SCTE Prague 2024

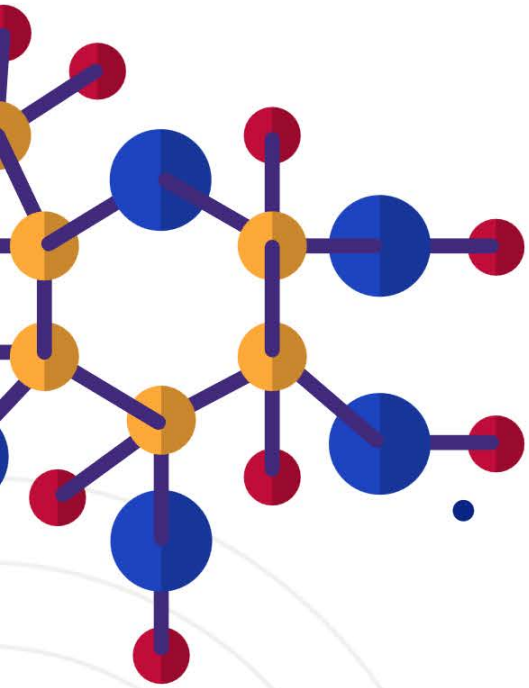

SCTE 2024

24th International Conference on Solid Compounds of Transition Elements

ABSTRACT BOOK / PROGRAM

WWW.SCTE2024.ORG

facebook.com/scte2024

Organizer

FACULTY OF MATHEMATICS AND PHYSICS
Charles University

DEPARTMENT OF CONDENSED MATTER PHYSICS
Faculty of Mathematics and Physics
Charles University

Administrator

OPTIVERSO s.r.o.
MAKE EVERYTHING OPTIMAL

Bronze partner

Crystal Systems Corporation

Other partners

CLASIC
Electric furnaces, measurement and control

MGML

VAKUUM PRAHA

labo sk

Abstract book and conference badge designed by Freepik.

Dear Friends and Colleagues,

We welcome you to the International Conference on Solid Compounds of Transition Elements 2024 (SCTE2024) in Prague, Czech Republic. This is the 24th SCTE conference since its inception and like so many previous SCTE meetings, we hope that SCTE24 will provide a mix of interesting and engaging research for all attendees.

At SCTE2024, you will hear the latest developments across a broad selection of fields from leading scientists, including 10 plenary speakers and 29 invited speakers. And there will be 54 contributed talks and around 52 poster presentations.

In addition to the scientific content, SCTE2024 offers a social program that includes a welcome party in the garden and terrace of Hotel Duo from 17:30 on Monday. On Thursday from 19:15 we will have the conference dinner at Plzenka U Brabcu restaurant, a short walk or metro ride from the conference site passing through a natural rock formation with beautiful views over Prague.

With over 100 participants, we hope that SCTE24 will be remembered as a meeting where you will meet old and new friends, and exchange fresh ideas with peers. We anticipate your kind participation and contributions to continuously strengthening the long tradition of SCTE conferences.

We wish you all to enjoy SCTE24.

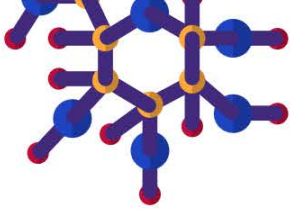

Information

The 24th International Conference on Solid Compounds of Transition Elements (SCTE2024) will be held in Hotel Duo during the week of June 17-21, 2024.

The SCTE conferences allow every 2 years to report new discoveries in chemistry and solid state physics of compounds and materials based on d and f electron elements. Several axes are discussed such as the crystal structure, the chemical bond as well as the various and varied physical properties (magnetic, transport and spectroscopic) of various families of intermetallics (and derivatives such as: hydrides, borides, carbides, silicides, pnictides, chalcogenides, oxides, halides).

The previous editions of SCTE took place in: Bordeaux in 2022, Wrocław in 2020 (in distance and in 2021 in reality), Vienna (2018), Zaragoza (2016), Genoa (2014), Lisbon (2012), Annecy (2010), Dresden (2008) and Krakow (2006).

Topics

- Synthesis and characterization of solid compounds of *d*- or *f* -elements
- Thermodynamics, phase equilibria, phase transitions
- Metastable, amorphous, and nanostructured materials
- Cooperative and topological phenomena (magnetism, ferroelectricity, electrical transport including superconductivity, charge density waves, strongly correlated systems, quantum criticality, spectroscopy)
- Theory (chemical bonding, electronic structure, phonons, machine learning)
- Energy (hydrogen production and storage, fuel cells, thermoelectrics, magnetocalorics, catalysis)
- Applications (production, recycling and other industrial processes, nuclear fuel and waste issues)

Committees

LOCAL
Ross H. Colman (Chair)
Vladimír Sechovský (Vice-chair)
Ladislav Havela (Chair of PC)
Štěpán Sechovský (Admin)
Martina Rážová
Pavel Javorský
Petr Čermák
Jiří Pospíšil
Jan Prokleška
Milan Klicpera (Proceedings)
(all are from Charles University)

PROGRAM
Ladislav Havela
(Charles Uni, Prague) - Chair
Milan Dopita
(Charles Uni, Prague)
Jeroen Custers
(Charles Uni, Prague)
Stanislav Kamba
(Institut of Physics, ASCR)
David Sedmidubský
(UCT Prague)
Čestmír Drašar
(Pardubice University)
Mathieu Pasturel
(Université de Rennes 1)

ADVISORY
Adriana Saccone (Italia)
Andrzej Szytuła (Poland)
Anna Tursina (Russia)
Antonio P. Goncalves (Portugal)
Arthur Mar (Canada)
Daniel Fruchart (France)
Dariusz Kaczorowski (Poland)
Ernst Bauer (Austria)
Fernando Bartolome (Spain)
Herbert Boller (Austria)
Jean-Louis Bobet (France)
Mathieu Pasturel (France)
Peter Rogl (Austria)
Roman Gladyshevskii (Ukraine)
Takao Mori (Japan)
Vladimir Sechovsky (Czechia)
Yuri Grin (Germany)

Wifi

SSID: **SCTE2024** Password: **2s0c2t4E**

Venue

- Hotel DUO, Teplická 492, 190 00 Prague 9, Czech republic
- Easily accessible center of the city (15min by metro) – hotel is located next to the metro station Střížkov (red line) – see map below
- Dividable congress hall (Prague EAST/WEST) for up to 410 participants

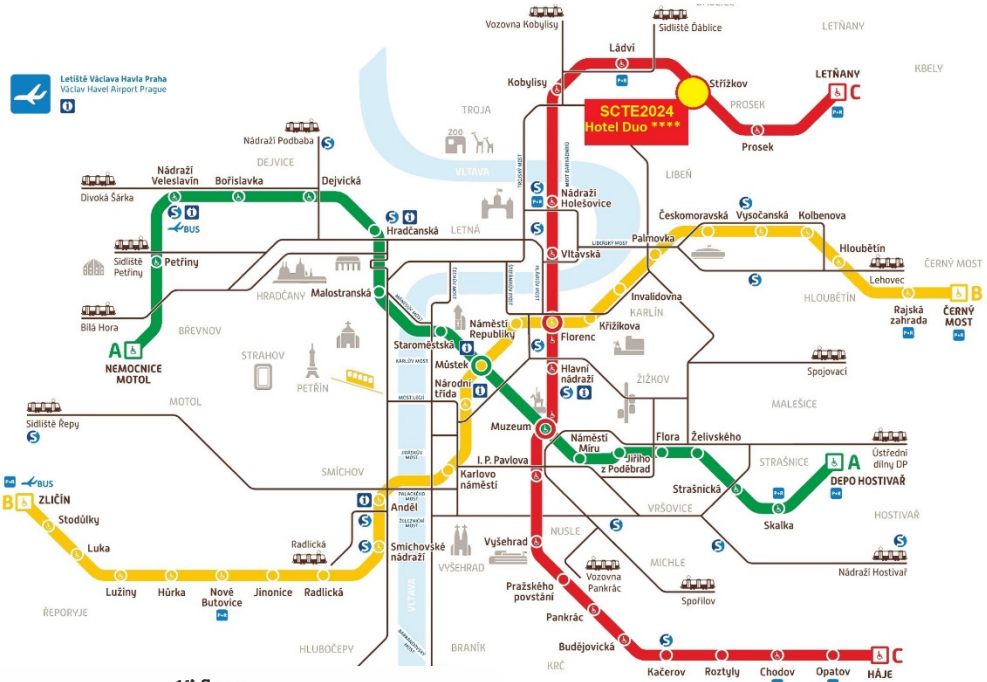

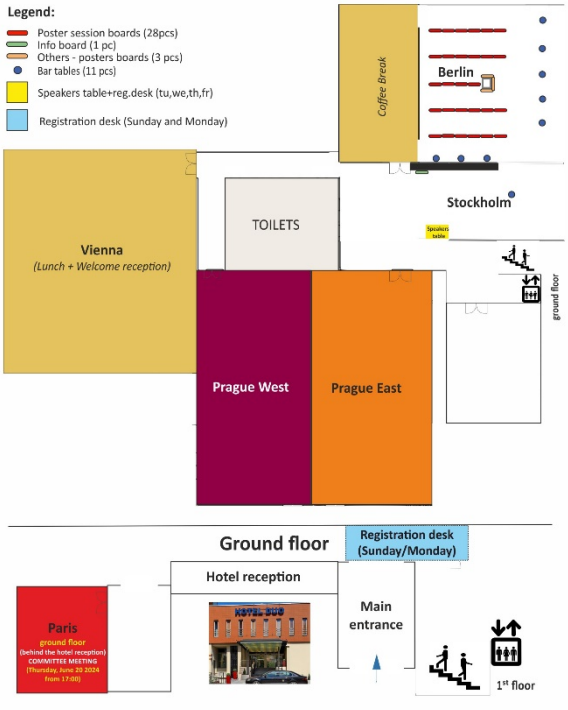

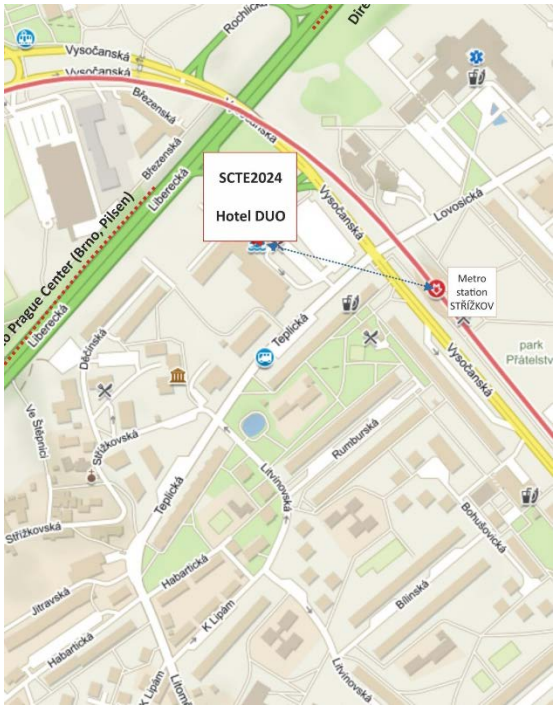

Program

SUNDAY 16.06.2024

16:00-18:00	**REGISTRATION** – Hotel Duo (opposite the main entrance)			

MONDAY 17.06.2024

8:00	**REGISTRATION** – Hotel Duo (opposite the main entrance)			
9:00	**Room Prague EAST**		**OPENING**	**R. Colman**
9:15	**PLENARY I** session chair: T. Klimczuk	**pl01**	Design and discovery of novel transition metal based compounds—What happens when a Physicist tries to be a Chemist	Paul Canfield *Ames, Iowa, USA*
10:00			COFFEE	
			Room Prague EAST	
10:30	**Lanthanide systems - Magnetism** Session chair: P. Čermák	**o01**	Electronic properties of Eu-T-X (T: transition metal, X: metalloid) compounds under high pressure	Fuminori Honda *Kyushu, JP*
11:00		**o02**	Structural, magnetic and electronic properties of $EuZn_2As_2$ single crystals	Damian Rybicki *Cracow, PL*
11:15		**o03**	Complex magnetic order in Eu_2Pd_2Sn and $EuPdSn_2$	Mauro Giovannini *Genoa, IT*
11:30		**o04**	Synthesis of europium-based crystals by flux method	Karolina Podgórska *Cracow, PL*
11:45		**o05**	Magnetic properties of the rare-earth aluminides $RECo_2Al_8$ (RE = La, Ce, Pr, Nd and Sm).	Raquel Ribeiro *Ames, Iowa, USA*
12:00		**o06**	Massive electronic state and field-induced ordering in $YbCo_2$	Naohito Tsujii *Tsukuba, JP*
			Room Prague WEST	
10:30	**Oxidic materials, frustration** Session chair: R. Colman	**o07**	Electric dipole frustration in the ferromagnet $EuAl_{12}O_{19}$	Gael Bastien *Prague, CZ*
11:00		**o08**	Gapless quantum spin liquid in triangular antiferromagnet hexa-aluminate $PrMgAl_{11}O_{19}$	Sonu Kumar *Prague, CZ*
11:15		**o09**	Out-of-equilibrium monopole dynamics in classical spin ices using the fluctuation-dissipation theorem	Félix Morineau *Grenoble, FR*
11:45		**o10**	Possible to control metastable charge-ordered states in δ-$Ag_{2/3}V_2O_5$	Masahiko Isobe *Stuttgart, DE*
12:00		**o11**	Effects of antiferromagnetic domain walls in single crystal $Lu_2Ir_2O_7$	Daniel Staško *Prague, CZ*
12:15			LUNCH	

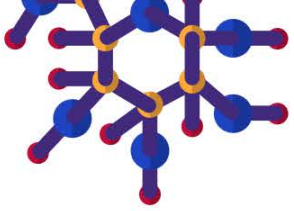

13:45	**PLENARY II** session chair: L. Havela	**pl02**	Effect of the Synthesis Route on the Microstructure and hydrogen storage of $Hf_xTi_{(1-x)}NbVZr$ Refractory High-Entropy Alloys	Jacques Huot *Quebec, CA*
14:30	**PLENARY III** session chair: E. Chitrova	**pl03**	Actinide science at high magnetic fields: piezomagnetism in uranium dioxide	Krzysztof Gofryk *Idaho Falls, USA*
15:15			COFFEE	
			Room Prague EAST	
15:45	**Lanthanide systems - Magnetism** Session chair: A. Pikul	**o12**	Unusual magnetotransport in half-Heusler topological materials	Orest Pavlosiuk *Wrocław, Poland*
16:15		**o13**	Comparison of complex magnetic structures in $RE_5T_2In_4$ (RE = rare earth element; T = Ni, Pd, Pt) compounds	Stanisław Baran *Cracow, PL*
16:30		**o14**	Physical properties studies of the multiple CDW phase transitions in quasi-1D $RNiC_2$ compounds (R = rare earth metal)	Marta Roman *Vienna, AT*
17:00		**o15**	Bulk physical properties and enantiomorph-resolved electrical transport of chiral narrow-band semiconductors $RRhC_2$ (R = La, Ce)	Volodymyr Levytskyi *Freiberg, DE*
			Room Prague WEST	
15:45	**Applications** Session chair: Č. Drašar	**o16**	Uranium Nuclear Safeguards: Automated Fission Track Analysis via Synthetic Model Generation and Image Analysis Tools	Itzhak Halevy *Beer Sheva, IL*
16:15		**o17**	Impact of Rare Earth Element Integration on Glass Forming Ability and Thermal Stability of Zr-Based Bulk Metallic Glasses	Juhi Rani Verma *Nagpur, IN*
16:30		**o18**	Fabrication of porous aluminum alloys for hydrogen production	Laurent Cuzacq *Bordeaux, FR*
16:45		**o19**	Scalability of the magnesiothermic synthesis of skutterudites and their protective coatings against oxidation	Arige Hodroj *Rennes, FR*
17:00		**o20**	MAX Phase / MXene / Metal Nanomaterials for Energy Conversion Application	Sergii Sergiienko *Prague, CZ*
17:30-19:30	***Welcome Party*** (Hotel Duo garden or inside - 1st floor by the weather)			

TUESDAY

18.06.2024

9:00	**PLENARY IV** session chair: R. Freccero	**pl04**	Targeted Catalyst Development: An Innovative Playground for Intermetallic Compounds	Marc Armbrüster *Chemnitz, DE*
9:45	**PLENARY V** session chair: J. Tobin	**pl05**	High energy resolution X-ray spectroscopy for Material Science	Kristina Kvashnina *Grenoble, FR* *Dresden, DE*
10:30			COFFEE	
11:00	Room Berlin		**POSTERS - see list of posters below**	
12:30			LUNCH	
			Room Prague EAST	
14:00	**Spectroscopy, Uranium** Session chair: K. Kvashnina	**o21**	Unraveling the Actinides 5f Enigma with X-Ray Emission Spectroscopy	James G. Tobin *Oshkosh, WI, USA*
14:30		**o22**	Fundamentals of the Uranium Halides	Clara L. Silva *Grenoble, FR*
15:00		**o23**	On valence-band photoemission from actinides	Jindřich Kolorenč *Prague, CZ*
15:30		**o24**	Electronic structure of U hydrides probed by XPS and UPS	Oleksandra Koloskova *Prague, CZ*
			Room Prague WEST	
14:00	**New compounds** Session chair: M. Armbrüster	**o25**	Crystal Structure and Chemical Bonding Analysis of Be-Ru Intermetallic Compounds	Laura Agnarelli *Caen, FR*
14:30		**o26**	Electronic structure of modified Ti_2MnAl compound.	Wojciech Gumulak *Chorzów, PL*
14:45		**o27**	Tuning the Weyl-Kondo Semimetal $Ce_3Bi_4Pd_3$ via Stoichiometry	Nikolas Reumann *Vienna, AT*
15:00		**o28**	Superconductivity in the Heusler and a related type intermetallic compounds	Tomasz Klimczuk *Gdansk, PL*
15:30		**o29**	Crystallochemistry, Thermodynamic and Physical Properties of the novel $Cu_{3-x}(As_ySb_{1-y})$ intermetallic compound	Pietro Manfrinetti *Genoa, Italy*
15:45			COFFEE	
			Room Prague EAST	
16:15	**Spectroscopy, Uranium** Session chair: J. Kolorenč	**o30**	Electronic Structure and Local Magnetic Properties of Uranium Compounds Probed with XANES and XMCD.	Fabrice Wilhelm *Grenoble, FR*
16:45		**o31**	Complex magnetic behaviours in $U_6T_4Al_{43}$ (T = V, Nb, Ta, Cr, Mo, W) with isolated U-dumbells	Mathieu Pasturel *Rennes, FR*
17:15		**o32**	Electrical resistivity of the Zintl phase UCu_2P_2	Silvie Černá, *Prague, CZ*
17:30		**o33**	Exploration of the Exceptional Curie Temperatures in Uranium-Based UCu_2P_2 Ferromagnet Using Dilatometry	Volodymyr Buturlim *Idaho, USA*
17:45		**o34**	High-pressure investigation of the crystal structure of UCu_2P_2	Oleksandr Kolomiets *Lviv, UA*

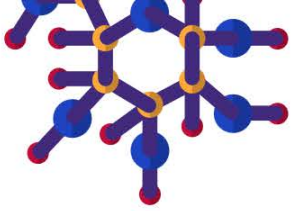

		Room Prague WEST		
16:15	**New Materials** Session chair: E. Svanidze	**o35**	New Ternary Arsenide of Ytterbium and Iron–a Novel Ferromagnetic Material	Oksana Karychort *Lviv, UA*
16:30		**o36**	Synthesis and characterization of a new ferrimagnetic $SmFe_5As_3$ pnictide	Mitja Krnel *Dresden, DE*
16:45		**o37**	Functionalization of selected 2D materials with π-conjugated bis-hydrazone coordination complex	Piotr Zabierowski *Prague, CZ*
17:00		**o38**	Magnetically soft CoFeNi-based high-entropy alloys	Primož Koželj *Ljubljana, SL*
17:15		**o39**	Effect of sputtering power on the structural, optical and electrical properties of aluminum-doped zinc oxide thin film	Chonthicha Wannasiri *Bangkok, TH*
17:30		**o40**	Transition temperature enhancement in superconducting high entropy alloy films through nitrogen addition	Karol Flachbart *Košice, SK*

WEDNESDAY

19.06.2024

9:00	**PLENARY VI** session chair: T. Mori	**pl06**	Towards the Metal Age of Thermoelectricity: High Thermoelectric Performance in Metallic Materials via Interband Scattering	Andrej Pustogow *Vienna, AT*
9:45	**PLENARY VII** session chair: J. Custers	**pl07**	Geometrically frustrated Ytterbium-oxides for milli-Kelvin adiabatic demagnetization refrigeration	Philipp Gegenwart *Augsburg, DE*
10:30			COFFEE	
11:00	Room Berlin		**POSTERS - see list of posters below**	
12:30			LUNCH	
			Room Prague EAST	
14:00	**Thermoelectrics magnetocalorics** Session chair: E. Bauer	**o41**	Mechanisms to inhibit thermal conductivity and enhance thermoelectric performance	Takao Mori *Tsukuba, JP*
14:30		**o42**	Thermoelectric properties of new transition metal chalcogenides and phosphides	David Berthebaud *Nantes, FR*
15:00		**o43**	Is the presence of Sn^{2+} a crucial factor for the generation of low thermal conductivity in tin -based sulphides?	Florentine Guiot *Rennes, FR*
15:15		**o44**	Room Temperature Giant Magnetocaloric Materials $(MnFe)_{1.9}(PSi)$ Fe-Rich Compounds for Heat Pump Application	Hang Hanggai *Delft, NL*
15:30		**o45**	Accelerating Material Synthesis Optimization with Bayesian Optimization: Investigating the Magnesioreduction Synthesis of Magnetocaloric $Mn_{5-x}Fe_xSi_3$	Sylvain Le Tonquesse *Caen, FR*
			Room Prague WEST	
14:00	**Theory** Session chair: D. Legut	**o46**	Discovery of Inorganic Solids with Desired Structure Motifs Guided by Machine Learning	Arthur Mar *Alberta, CA*
14:30		**o47**	What is the true ground-state of intermetallic compound Fe_3Al?	Mojimír Šob *Brno, CZ*
14:45		**o48**	Predictive theory of the spontaneous volume magnetostriction in Fe-Ni alloys: bond repopulation model of Invar effect.	Sergii Khmelevskyi *Vienna, AT*
15:15		**o49**	Self-Consistent Renormalization Theory of Anisotropic Spin Fluctuations in Nearly Antiferromagnetic Metals	Rikio Konno *Nabari-shi, Mie, Japan*
15:30		**o50**	Intrinsic spin currents in noncentrosymmetric ferromagnets	Ilja Turek *Brno, CZ*
15:45			COFFEE	

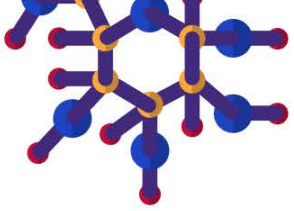

		Room Prague EAST		
16:15	**f-materials** Session chair: P. Rogl	**o51**	Two-fluid model analysis of the terahertz conductivity of YBaCuO samples: optimally doped, underdoped and overdoped cases	Christelle Kadlec *Prague, CZ*
16:30		**o52**	Effect of Hydrogenation on the Crystal Structure and Magnetism of Nd_2Ni_2Sn	Khrystyna Miliyanchuk *Lviv, UA*
16:45		**o53**	Phase stability of solid solution $La_{1-x}R_xRh_3B$ (R = Gd, Lu and Sc) with anti-perovskite cubic type structure	Kunio Yubuta *Fukuoka, JP*
17:00		**o54**	Unveiling exotic magnetic phase diagram of a non-Heisenberg quasicrystal approximant	Farid Labib *Tokyo, JP*
17:15		**o55**	Revisiting the $RE_2Pd_3Si_5$ series: flux growth, crystal structure and chemical bonding	Riccardo Freccero *Genoa, IT*
17:45		**o56**	The new $PrNi_6Si_6$ intermetallic: crystal structure, thermal and electrical transport properties in the temperature range 2 - 900 K	Alessia Provino *Genoa, IT*
		Room Prague WEST		
16:15	**Theory** Session chair: M. Šob	**o57**	An ab-initio theory of vibrational inelastic tunneling spectrum of magnetic molecules adsorbed on superconductors	Athanasios Koliogiorgos *Prague, CZ*
16:45		**o58**	Large Magnetostriction and Anisotropy Energy in FePt and Fe_5Ta_2	Dominik Legut *Prague/Ostrava, CZ*
17:15		**o59**	Phonons and superconductivity of high entropy alloys	Sylwia Gutowska *Vienna, AT*
17:30		**o60**	Lattice Dynamical Properties and its Thermal Conductivity in Two-Dimensional Boron Nitride (BN) and Graphene	Svitlana Pastukh *Cracow, PL*

THURSDAY

20.06.2024

9:00	**PLENARY VIII** session chair: J. Custers	**pl08**	Mass renormalisation and superconductivity in quantum materials	Malte Grosche *Cambridge, UK*
9:45	**PLENARY IX** session chair: S. Kamba	**pl09**	Optical detection of symmetry breakings in ferroic and multiferroic materials	Tsuyoshi Kimura *Tokyo, JP*
10:30			COFFEE	
			Room Prague EAST	
11:00	**Hydrogen** Session chair: R. Gladyshevskii	**o62**	Metal hydridoborates, novel energy storage materials.	Radovan Černý *Geneva, CH*
11:30		**o63**	H_2 production and storage: New active and stable Ni_xFe_y catalysts supported on conductive ball-milling prepared titanium oxides for OER in alkaline medium and design of light HEA's for H_2 storage.	Victor RAUD *Poitiers/Bordeaux, FR*
11:45		**o64**	Light elements (H, O, F) insertion into the RScSi (R = La, Nd, Pr) intermetallics: Structural studies and a gateway to catalysis applications	Khaled Alabd *Bordeaux, FR*
			Room Prague WEST	
11:00	**Ferroics** Session Chair: A. Maignan	**o65**	Collinear magnetic structures induced by ferroelectric distortion in multiferroic quadruple perovskites BiM3Cr4O12 and BiMn7O12	Stanislav Kamba *Prague, CZ*
11:30		**o66**	$RuIn_6Sn_6O_{16}$, $Ru_4In_2Sn_{20}O_{21}$ and $Ir_3In_3Sn_{12}O_{14}$ - Synthesis and structural characterization of novel transition metal oxide clusters	Tilo Söhnel *Auckland, NZ*
11:45		**o67**	Sliding ferroelectricity in bulk misfit layered compound $(BiS)_{1.24}CrS_2$	Jiří Volný *Prague, CZ*
12:00			LUNCH	
			Room Prague EAST	
13:30	**New materials** Session chair: M. Pasturel	**o68**	Structure and bonding of compounds in the Sc-rich part of the Sc-{Mn,Fe,Co,Ni,Pd,Pt}-Ga systems	Vitaliy Romaka *Dresden, DE*
14:00		**o69**	Lattice, magnetic, and in-gap optical states in van der Waals antiferromagnet VCl_3	Dávid Hovančík *Prague, CZ*
14:15		**o70**	Unconventional magnetic and magneto-transport properties of tetragonal $RbCo_2As_2$	Abhishek Pandey *Johannesburg, ZA*
14:30		**o71**	Comparative study of magnetocaloric effect in the $RE_5T_2In_4$(RE = Gd–Tm, T – transition metals = Pt, Pd, Rh) compounds	Altifani Rizky Hayyu *Cracow, PL*
14:45		**o72**	Magnetic properties at ambient and under high pressure in Ho_3Co	Srikanta Goswami *Prague, CZ*
15:00		**o73**	Misfit layered compounds, a route towards natural morié lattices	Klára Uhlířová *Prague, CZ*

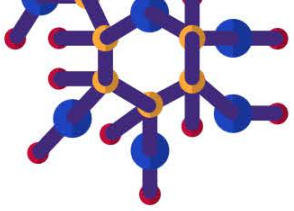

		Room Prague WEST		
13:30	**UTe_2 and other U systems** Session chair: M. Grosche	**o74**	Physics and chemistry of UTe_2	Eteri Svanidze *Dresden, DE*
14:00		**o75**	Lattice dynamics of UTe_2 in high magnetic fields studied by ultrasound	Michal Vališka *Prague, CZ*
14:30		**o76**	Evolution of electronic structure across the U-Te series of compositions	Evgenia Tereshina-Chitrova *Prague, CZ*
15:00		**o77**	New uranium-based arsenides: A small review	Nazar Zaremba *Dresden, DE*
15:15			COFFEE	
		Room Prague EAST		
15:45	**Phase diagrams** Session chair: R. Černý	**o78**	System Thorium - Boron - Carbon, revisited	Peter Franz Rogl *Vienna, AT*
16:15		**o79**	Revisiting the Strontium-Mercury Phase Diagram	Rachel Nixon *Dresden, DE*
		Room Prague WEST		
15:45	**Applications** Session chair: I. Halevy	**o80**	From Industry to Lab: Pioneering Automated Sample Preparation	Petr Čermák *Prague, CZ*
16:15		**o81**	Elevating Cancer Treatment with Advanced Dosimeters and Crystal Precision	Cristiana Rodrigues *Lisbon, PT*
16:45	**Conference photo**			
17:00	**Committee meeting (room Paris)**			
18:00				
19:15	**Conference dinner**		**PLZEŇKA U BRABCŮ - https://plzenkaubrabcu.cz/**	
22:15				

FRIDAY

21.06.2024

		Room Prague EAST		
9:00	**Borides** Session chair: M. Giovannini	**o82**	Elastic and inelastic neutron scattering studies in ternary boride $YbPt_5B_2$	Ernst Bauer *Vienna, AT*
9:30		**o83**	Angle-resolved magnetoresistance in the strongly anisotropic quantum magnet TmB_4	Slavomír Gabáni *Košice, SK*
9:45	**PLENARY X** session chair: P. Canfield	**pl10**	Antiferromagnetism, ferrimagnetism, magnetization reversal and linear magnetoelectricity in $A_4Nb_2O_9$ where A=3d (Mn,Fe,Co,Ni) magnetic elements	Antoine Maignan *Caen, FR*
10:30			COFFEE	
11:00	**Conference summary - Session chair: R. Colman** **Prizes** **Announcement of next SCTE** **CLOSING**			

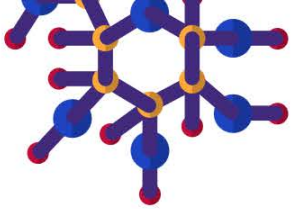

LIST OF POSTERS

P01	High-field magnetoacoustics of a $Dy_2Fe_{14}Si_3$ single crystal	Alexander V. Andreev	Prague, CZ
P02	Enhanced Superconducting Critical Parameters in a New High-Entropy Alloy $Nb_{0.34}Ti_{0.33}Zr_{0.14}Ta_{0.11}Hf_{0.08}$	Adam Pikul	Wrocław, PL
P03	Possible realization of the Majumdar-Ghosh point in the mineral szenicsite	Adam Berlie	Oxfordshire, UK
P04	Investigation of vacuum cryodeposited water films capturing carbon monoxide on an optical surface	Yevgeniy Korshikov	Almaty, KZ
P09	In situ diffraction study of the phase transformations occurring in the thermoelectric colusite $Cu_{26}V_2Sn_6S_{32}$	Florentine Guiot	Rennes, FR
P10	Thickness Dependence on the Properties of Sputtered-AZO Thin Film on Flexible Substrate for Transparent Heater	Watcharee Rattanasakulthong	Bangkok, TH
P11	Strong electron-phonon coupling and superconducting gap in Heusler-type superconductor $ScAu_2Al$	Gabriel Kuderowicz	Cracow, PL
P12	Superconductivity in medium- and high-entropy alloy thin films	Gabriel Pristáš	Košice, SK
P13	Exploring a new method in the field of metal hydrides	Christohe Cona	Bordeaux, FR
P14	Magnetic Structures of $UnRhIn_{3n+2}$ Materials	Jeroen Custers	Prague, CZ
P15	Tailoring the size and shape of actinide compounds	Karin Popa	Karlsruhe, DE
P16	Syntheses and some properties of solid solution $Yb(Al,T)B_4$ (T=Fe,Cr,Mo,Mn,W) compounds	Kaoru Kouzu	Tokyo, JP
P17	Exploring Magnetic Transition Metal Sulfides and their Thermoelectric Properties	Laura Agnarelli	Caen, FR
P18	Coupled magnetic-crystallographic transition and associated multi-functional properties in $La_{0.9}Ce_{0.1}Fe_{12}B_6$	Léopold Diop	Nancy, FR
P19	Magnetic Field-Induced Phase Transition and Weak Ferromagnetism in the Underdoped PrBCO Cuprate	Mahieddine Lahoubi	Annaba, DZ
P20	Magnetization Study of the Low Temperature Anomalies in the Substituted Dysprosium-Yttrium Iron Garnets	Mahieddine Lahoubi	Annaba, DZ
P22	Quantum Spin Liquid vs. Spin-glass: S(eff) = ½ Pyrochlore Fluoride Antiferromagnets $NaCdCu_2F_7$ & $NaCdCo_2F_7$	Andrej Kancko	Prague, CZ
P23	Fluctuation conductivity and pseudogap in slightly doped $HoBa_2Cu_3O_{7-\delta}$ single crystals	Liudmyla Bludova	Kharkiv, UA
P24	Magnetoelastic properties of UIrGe studied by ultrasound	Tetiana Haidamak	Prague, CZ
P25	Magnetoelastic coupling in HoB_4	Cinthia Antunes Correa	Prague, CZ
P26	Magnetism and anisotropy of vdW antiferromagnet VCl_3	Ondřej Michal	Prague, CZ

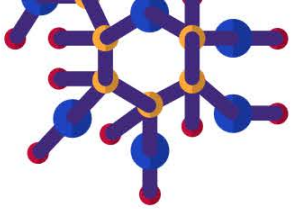

P27	Exploring electrical and magnetical properties of $NiBr_2$	Parvez Ahmed Qureshi	Prague, CZ
P28	Structural and magnetic properties of R_2Cu_2In intermetallics	Petr Král	Prague, CZ
P29	Strong magnetocaloric effect induced by anisotropic ferromagnetism in $EuAl_{12}O_{19}$	Adam Eliáš	Prague, CZ
P30	Crystal Structure and Magnetic Properties of Uranium-Hafnium Hydrides	Shanmukh V. V. Devanaboina	Prague, CZ
P31	Universal anomalous low-temperature properties of the binary ZnO-P_2O_5 glasses	Vladimír Tkáč	Košice, SK
P32	Anomalous Hall effect and chiral anomaly in antiferromagnetic DyPtSb	Abhinav Agarwal	Wroclaw, PL
P33	Spin-orbit interactions and magnetism in open d-shell oxides: $CdVO_3$ and Ba_2LuMoO_6	Ryszard Radwanski	Cracow, PL
P34	Physical properties of a Kondo lattice oxypnictide $Ce_3Cu_4P_4O_2$	Szymon Królak	Gdansk, PL
P35	Formation, structure, and properties of R_2Pt_2Sn intermetallics (R = Sc, Y, La-Sm, Gd-Lu)	Vitaliy Romaka	Dresden, DE
P36	Phase equilibria, crystal structure, physical properties, and DFT study of ternary stannides in Hf-Cu-Sn system	Vitaliy Romaka	Dresden, DE
P37	Structure, properties, and DFT study of RCr_6Ge_6 (R = Gd-Lu) compounds with kagome lattice	Vitaliy Romaka	Dresden, DE
P38	Magnetic anisotropy of $YCo_{12}B_6$ single crystals	Léopold V. B. Diop	Nancy, FR
P39	Structural and magnetic properties of the chiral solid solution $La_{1-x}Ce_xRhC_2$	Volodymyr Levytskyi	Freiberg, DE
P40	The $NdTIn_{1-x}Al_x$ (T = Ni, Pd) continuous solid solutions	Galyna Nychyporuk	Lviv, UA
P41	Influence of Ti/Zr-Based Intermetallics on Hydrogen Storage and Generation Properties of MgH_2 Composites	Ihor Zavaliy	Lviv, UA
P42	New Quaternary Compounds $R_2CoAl_4Si_2$	Svitlana Pukas	Lviv, UA
P43	New ternary gallide $Zr_7Pd_7Ga_3$:preparation, crystal and electronic structures	Volodymyr Babizhetskyy	Lviv, UA
P44	Crystal structure of the $Mg_{5.57}Ni_{16}Ge_{7.43}$ ternary compound	Volodymyr Pavlyuk	Lviv, UA
P45	Crystal structure of the new ternary indide $ErCo_2In$	Yuriy Tyvanchuk	Lviv, UA
P46	Crystal Structure of the New Ternary Phases in the Nd-Tm-Ge System	Zinoviya Shpyrka	Lviv, UA
P47	Crystal structure of the $R_{1.33}Ni_3Ga_8$ (R = Tb, Dy, Ho, Er, Tm, Lu) compounds	Nataliya Muts	Lviv, UA
P48	More about the $BaO–Lu_2O_3–CuO$ system	Oksana Zaremba	Lviv, UA
P49	Phase Equilibria in the Ternary System Gd–Mn–Zn and Electrochemical Hydrogenation of the Phases	Oksana Zelinska	Lviv, UA

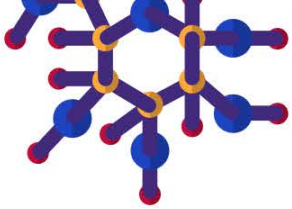

P50	Structural Characterization of Sol-Gel Derived High-Entropy Perovskite $(Y_{0.2}Nd_{0.2}Sm_{0.2}Eu_{0.2}Er_{0.2})AlO_3$	Leonid Vasylechko	Lviv, UA
P51	Spark Plasma Sintering of the $B_{13}C_2$–VB_2 Composition	Andriana Ivanushko	Lviv, UA
P52	Synthesis Method for Single Crystals of the Compound Ti_3SiC_2	Anastasiia Broda	Lviv, UA
P53	Exploring high magnetocrystalline anisotropy in $Ni_{50}Mn_{25}Ga_{20}Fe_5$ single crystals	Taras Kovaliuk	Prague, CZ

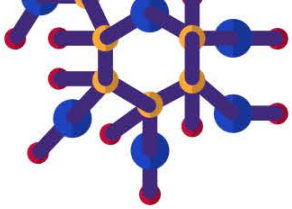

Abstracts

pl01

PLENARY: Design and discovery of novel transition metal based compounds—What happens when a Physicist tries to be a Chemist.

Paul Canfield

Ames Laboratory, Ames, Iowa, USA. Iowa State University, Ames, Iowa, USA

Over the past 30 plus years my group has made over 10,000 solution growth attempts to grow or explore 1,000's of different compounds or phase spaces. Over the past decade we have been developing a variety of different algorithms for identifying and accessing poorly explored spaces, partly with an eye toward discovering new phases, partly with an eye toward discovering new electrical or magnetic phase transitions and ground states. In this talk I will try to address the basic research questions of, "where should I look for new materials or physics?" and "how can I enhance my chances of discovering X, Y, or Z (where XYZ can be your favorite state, structure or behavior)?". Specific examples spanning superconductors, quasicrystals, heavy fermions, fragile magnets, topological electronic systems, local moment magnets and a few lost puppies will be given and reviewed.

The goal of this talk is to inspire and entertain, any resemblance to persons living or dead is coincidental. This talk is based on parts of my recent review article, "New Materials Physics" [1] as well as recent technical papers on solution growth. [2,3]

[1] P. C. Canfield, Rev. Prog. Phys. **83**, 016501 (2020).
[2] T. J. Slade and P. C. Canfield, Z. Anorg. Allg. Chem., **648**, e202200145 (2022).
[3] P. C. Canfield, T. Kong, U. S. Kaluarachchi, N-H. Jo, Philosophical Magazine **96**, 84-92 (2016).

o01

Electronic properties of Eu-T-X (T: transition metal, X: metalloid) compounds under high pressure

Fuminori Honda[1], Naomi Kawamura[2], Ryu Nakachi[3], Dexin Li[4], Ai Nakamura[4], Yoshiya Homma[4], Masato Hedo[5], Tatsuma D. Matsuda[3], Dai Aoki[4], Yoshichika Onuki[6,3]

[1]Central Institute of Radioisotope Science and Safety, Kyushu University, Fukuoka-Nishi, Fukuoka, Japan. [2]JASRI/SPring-8, Koto, Hyogo, Japan. [3]Grad. Sch. of Sci. Tokyo Metropolitan Univ., Hachioji, Tokyo, Japan. [4]IMR Tohoku University, Oarai, Ibaraki, Japan. [5]The Univ. of Ryukyus, Nishihara, Okinawa, Japan. [6]RIKEN CEMS, Wako, Saitama, Japan

It is widely recognized that the valence state of Eu can be controlled by pressure. We proposed there are three typical pressure-temperature phase diagrams on Eu-compounds under pressure [1]. One is the well-known pressure-induced valence transition (PIVT) case, which is observed in $EuRh_2Si_2$ etc [2]. The second one is the Doniach type found in $EuPt_2Si_2$ and $Eu_2Ni_3Ge_5$, *i.e.*, like some Ce-compounds the magnetism is gradually suppressed and disappears with pressure. The third one is the “sharp valence crossover” case. The magnetic ordering temperature suddenly becomes zero and simultaneously Eu valence state is slightly changed, which is found in $EuCu_2Ge_2$ [3] and $EuPt_3Al_5$ [1].

Recently, we succeeded in growing high-quality single crystals of several Eu-T-X compounds (T: transition metal, X: metalloid) and performed a series of pressure experiments. Recently, we have found that $EuRu_2Ge_2$ ferromagnet with T_C = 62 K and discovered a new PIVT. We confirmed that there is no PIVT in the isostructural (but without transition elements) compound $EuGa_4$, which was believed to exhibit PIVT around 6 GPa, by the XAS. Besides, we observed a significant valence crossover in $EuRu_2P_2$ above the critical pressure of QCP. In the presentation, single crystal growth and various pressure studies of Eu compounds will also be reviewed.

[1] T. Koizumi, F. Honda et al., J. Phys. Soc. Jpn. **91**, 043704 (2022).
[2] F. Honda Physica B **536**, 182 (2018).
[3] J. Gouchi . Phys. Soc. Jpn. **89**, 053703 (2020).

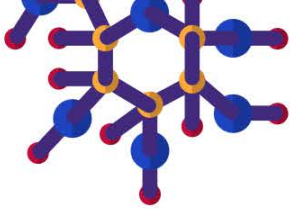

o02

Structural, magnetic and electronic properties of $EuZn_2As_2$ single crystals

Damian Rybicki[1], Zbigniew Bukowski[2], Michał Babij[2], Łukasz Gondek[1], Janusz Przewoźnik[1], Jan Żukrowski[1], Czesław Kapusta[1]

[1]AGH University of Krakow, Faculty of Physics and Applied Computer Science, Kraków, Poland. [2]Institute of Low Temperature and Structure Research, Polish Academy of Sciences, Wrocław, Poland

Compounds containing Eu show a vast range of unique physical properties due to the interplay of electronic and magnetic properties, which can lead to a nontrivial electronic topology combined with magnetic order. We report on the growth of trigonal (*P*3*m*1 space group) $EuZn_2As_2$ single crystals and on the studies of their structural, electronic and magnetic properties. A range of experimental techniques was applied including X-ray diffraction, electron microscopy, magnetic susceptibility, magnetization, heat capacity and Mössbauer spectroscopy in the study. We found that Eu has solely a 2+ valence state and its magnetic moments below T_N = 19.2 K form a canted antiferromagnetic structure, tilted from the basal plane [1].

We acknowledge financial support by National Science Centre, Poland (Grant No. 2018/30/E/ST3/00377 and 2017/25/B/ ST3/02868). Part of the work was performed with the apparatus purchased within the IDUB Project.

[1] Z. Bukowski, D. Rybicki, M. Babij, J. Przewoźnik, Ł. Gondek, J. Żukrowski, Cz. Kapusta, Scientific Reports **12**, 14718 (2022).

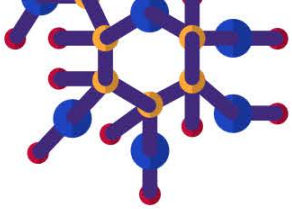

o03

Complex magnetic order in Eu_2Pd_2Sn and $EuPdSn_2$

Mauro Giovannini[1,2], Alberto Martinelli[3], Dominic Ryan[4], Julian Sereni[5], Clemens Ritter[6], Ivan Čurlik[7], Riccardo Freccero[2]

[1]INFN, Genoa, Italy. [2]University of Genoa, Genoa, Italy. [3]SPIN-CNR, Genoa, Italy. [4]McGill University, Montreal, Quebec, Italy. [5]CAB-CNEA, CONICET, San Carlos de Bariloche, Argentina. [6]Institut Laue - Langevin, Grenoble, France. [7]University of Prešov, Prešov, Slovakia

The magnetic behaviour of intermetallic compounds based on Eu^{2+} is often unexpected. In fact, these compounds constitute a pure spin system with $J = S = 7/2$ and $L = 0$ which preclude CEF effects. Nevertheless, these compounds frequently exhibit a complex anisotropic magnetic ordering. The structural and magnetic properties of Eu_2Pd_2Sn and $EuPdSn_2$ compounds have been investigated by synchrotron X-ray and neutron powder diffraction and ^{151}Eu Mössbauer spectroscopy. The study of magnetism in non-centrosymmetric compounds like Eu_2Pd_2Sn is of great interest due to topologically non-trivial magnetic textures, which offer the potential for new magnetic information manipulation and storage technologies [1].

The magnetic phase that develops for Eu_2Pd_2Sn below 14 K is characterized by an incommensurate cycloidal ordering in the *ac* plane of the Eu substructure. This magnetic structure shows significant analogies to the structure observed in $EuNiGe_3$, possibly indicating the occurrence of a skyrmion lattice also for Eu_2Pd_2Sn [2].

In $EuPdSn_2$, the magnetic behavior is unconventional: we will show that antiferromagnetic and ferromagnetic domains compete and coexist in the ground state which is also confirmed by theoretical calculations [3].

[1] N. Nagaosa et al. Nat. Nanotechnol. **8** (2013) 899.
[2] J.G. Sereni et al., Phys. Rev. B **108** (2023) 014427.
[3] A. Martinelli et. al. J. Materials Chemistry C **11** (2023) 7641

o04

Synthesis of europium-based crystals by flux method

Karolina Podgórska[1], Michał Babij[2], Wojciech Tabiś[1,3], Damian Rybicki[1]

[1]AGH University of Kraków, Faculty of Physics and Applied Computer Science, Aleja Mickiewicza 30, 30-059 Kraków, Poland. [2]Institute of Low Temperature and Structure Research, Polish Academy of Sciences, ul. Okólna 2, 50-422 Wrocław, Poland. [3]Institute of Solid State Physics, TU Wien, 1040 Vienna, Austria

A flux growth methods are widely used to obtain inorganic compounds in form of single crystals. In order to obtain a specific stoichiometry, it is necessary to: select the right flux, its ratio, use the proper heating profile and choose the right crucible material in which the reaction is carried out. All these factors have an influence on whether the crystals with the assumed stoichiometry will be obtained in the end. The synthesis of new compound implies the need to test different fluxes and conditions of the synthesis with the need to improve it in order to get crystals of assumed stoichiometry. Since it is known that EuAgAs compound can be obtained from Bi flux [1], one can try, using the same synthesis method (with the same flux), to synthesize the potentially topological EuAgP, which is currently obtained only in a polycrystalline form [2]. It turns out that trying to create such an analogue between arsenides and phosphides is not so obvious at all. It will be shown how changing the chosen flux and synthesis conditions affects the material obtained. X-ray diffraction and energy X-ray dispersive spectroscopy studies of the obtained crystals clearly show that different fluxes result in different compound, with different stoichiometry.

Acknowledgements: We acknowledge the support from NCN (SONATA BIS: 2018/30/E/ST3/00377, OPUS: 2021/41/B/ST3/03454).

[1] A. Laha et al., Phys. Rev. B **103**, L241112 (2021).
[2] C. Tomuschat et al., Z. Naturforsch. B, **36** (1981).

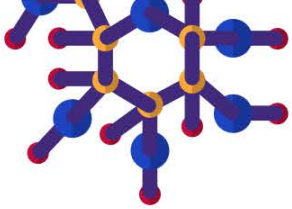

o05

Magnetic properties of the rare-earth aluminides $RECo_2Al_8$ (RE = La, Ce, Pr, Nd and Sm).

Raquel Ribeiro[1,2], Fernando Garcia[2,3], Sushma Kumari[2], Juan Schmidt[2], Aashish Sapkota[2], Paul Canfield[1,2]

[1]Iowa State University, Ames, IA, USA. [2]Ames National Laboratory, Ames, IA, USA. [3]Instituto de Física, Universidade de São Paulo, Sao Paulo, SP, Brazil

We present the magnetic, thermal and transport properties of single crystals of the $RECo_2Al_8$ (RE = La, Ce, Pr, Nd and Sm) rare-earth aluminides. The Ce-based material is characterized as a Kondo system and moderate heavy fermion, for which the Sommerfeld coefficient is about ten times that determined for the La-based material (g_{Ce} = 138 mJ/mol.K and g_{La} = 14 mJ/mol.K, respectively). The Pr-, Nd- and Sm-based materials all present antiferromagnetic (AFM) order that develops below 4.93 K, 8.2 K and 21.4 K, respectively. In the cases of the Nd- and Sm-based materials, frustrated in plane AFM interactions are observed. For the Pr-based compound, indeed two consecutive AFM transitions are observed in heat capacity and magnetization measurements (at 4.77 K and 4.93 K). Supported by isothermal magnetization and heat capacity measurements, we construct the T vs. H phase diagrams for the Pr- and Nd- based materials. Metamagnetic transitions from the low field AFM phase to a high field FM phase are observed. The FM phase is suppressed at further higher fields. Resistivity measurements are compatible with metallic behavior.

This work was done at Iowa State University and supported by the Ames National Laboratory, US DOE, Basic Sciences, Material Science and Engineering Division under Contract No DE-AC02-07CH11358

o06

Massive electronic state and field-induced ordering in $YbCo_2$

Naohito Tsujii[1], Jaroslav Valenta[1,2], Hitoshi Yamaoka[3], Fuminori Honda[4], Yusuke Hirose[5], Hiroya Sakurai[1], Takao Mori[1], Masashi Hase[1]

[1]National Institute for Materials Science, Tsukuba, Japan. [2]Institute of Physics, Czech Academy of Science, Prague, Czech Republic. [3]RIKEN, Sayo, Hyogo, Japan. [4]Kyushu University, Fukuoka, Japan. [5]Niigata University, Niigata, Japan

Cubic Laves-phase compounds RCo_2 (R = rare earth) have been widely interested because of their interesting physical properties such as itinerant electron metamagnetism etc. [1,2]. Here we report distinct magnetic properties of $YbCo_2$ [3]. The magnetic susceptibility shows that both the Yb and Co contribute to the Curie-Weiss paramagnetic moment. While no evidence of magnetic ordering has been detected down to 0.4 K, the specific heat divided by temperature, C/T, drastically increases below 2 K, reaching a very large value of C/T = 7 J/K^2 Yb-mol at T = 0.4 K. Electrical resistivity shows a non-Fermi liquid behavior at low temperature. Interestingly, a novel ordered phase appears in magnetic fields above H = 1 T. The transition temperature T_t increases with H, reminiscent of a field-induced ferromagnetic transition. Hence, both the magnetic instability of Co-3*d* and the heavy-fermion state of Yb-4*f* electrons are likely to be closely connected in $YbCo_2$. Cases of such strongly correlated *d*+*f* electron systems will be discussed.

[1] E. Gratz and A. S. Markosyan, J. Phys.: Condens. Matter **13**, R385 (2001).
[2] T. Goto et al., Physica B **300**, 167 (2001).
[3] J. Valenta et al., J. Phys.: Condens. Matter **35**, 285601 (2023).

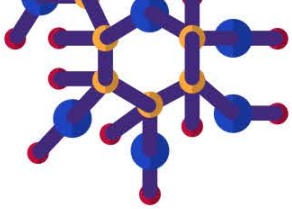

o07

Electric dipole frustration in the ferromagnet $EuAl_{12}O_{19}$

Gaël Bastien[1], Dalibor Repček[2,3], Adam Eliáš[1], Andrej Kancko[1], Maxim Savinov[2], Viktor Bovtun[2], Martin Kempa[2], Michal Vališka[1], Marie Kratochvílová[1], Petr Doležal[1], Sarah Barnett[4], Quentin Courtade[1], Tetiana Haidamak[1], Petr Proschek[1], Stanislav Kamba[2], Christelle Kadlec[2], Petr Kužel[2], Ross Colman[1]

[1]Charles University, Faculty of Mathematics and Physics, Department of Condensed Matter Physics, Prague, Czech Republic. [2]Institute of Physics, Czech Academy of Sciences, Prague, Czech Republic. [3]Czech Technical University in Prague, Faculty of Nuclear Sciences and Physical Engineering, Department of Solid State Engineering, Prague, Czech Republic. [4]Diamond Light Source, Didcot, United Kingdom

$EuAl_{12}O_{19}$ is quasi-two-dimensional ferromagnet with T_C = 1.3 K and large spins S = 7/2. In addition to the magnetic lattice, $EuAl_{12}O_{19}$ harbors a triangular lattice of uniaxial electric dipoles formed by bipyramid AlO_5. At T_S = 49 K $EuAl_{12}O_{19}$ undergoes a phase transition accompanied by a strong increase of the electrical permittivity. However low temperature single crystal diffraction experiments performed with synchrotron source rule and measurement of second harmonic generation rule out any long-range ordering of the electric dipoles hosted by the bipyramid AlO_5. In addition, THz spectroscopy and electrical permittivity measurements reveal a slowing down of the dynamics of the electric dipoles upon cooling following to an Arrhenius law. Based on these results, we propose that the lattice of electric dipoles in $EuAl_{12}O_{19}$ is a geometrically frustrated system, analogous to the Ising triangular lattice antiferromagnet.

o08

Gapless quantum spin liquid in triangular antiferromagnet hexa-aluminate $PrMgAl_{11}O_{19}$

Sonu Kumar[1,2], Milan Klicpera[1], Adam Elias[1], Marie Kratochvílová[1], Ross Colman[1], Anar Rzayev[2], Malgorzata Sliwinska-Bartkowiak[2], Gael Bastien[1]

[1]Department of Condensed Matter Physics, Charles University, Prague, Prague, Czech Republic. [2]Faculty of Physics, Adam Mickiewicz University, Poznan, Wielkopolska, Poland

Geometric frustration among interacting spins combined with strong quantum fluctuations can lead to the formation of exotic magnetic states without conventional spin freezing such as quantum spin liquid (QSL). Experimental realization of QSL state is a challenge in condensed matter physics. Recently the realization of a quantum spin liquid has been proposed in the triangular lattice antiferromagnet (TLAF) $PrZnAl_{11}O_{19}$ based on specific heat, neutron scattering, and muon spectroscopy measurements on polycrystalline samples [1]. Here, we report the single crystal growth and study of sister compound, the hexaalumate $PrMgAl_{11}O_{19}$. Based on specific heat and magnetization measurements, we demonstrate the absence of magnetic order down to 0.4 K, despite strong antiferromagnetic correlations indicated by the relatively large negative Curie-Weiss temperature. Magnetization measurements further revealed a strong magnetic anisotropy implying a proximity the to Ising limit, which could explain the arise of the QSL state. Quantitative analysis of the magnetic entropy determined using nonmagnetic analog $LaMgAl_{11}O_{19}$ confirms the formation of effective spin S=1/2. Moreover, the specific heat follows a power-law dependence at low temperatures, further indicating experimental realization of a gapless QSL ground state in the TLAF hexa-aluminate, $PrMgAl_{11}O_{19}$.

[1] H. Bu, *Phys. Rev. B* **106**, 134428, (2022)

o09

Out-of-equilibrium monopole dynamics in classical spin ices using the fluctuation-dissipation theorem

Félix Morineau[1], Kazuyuki Mastuhira[2], Carley Paulsen[1], Elsa Lhotel[1]

[1]CNRS, Grenoble, France. [2]Kyushu Institute of Technology, Kitakyushu, Japan

Amongst the exotic magnetic states which emerge from frustrated spin systems, spin ices have aroused a strong interest [1]. This is due to the excitations being described as magnetic charges, called magnetic monopoles, which govern the dynamics described by the strongly diverging relaxation times at very low temperatures. Understanding the monopole dynamics in spin ices is a central challenge of frustrated magnetism, and the low temperature out-of-equilibrium properties remain poorly understood due to the difficulty of experimental and theoretical investigations. Recently, we developed a new experimental setup, which allow us to access these properties with the simultaneous measurement of the AC susceptibility and noise spectra and thus directly probe the fluctuation dissipation theorem.

Here we experimentally address the physics in both the equilibrium and out-of-equilibrium regimes of two classical spin ice compounds: $Dy_2Ti_2O_7$ and $Ho_2Ti_2O_7$. We show that in both systems the fluctuation-dissipation relation is obeyed down to approximately 450 mK, despite the out-of-equilibrium regime being reported below about 600 mK from magnetisation measurements [2]. Below 500 mK, the $Ho_2Ti_2O_7$ dynamics can be described by the fluctuation-dissipation relation by considering an effective temperature instead of the sample temperature, in the same way as in spin glass compounds [3]. By renormalising, we can quantitatively understand the monopole dynamics in this strongly diverging regime and relate the dynamics to the out-of-equilibrium state.

[1] Harris et al., *Phys. Rev. Lett.*, **79**, 2554 (1997)
[2] Snyder et al., *Phys. Rev. B.*, ***69,*** 064414 (2004)
[3] D. Hérisson and M. Ocio, *Phys. Rev. Lett*., **88**, 257202 (2002)

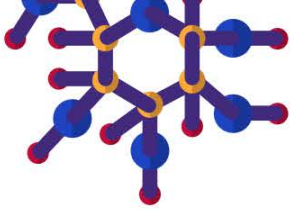

o10

Possible to control metastable charge-ordered states in δ-$Ag_{2/3}V_2O_5$

Masahiko Isobe[1], Taisei Kubo[2], Naoyuki Katayama[2], Robert E. Dinnebier[1]

[1]Max Planck Institute for Solid State Research, Stuttgart, Germany. [2]Department of Applied Physics, Nagoya University, Nagoya, Japan

Vanadium bronzes are essentially mixed valence oxides where metallic conductivity and novel phenomena with spin, charge and orbital degrees of freedom are exhibited. They have therefore attracted much interest as a playground for various quantum phenomena. Recently, we have studied the δ-phase of silver vanadium bronze, δ-$Ag_{2/3}V_2O_5$, focusing on the phase transition, where it exhibits characteristic super-cooling effects. The structure consists of double trellis layer formed by edge/corner-shared VO_6 octahedra and Ag ions occupied between the layers. We have observed the phase transition at around 220 K, accompanied by jumps in magnetic susceptibility and resistivity. Structural analysis of the low-temperature triclinic phase reveals that Ag ion ordering and vanadium dimer formation. Below the transition temperature the magnetic susceptibility shows a broad maximum around 110 K followed by spin gap behavior. We conclude that the phase transition in δ-$Ag_{2/3}V_2O_5$ is a charge ordering into V^{4+} and V^{5+} induced by Ag ion ordering. The V^{4+} ions form dimers with the spin-gapped ground state. We also found that it shows characteristic super-cooling effects. Interestingly, this is similar to the charge glass behavior reported for the organic compounds. In addition, we have recently observed the metastable ordered states induced by low temperature annealing.

o11

Effects of antiferromagnetic domain walls in single crystal Lu2Ir2O7

Daniel Staško[1], Kristina Vlášková[1], Filip Hájek[1], Jiří Kaštil[2], Milan Klicpera[1]

[1]Charles university, Prague, Czech Republic. [2]Institute of Physics of the Czech Academy of Sciences, Prague, Czech Republic

Rare-earth $A_2Ir_2O_7$ oxides have attracted considerable attention of the condensed-matter scientific community for frequently exhibiting complex magnetic and conductive properties. Crystalizing in the ordered pyrochlore structure throughout the whole rare-earth series, the innate geometrical frustration together with strong spin-orbit coupling, Coulomb repulsion and magnetic exchange interactions can result in frequently exotic states such as Weyl semimetal [1], spin ice [2], spin-liquid [3], or fragmented state [4].

The current study focuses on the $Lu_2Ir_2O_7$ member which has a non-magnetic rare-earth ion Lu and therefore all magnetic properties are connected to the Ir magnetic ions. All-in-all-out magnetic ordering of Ir ions is accompanied by the creation of antiferromagnetic domain walls and interfaces. We present the results of our magnetization measurements of $Lu_2Ir_2O_7$ single crystal; most importantly, magnetic anisotropy and thermal-magnetic field hysteresis of magnetic properties reflecting the domain structure of the material.

[1] X. Liu et al., Phys. Rev. Lett. **127**, 277204 (2021).
[2] E. Lefrançois et al., Nat. Commun. **8**, 209 (2017).
[3] M. Kavai et al., Nat. Commun. **12**, 1377 (2021).
[4] V. Cathelin et al., Phys. Rev. Research **2**, 032073(R) (2020).

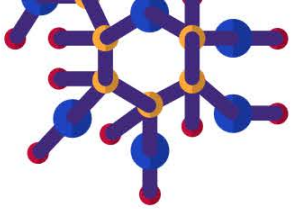

pl02

PLENARY: Effect of the synthesis route on the microstructure and hydrogen storage of $Hf_xTi_{(1-x)}NbVZr$ refractory high-entropy alloys

Maria Moussa[1,2], Stéphane Gorsse[2], Jacques Huot[1], Jean Louis Bobet[2]

[1]UQTR, Trois-Rivieres, Quebec, Canada. [2]Université de Bordeaux, Bordeaux, France

In this talk, we will present the effects of (i) Ti replacement by Hf and (ii) the synthesis method on the microstructure and crystal structure evolution in the high-entropy alloy $Hf_xTi_{(1-x)}NbVZr$. The hydrogen storage properties will also be show. The results of scanning electron microscopy and X-ray diffraction analysis of alloys prepared by both arc-melting and induction-melting are compared with theoretical thermodynamic calculations using the CALPHAD approach. The non-equilibrium thermodynamic calculations agree well with the experimental observations for the arc-melted alloys: a mixture of body-centered cubic (BCC) and cubic C15 Laves phases occurs for low-Ti-concentration alloys and a single BCC phase is obtained for high-Ti alloys. The agreement is not as good when using the induction-melting ethod: equilibrium solidification calculations predict that the most stable state is a phase mixture of BCC, hexagonal close-packed, and a cubic C15 Laves phase, while experimentally only one BCC and one hexagonal C14 Laves phase were found. The estimation of the exact cooling rate and the lack of a thermodynamic database can explain the difference. In addition, for both methods, the thermodynamic calculation confirms that for a high Ti concentration, the BCC phase is stable, whereas phase separation is enhanced with a higher Hf concentration.

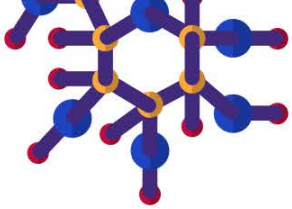

pl03

PLENARY: Actinide science at high magnetic fields: piezomagnetism in uranium dioxide

Krzysztof Gofryk[1], Marcelo Jaime[2], Daniel Antonio[1], Rico Schönemann[3], Zahir Islam[4], Andres Saul[5], Myron Salamon[6]

[1]Idaho National Laboratory, Idaho Falls, Idaho Falls, USA. [2]Physikalisch-Technische Bundesanstalt, Braunschweig, Germany. [3]Los Alamos National Laboratory, Los Alamos, USA. [4]Advanced Photon Source, Argonne, USA. [5]Aix-Marseille University, Marseille, France. [6]National High Magnetic Field Laboratory, Los Alamos, USA

The spin-lattice coupling in uranium dioxide remains an unsolved puzzle resulting from the lack of a thorough understanding of the strong coupling between 5*f*-electron magnetism and lattice vibrations. Besides being the main nuclear fuel material, UO_2 is a Mott-Hubbard insulator with well-localized 5*f*-electrons (U^{4+} electronic configuration) and its magnetic state is characterized by a non-collinear antiferromagnetic structure of 3***k*** type and multidomain Jahn-Teller distortions. In the magnetic state, a UO_2 single crystal subjected to strong magnetic fields exhibits the abrupt appearance of positive linear magnetostriction leading to a trigonal distortion and piezomagnetism. This is the first example of piezomagnetism in the *f*-electron spin system. The unusually strong correlations between the magnetic moments in U-atoms and lattice distortions are a direct consequence of the non-collinear symmetry of the magnetic state that breaks time-reversal symmetry in a non-trivial way. The microscopic nature of these interactions, however, remains unclear. During the talk, we will demonstrate how detailed thermodynamic and structural measurements, performed in high and ultra-high magnetic fields, can be used to study these interactions and their couplings. We will discuss the implications of these results in the context of the origin of the piezomagnetic ground state in this material.

o12

Unusual magnetotransport in half-Heusler topological materials

Orest Pavlosiuk, Piotr Wiśniewski, Dariusz Kaczorowski

Institute of Low Temperature and Structure Research, Polish Academy of Sciences, Wrocław, Poland

Topological materials exhibit non-trivial electronic structures that result in their exceptional magnetotransport properties [1]. Half-Heusler family of materials was one of the first groups of topological materials identified over a decade ago [2], but it continues to be of significant interest.

This work presents a review of our recent magnetotransport investigations carried out on high-quality single crystals of half-Heusler compounds with chemical compositions *RE*PtBi and *RE*PdBi (where *RE* = Sm, Gd, Dy, Ho, Tb and Sc). Transverse magnetoresistance of these compounds is large, does not show saturation in high magnetic fields, and is positive for *RE*PtBi and negative for *RE*PdBi. Their longitudinal magnetoresistance (LMR) is negative or at least demonstrates a pronounced negative contribution to the total LMR, which is a hallmark of chiral magnetic anomaly typical for topological semimetals. Hall effect analysis reveals multiple-band conductivity in all studied compounds and discloses anomalous Hall effect in all compounds containing magnetic rare-earth element. The findings of our research support the topologically non-trivial nature of the electronic structure in the half-Heusler compounds investigated.

*This work was supported by the National Science Centre (Poland), grant no. 2021/40/Q/ST5/00066.

[1] B. Q. Lv et al., *Rev. Mod. Phys*. **93**, 025002 (2021).
[2] H. Lin et al., *Nat. Mat*. **9**, 546 (2010).

o13

Comparison of complex magnetic structures in $RE_5T_2In_4$ (RE = rare earth element; T = Ni, Pd, Pt) compounds

Stanisław Baran

Jagiellonian University, Faculty of Physics, Astronomy and Applied Computer Science, M. Smoluchowski Institute of Physics, Kraków, Poland

The $RE_5T_2In_4$ (RE = rare earth element; T = Ni, Pd, Pt) intermetallics crystallize in the $Lu_5Ni_2In_4$-type orthorhombic crystal structure (*Pbam* space group, No. 55). The rare earth atoms occupy three nonequivalent Wyckoff sites, namely, the 2a site as well as 4g1 and 4g2 sites with different atomic positional parameters. The recent reports show that the complex crystal structure leads to complex magnetic properties manifesting themselves in a number of temperature-induced magnetic transitions. The neutron diffraction experiments reveal presence of complex magnetic structures in $RE_5T_2In_4$ – the structures have both the ferro- and antiferromagnetic components, magnetic moments at different Wyckoff sites have different magnitudes and point at different directions, both commensurate and incommensurate components of the magnetic structures are detected, etc. The magnetic moments are localized solely on the rare earth atoms. It has been found that magnetic moments at the 2a and 4g2 sites order at higher temperatures that the moments at the 4g1 site. In this study, magnetic structures in $RE_5T_2In_4$ (RE = rare earth element; T = Ni, Pd, Pt) are summarized and compared in order to understand how they are affected by chemical composition.

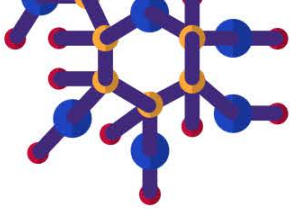

o14

Physical properties studies of the multiple CDW phase transitions in quasi-1D *R*NiC_2 compounds (*R* = rare earth metal)

Marta Roman[1,2], Berthold Stoeger[1], Simone Di Cataldo[3], Kamil Kolincio[2], Herwig Michor[1]

[1]TU Wien, Vienna, Austria. [2]Gdansk University of Technology, Gdansk, Poland. [3]Sapienza University of Rome, Rome, Italy

Ternary rare-earth nickel dicarbides *R*NiC_2 crystallize in the orthorhombic crystal structure with broken inversion symmetry. Since decades, these compounds attract much attention due to the presence of large variety of ground states, such as: unconventional superconductivity, magnetism, multiple charge density waves (CDWs), as well as complex interplay between CDW and rare-earth magnetism, and then finally, recently reported topological features of their quasi-1D electronic structure.

In this presentation we will discuss multiple CDW phase transitions observed in *R*NiC_2 (*R* = Pr - Lu, Y) compounds with the ordering temperature scaling linearly with the unit-cell volume. We will focus on the difference between two competing types of CDW order adapted in the *R*NiC_2 family: the incommensurate q_1-CDW preferred by the early lanthanide-based *R*NiC_2 (*R* = Pr - Sm) and the commensurate q_2-CDW state formed in the late lanthanide-based *R*NiC_2 (*R* = Ho - Lu). We will also refer to the CDWs interplay with the magnetic order as well as topology of the electronic structure. We will present crystallographic characteristics explored via single-crystal XRD, as well as electronic, thermoelectric, thermodynamic and magnetic properties studied by a variety of techniques revealing anisotropic features of selected *R*NiC_2 single crystals.

Acknowledgement: Financial support for M.R. by grant BPN/BEK/2021/1/00245/DEC/1 of The Polish National Agency for Academic Exchange (NAWA) is gratefully acknowledged.

o15

Bulk physical properties and enantiomorph-resolved electrical transport of chiral narrow-band semiconductors *R*RhC$_2$ (*R* = La, Ce)

Volodymyr Levytskyi[1], Ulrich Burkhardt[2], Markus König[2], Eteri Svanidze[2], Yuri Grin[2], Roman Gumeniuk[1]

[1]*Institut für Experimentelle Physik, TU Bergakademie Freiberg, 09599 Freiberg, Germany.* [2]*Max-Planck-Institut für Chemische Physik fester Stoffe, 01187 Dresden, Germany*

*R*RhC$_2$ (*R* = La, Ce) compounds are the only representatives with a chiral crystal structure (space groups $P4_1/P4_3$) among the rare-earth transition-element dicarbides [1-3]. Our studies indicated LaRhC$_2$ and CeRhC$_2$ to form incongruently at 1670 and 1600 (±25)K, respectively. Detailed electron backscatter diffraction (EBSD) analyses on polycrystalline materials prepared by arc-melting followed by annealing at 1520 K revealed different enantiomorphs to exist within individual grains. Using EBSD-based enantiomorph distribution maps [4, 5], micro-structured devices with well-defined handedness and orientation of the 4-fold screw axis were prepared using the focused ion beam technique. The magnetization, heat capacity, electrical resistivity, thermal conductivity, and thermopower were studied on polycrystalline materials, as well as the electrical transport on oriented microdevices. For the latter, electrical resistivity and the Hall effect were examined parallel and perpendicular to the 4_1 and 4_3-axis, respectively. The estimated energy gaps are up to 30 meV. The anisotropic and enentiomorph-dependent properties of LaRhC$_2$ and CeRhC$_2$ are discussed in detail.

[1] Babizhetskyy V. *et al*. In: *Handbook on the Phys. and Chem. of Rare Earths*, **52**, Elsevier, 2017, 1-263.
[2] Tsokol A.O. *et al*., *Sov. Phys. Crystallogr.* **31** (1986) 39.
[3] Hoffmann R.-D. *et al*., *Chem. Mater*. **1** (1989) 580.
[4] Burkhardt U. *et al*., *Sci. Rep*. **10** (2020) 4065.
[5] Carillo-Cabrera W. *et al*., *Commun. Mater*. **4** (2023) 109.

o16

Uranium nuclear safeguards: Automated Fission Track Analysis via Synthetic Model Generation and Image Analysis Tools

Itzhak Halevy[1], Rami Babayew[2,1], Yaacov Yehuda-Zada[2,1], Noam Elgad[2,1], Shay Dadon[2], Jan Lorincik[3], Itzhak Orion[1], Aryeh Weiss[4], Galit Katarivas Levy[1]

[1]Ben Gurion Uni, Beer Sheva, Israel. [2]Nuclear Research Centre Negev, Beer Sheva, Israel. [3]Research Centre Řež, Husinec, Czech Republic. [4]Bar Ilan Uni., Ramat Gan, Israel

The Fission Track Analysis method is a cornerstone in nuclear and safeguard investigations. This presentation unveils a pioneering approach that focuses on the automation of FTA through advanced image processing algorithms applied to microscope images. As a critical prelude to our research and development endeavors, our research group has successfully developed an application capable of generating synthetic models of fission tracks, namely uranium tracks.

Leveraging trajectory data from the fission products trajectory database, created through GEANT4 simulations, we generate synthetic models of fission tracks. This synthetic bank of images closely resembles light microscope images, providing a controlled dataset for R&D processes for developing robust image analysis tools. These tools aim to automate the identification of fission track clusters without human intervention, representing a significant leap toward the elimination of manual methods.

The preliminary software for image processing demonstrates its efficacy in detecting fission track clusters. The software calculates the number of tracks, enhancing the efficiency of data interpretation. The automation of Fission Track Analysis not only streamlines the identification process but also serves as a proactive measure to reduce the likelihood of human errors inherent in manual procedures. This is paramount for enhancing the accuracy and reliability of nuclear investigations. For further development we are using AI as well.

o17

Impact of rare earth element integration on glass forming ability and thermal stability of Zr-based bulk metallic glasse

Juhi Rani Verma, Yogesh Prabhu, Jatin Bhatt

Visvesvaraya National Institute of Technology, Nagpur, Maharashtra, India

The present study examines the effect of minor alloying on Zr-based bulk metallic glasses (BMGs).The investigation of minor alloying has been motivated by the search for novel materials with improved properties. The thermal stability and glass forming ability (GFA) has been evaluated by addition 1 at. % Dy to the Zr-Cu-Al-Ag glass forming system. Schematically, we discussed the role of Dy addition in Zr-based alloys. This study examines the influence of Dy in the Zr-Cu-Al-Ag system by taking various factors into consideration such as positive heat of mixing between Dy and Zr, high oxygen affinity of Dy and larger covalent diameter of Dy. These factors favour easy synthesis of glassy alloys, influencing the atomic environment during cooling, inducing distortion in the local atomic environment, and enhancing atomic packing density, structural stability, and GFA. Minor alloying considerably influences the glass-forming ability and thermal stability of Zr-based BMGs. The introduction of rare earth metals presents exciting potential for tailoring materials with enhanced material properties. This study contributes to improving minor alloying knowledge and application in developing high-performance materials for upcoming applications.

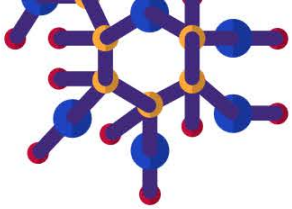

o18

Fabrication of porous aluminum alloys for hydrogen production

Laurent Cuzacq[1], Chloé Polido[1], Jean-François Silvain[1,2], Jean-Louis Bobet[1]

[1]Univ. Bordeaux, CNRS, Bordeaux INP, ICMCB, UMR 5026, Pessac, France. [2]Department of Electrical and Computer Engineering, University of Nebraska, Lincoln, Nebraska, USA

Aluminum (Al) is used for its physical properties (density, thermal and electrical conductivity) and Al alloys for its mechanical properties in numerous domains of industry like electronic or automobile. Moreover, it is one of the more common and cheapest metal. Recently, the utilization of Al and Al alloys to produce hydrogen is emerging. Porous materials exhibit very interesting properties for the hydrogen production. Indeed, their large specific surface tend to increase contacts with the reactive medium leading to homogeneous hydrolysis. Uniaxial hot-pressing technique was used for the fabrication of porous Al-Mg materials. Parameters were optimized in order to control the porosity volume fraction (ranging from 0 to 50) and the crystallographic structure of the materials. Correlations between the porosity volume fraction, the crystallographic structure of the materials and the hydrogen production were established.

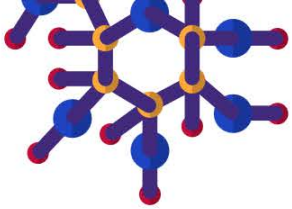

o19

Scalability of the magnesiothermic synthesis of skutterudites and their protective coatings against oxidation

Arige Hodroj[1], Ilyes Talbi[1], Valerie Bouquet[1], Sophie Ollivier[1], Ronan Lebullenger[1], Valerie Demange[1], Carmelo Prestipino[2], Ruchi Bhardwaj[3], Eric Alleno[3], Mathieu Pasturel[1]

[1]ISCR, Rennes, France. [2]CRISMAT, Caen, France. [3]ICMPE, Thiais, France

Skutterudites, particularly those derived from $CoSb_3$, are promising for mid-temperature thermoelectric applications due to unique properties like dual doping capability, high electron/hole mobility, and large Seebeck coefficient [1]. However, their practical use is hindered by complex synthesis and susceptibility to oxidation. Our research presents the magnesioreduction method as a novel synthesis approach, offering advantages such as lower temperatures, shorter reaction times, and scalability [2,3].

I will present the scale up results (up to 20g) for both n-type ($In_{0.22}Co_4Sb_{12}$) and p-type ($Ce_{0.8}Fe_{3.5}Co_{0.5}Sb_{12}$) skutterudites.

Additionally, protective layers against oxidation, sourced from both commercially available options and laboratory-prepared alternatives, are incorporated via dip coating. Preliminary results of aging tests at 750 and 800 K in air for both n- and p-type skutterudites will be shown and compared to the state-of-the-art.

[1] Rogl, G., and P. Rogl. "Skutterudites, a most promising group of thermoelectric materials." *Current opinion in green and sustainable chemistry* ***4*** (2017): 50-57.
[2] Le Tonquesse, Sylvain, et al. "Innovative synthesis of mesostructured $CoSb_3$-based skutterudites by magnesioreduction." *Journal of Alloys and Compounds* **796** (2019): 176-184.
[3]Le Tonquesse, Sylvain, et al. "Reaction mechanism and thermoelectric properties of $In_{0.22}Co_4Sb_{12}$ prepared by magnesiothermy." *Materials Today Chemistry* **16** (2020): 100223.

o20

MAX phase / MXENE / metal nanomaterials for energy conversion application

Sergii Sergiienko

University of Chemistry and Technology, Prague, Czech Republic

The emergence of new multifunctional materials continuously increases the expectations for the performance of energy conversion and storage devices. MXenes, a family of two-dimensional transition metal carbides has been discovered as candidate for these applications [1], [2]. This work explores the possibilities for the processing of Ni, MAX phase and MXene- containing composite electrodes for energy conversion and storage application. Synthesis of powder mixtures with extra Ni and Al content (e.g. Ni:Mo:Ti:Al:C = 1:2:1:7:2) resulted in products containing modified molybdenum- and titanium-based MAX phase material and metal-Al alloys [2]. It was found that the presence of Ni and Al excess in the reaction mixture promotes the formation process of conventional (Mo_2TiAlC_2) and modified (probably $Mo_2TiAl_2C_2$) MAX phases due to generating Al-rich metal-Al alloys with a lower melting point. Further etching of these products in 10M NaOH allowed the direct formation of electrodes with active surface containing MAX phase, MXene and nanoporous metal composites [2, 3] with a well-developed 3D porous MAX phase-based structure acting as a support for electrocatalytic species, including MXene, and nano-metal possessing good mechanical integrity [2].

[1] Y. Gogotsi *et al.,* ACS nano. **13,** 8491–8494 (2019).
[2] S. A. Sergiienko *et al., RSC advances* **14(5)**, 3052–3069 (2024).
[3] S. A. Sergiienko *et al., Int. J. of Hydrogen Energy* **46(21)**, 11636–11651 (2021).

pl04

PLENARY: Targeted catalyst development: An innovative playground for intermetallic compounds

Marc Armbrüster

Chemnitz University of Technology, Chemnitz, Germany

Catalysis is massively contributing to modern life – giving access to countless chemicals needed for food (fertilizer), transportation (fuel) and medicine (pharmaceuticals). The overwhelming part of industrial catalysis is based upon heterogeneous catalysis.

Unsupported intermetallic compounds are a versatile class of materials for catalysis as they provide crystal structures which are not realized by elements.[1] This results in new electronic scaffolds with altered adsorption properties, which in turn, are responsible for the catalytic properties. These, as well as the geometric properties, can be finely tuned within an intermetallic compound by isostructural substitution. Together with investigating the stability under reaction conditions this allows retrieving reliable structure-property relations in (electro)catalysis and creating materials which are outperforming known systems.

Application of such a development is outlined on two examples – the semi-hydrogenation of acetylene[2] and methanol steam reforming[3], and has also been applied successfully to electrocatalysis[4].

[1] M. Armbrüster *Sci. Technol. Adv. Mater.* 2020, **21**, 303.
[2] R. Zerdoumi, O. Matselko, L. Rößner, B. Sarkar, Y. Grin, M. Armbrüster *J. Amer. Chem. Soc.* 2022, **144**, 8379.
[3] N. Köwitsch, L. Thoni, B. Klemmed, A. Benad, P. Paciok, M. Heggen, I. Köwitsch, M. Mehring, A. Eychmüller, M. Armbrüster *ACS Catal.* 2021, **11**, 304.
[4] R. Zerdoumi, L. Rößner, M. Armbrüster *J. Electrochem. Soc.* 2019, **166**, F1079.

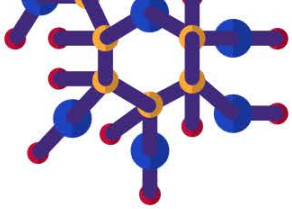

pl05

PLENARY: High energy resolution X-ray spectroscopy for Material Science

Kristina Kvashnina

The Rossendorf Beamline at ESRF – The European Synchrotron, Grenoble, France. Helmholtz-Zentrum Dresden-Rossendorf (HZDR), Institute of Resource Ecology, Dresden, Germany

Gaining insights into the properties and behaviour of materials at the atomic and molecular level is crucial for advancing materials science and fostering innovation in new technologies. Understanding the role of electrons in driving chemical reactions has long been a focal point of research. One of the most direct methods for probing the chemical and electronic structure of materials is done by X-ray absorption spectroscopy (XAS) or X-ray absorption near-edge structure (XANES) in high energy resolution fluorescence detection (HERFD) mode. The use of hard and tender X-rays offers distinct advantages, including their high penetration depth, which facilitates in-situ reaction studies in real-time and allows for the investigation of material production or performance under specific conditions. Such experiments are non-destructive and performed at the large-scale synchrotron facilities. This contribution will provide an overview of the recently performed HERFD-XANES studies on cerium [1,2], uranium [3], thorium [4,5] and plutonium [6,7] contained materials at the Rossendorf Beamline (ROBL) of the European Synchrotron (ESRF) in Grenoble (France). I will show that the experimental data, analysed by electronic structure calculations can provide detailed information about the electronic states and bonding characteristics of atoms within materials, helping researchers to elucidate the relationship between chemical composition, atomic structure, and material properties.

[1] Estevenon, P. *et al. Chem. Mater.* **35**, 1723–1734 (2023).
[2] Plakhova, T. V. *et al. Nanoscale* **11**, 18142–18149 (2019).
[3] Gerber, E. *et al. Inorg. Chem. Front.* **8**, 1102–1110 (2021).
[4] Amidani, L. *et al. Phys. Chem. Chem. Phys.* **21**, 10635–10643 (2019).
[5] Amidani, L. *et al. Chem. – A Eur. J.* **27**, 252–263 (2021).
[6] Kvashnina, K. O. *et al. Angew. Chemie Int. Ed.* **58**, 17558–17562 (2019).
[7] Gerber, E. *et al. Nanoscale* **12**, 18039–18048 (2020).

o21

Unraveling the Actinides 5f Enigma with X-Ray Emission Spectroscopy

JG Tobin

University of Wisconsin Oshkosh, Oshkosh, WI, US

The advent of new, powerful, highly efficient, multi-component, X-ray monochromators used in the detection of tender x-rays has revolutionized spectroscopic investigations of the 5f electronic structure. All of the new experiments are, in essence, variants of X-ray Emission Spectroscopy (XES), where the improved monochromatized detection plays a key role. In HERFD (High Energy Resolution Fluorescence Detection), the monochromatized XES detection allows the performance of a scattering experiment that devolves into a higher resolution version of X-Ray Absorption Spectroscopy (XAS). It has been shown that the M_4 and M_5 spectra are essentially direct measurements of the j-specific ($5f_{5/2}$ and $5f_{7/2}$) Unoccupied Density of States (UDOS), which can be directly correlated with the UDOS from Inverse Photoelectron Spectroscopy (IPES) and Bremsstrahlung Isochromat Spectroscopy (BIS). [1,2] Similarly, Resonant XES has been demonstrated to be Raman in nature, with a 5f-5f transition, not a simple charge transfer transition (ligand 2p to actinide 5f). [3] Finally, the 5f delocalization in U metal has been quantified with the combined 6p & 5f $M_{4,5}$ non-resonant XES, which exhibits strong angular momentum coupling effects. [4]

[1] J. G. Tobin et al. *Phys. Rev. B* (2022).
[2] J. G. Tobin et al., *J. Electron Spectr. Rel. Phen.* (2019).
[3] J.G. Tobin et al., *J. Phys. Cond. Matter* (2022).
[4] J.G. Tobin et al., *MRS Bulletin Impact Article* (2022)

o22

Fundamentals of the Uranium Halides

Clara L. Silva[1,2], Lucia Amidani[1,2], Marius Retegan[3], Elena F. Bazarkina[1,2], Stephan Weiss[2], Tim Graubner[4], Florian Kraus[4], Kristina Kvashnina[1,2]

[1]The Rossendorf Beamline of ESRF, Grenoble, France. [2]HZDR, Dresden, Germany. [3]ESRF, Grenoble, France. [4]Philipps University of Marburg, Malburg, Germany

Probing actinide chemistry is exceptionally challenging due to the radioactivity of actinide elements and their extremely rich chemistry. In the quest for a deeper understanding, assessing the actinide's valence state and the role of 5f electrons in the actinide bond are of primary importance. These physico-chemical properties can only be elucidated by a few spectroscopic and computational methods [1-2]. However, efforts to understand 5f electron systems have been hampered by the lack of high quality experimental data on the actinide compounds to be studied. We report here the first measurements of X-ray near-edge structure (XANES) in the high-energy resolution fluorescence detected (HERFD) mode at the uranium (U) M_4 edge for the U(III) and U(IV) halides, namely UX_3 and UX_4 (X=F, Cl, Br, I). The spectral shapes of these two halide families show clear differences, which can be comprehended within the framework of crystal field multiplet theory [3-4]. Electronic structure calculations were conducted for the 3d-4f Resonant Inelastic X-ray Scattering (RIXS) process, considering various strengths of electron-electron interactions between 3d, 4f, and 5f states. Our results confirm the capability of the HERFD-XANES method at the M_4 edges to detect the presence of low-valent compounds. Moreover, contrary to earlier expectations of increased ionicity in low-valent uranium compounds, our study reveals that the electronic structure of low-valent U systems exhibits heightened sensitivity to the influence of ligands surrounding the U atoms.

[1] Kvashnina, K. O., and S. M. Butorin. *Chemical Communications* **58**, 327 (2022).
[2] Leinders, G., Bes, R., Pakarinen, J., Kvashnina, K. & Verwerft, M. Evolution of the Uranium Chemical State in Mixed-Valence Oxides. *Inorg. Chem.* **56**, 6784–6787 (2017).
[3] Butorin, S. M. *Journal of Chemical Physics* **155**, 164103 (2021).
[4] Amidani, L. et al., *Inorg. Chem.* **60**, 16286 (2021).

o23

On valence-band photoemission from actinides

Jindřich Kolorenč

Institute of Physics (FZU), Czech Academy of Sciences, Prague, Czech Republic

The 4f states in lanthanides typically do not participate in chemical bonding and keep their atomic character even when built into a crystal lattice, as evidenced by atomic multiplets appearing in their photoemission spectra [1]. The 5f states in early actinides, on the other hand, have a tendency to form delocalized bands. Still, the spectra of some of their compounds (like PuSe or UH_3) display features not compatible with bands but resembling atomic multiplets instead [2-4]. In the same time, a $5f^6$ state analogous to lanthanides is expected in americium, yet, the Am photoemission cannot be fully understood in terms of the corresponding multiplets [5].

We show that the photoemission spectra of UH_3 and Am can be satisfactorily reproduced by the LDA+DMFT method. Furthermore, we analyze how the eigenstates of the DMFT impurity model evolve when the hybridization between the 5f shell and the other electronic states is ramped up from zero (ionic model appropriate for lanthanides) to its realistic value [6]. This theoretical experiment enables us to clearly link the observed spectral features to the atomic multiplets as suggested on empirical grounds earlier [3,5].

[1] J. K. Lang *et al.*, J. Phys. F: Met. Phys. **11** (1981) 121.
[2] T. Gouder *et al.*, PRL **84** (2000) 3378.
[3] T. Gouder *et al.*, PRB **70** (2004) 235108.
[4] L. Havela *et al.*, J. Electron Spectrosc. Relat. Phenom. **239** (2020) 146904.
[5] N. Mårtensson *et al.*, PRB **35** (1987) 1437.
[6] O. Koloskova *et al.*, PRB (2024), in print.

o24

Electronic structure of U hydrides probed by XPS and UPS

Oleksandra Koloskova[1], Evgenia Tereshina-Chitrova[2], Mykhaylo Paukov[1], Thomas Gouder[3], Jindřich Kolorenč[2], Ladislav Havela[1]

[1]Faculty of Mathematics and Physics, Charles University, Prague, Czech Republic. [2]Institute of Physics, Czech Academy of Sciences, Prague, Czech Republic. [3]European Commission, Joint Research Centre, Karlsruhe, Germany

Electronic structure is a common denominator of basic properties of actinide systems. U compounds are at the threshold of localization of the 5*f* states. This brings excellent opportunities to observe phenomena related to the onset of localization (as anomalous SC) but the degree of localization is difficult to quantify. U hydrides (α- or β-UH_3, UH_2) are FM with relatively high T_C (exceeding 100 K), and the question is whether they are conventional band magnets, well described by DFT calculations, or the e-e correlations play a more fundamental role. Electron spectroscopies (XPS, UPS, BIS) bring more direct information (taken with some precautions) on electronic states than bulk properties.

We used a combination of thin-film synthesis of U hydrides (provides clean surfaces for high-quality PES studies) with in-situ spectroscopic and ex-situ bulk (XRD, magnetic, transport) studies to reveal reasons for high T_C in UH_3 [1]. In addition, systems with Mo and Zr substitutions, which give elevated T_C values (up to 203 K), or stabilize transient α-UH_3 phase in bulk [2], were studied in film form. The confrontation with results of various computations indicates that DMFT-type of calculations are needed to understand the valence-band spectra, reflecting features of atomic multiplets, with intensity and energy of individual lines affected by hybridization.

[1] L. Havela *et al.*, *J. Electron Spectrosc. Relat. Phenom*. **239** (2020) 146904.
[2] L. Havela *et al.*, J. M. M. M. **400** (2016) 130-136.

o25

Crystal structure and chemical bonding analysis of Be-Ru intermetallic compounds

Laura Agnarelli[1], Yurii Prots[2], Mitja Krnel[2], Eteri Svanidze[2], Markus König[2], Marcus Schmidt[2], Ulrich Burkhardt[2], Andreas Leithe-Jasper[2], Yuri Grin[2]

[1]CRISMAT, Caen, France. [2]Max-Planck-Institut für Chemische Physik fester Stoffe, Dresden, Germany

In order to obtain new intermetallic compounds with potential semiconductor properties, it has been proven that charge transfer from the cationic to the anionic part of the crystal structure plays an important role.[1] In this scenario, the Be–Ru binary system was investigated, resulting in the discovery of two novel phases, Be_7Ru_4 and $Be_{12}Ru_7$. These phases show very close compositions (63.6 at.% Be and 63.2 at.% Be, respectively) and both represent new structural prototypes. Positioned in the phase diagram between Be_3Ru_2 (with a U_3Si_2-type structure) and Be_2Ru (with a Fe_2P-type structure),[2] this may explain why their crystal structures can be described as 2D intergrowths of Fe_2P and U_3Si_2 motifs, as determined through single-crystal X-ray diffraction analysis. The calculated electronic density of states (DOS) reveals that, contrary to typical intermetallic compounds, Be_7Ru_4 and $Be_{12}Ru_7$ exhibit a pronounced minimum in the vicinity of the Fermi level, suggesting their proximity to a semiconducting state. Position-space analysis of chemical bonding exhibits the formation of three- and four-atomic polar bonds involving both Ru and Be atoms, and a strong charge transfer from Be to the more electronegative Ru.

[1] A. Amon *et al. Angew.Chem.Int. Ed*. **2019**, 58, 15928-15933.
[2] L. Agnarelli *et al.* Chem. Eur. J. **2023**, 29, e202300578.

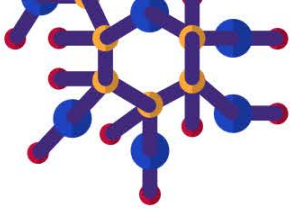

o26

Electronic structure of modified Ti_2MnAl compound.

Wojciech Gumulak, Jerzy Goraus, Jacek Czerniewski, Jerzy Kubacki

A.Chełkowski, Institute of Physic, University of Silesia, 75 Pułku Piechoty, Chorzów, Poland, Poland

In our presentation we show the band structure obtained for modified Ti_2MnAl where Mn was replaced by both iron and chromium, or Al was substituted by indium. In the first scenario, the manganese atom of Ti_2MnAl is replaced by equal amount of chromium and iron, so that the compound remains isoelectronic with base Ti_2MnAl. In the second scenario the equilibrium lattice should be of different volume than in pristine Ti_2MnAl simulating external pressure. It was reported earlier, that Ti_2MnAl might exhibit Spin-Gapless-Semiconductor state, if it would crystallize in the inverted Heusler structure. Most earlier reports show that pristine Ti_2MnAl does not crystallize in that structure, but it was also suggested by earlier papers, that substitued Ti_2MnAl may crystallize in such structure. We wanted to investigate that problem in details. We present both, the ab-initio calculations obtained within the KKR method, and the XPS spectra. We also deduce the crystal structure from the transition metal p-lines, as we have shown in our earlier papers that this is a quite appropriate approach.

o27

Tuning the Weyl-Kondo Semimetal $Ce_3Bi_4Pd_3$ via Stoichiometry

Nikolas Reumann, Diana Kirschbaum, Monika Lužnik, Sami Dzsaber, Mathieu Taupin, Gaku Eguchi, Xinlin Yan, Andrey Prokofiev, Silke Paschen

TU Wien, Vienna, Austria

The Weyl-Kondo semimetal Ce3Bi4Pd3 is a recent example of how the interplay of strong correlations and topology may lead to novel phases [1,2]. The combination of Berry curvature singularities at Weyl nodes and the Kondo effect, which may pin these nodes to the Fermi energy, boosts the topological response, in particular in the nonlinear Hall effect [3-5].

In this study a series of $Ce_3Bi_4Pd_3$ single crystals with slightly varying stoichiometry was synthesized and characterized in detail. The trends in terms of lattice parameter and various electrical transport properties will be presented and discussed, with special focus on the nonlinear Hall effect [6].

[1] J. G. Checkelsky et al., *arXiv:***2312.10659**, Nat. Rev. Mater., in press.
[2] S. Paschen and Q. Si, *Nat. Rev. Phys.* **3**, 9–26 (2021).
[3] S. Dzsaber et al., *PNAS* **118**, e2013386118 (2021).
[4] H.-H. Lai et al., *PNAS* **115**, 93 (2018).
[5] D. M. Kirschbaum et al., *J. Phys. Mater.* **7**, 012003 (2024).
[6] N. Reumann et al., *in preparation.*

o28

Superconductivity in the Heusler and a related type intermetallic compounds

Karolina Górnicka[1], Hanna Świątek[1], Sylwia Gutowska[2], Gabriel Kuderowicz[2], Michał Winiarski[1], Kamil Kutorasiński[2], Bartłomiej Wiendlocha[2], Tomasz Klimczuk[1]

[1]Gdansk University of Technology, Gdansk, Poland. [2]`AGH University of Science and Technology, Kraków, Poland

Over 1000 ternary intermetallic compounds are known to form in the Heusler structure, and their richness of physical properties make them one of the most interesting intermetallic families known. Superconductivity has been observed in no more than 50 members of this huge family and in this lecture I will discuss recently synthesized: $MgPd_2Sb$ [1], $LiPd_2Ge$ [2], $LiPd_2Si$ [3], $LiGa_2Rh$ [4] and $LiGa_2Ir$ [5]. $MgPd_2Sb$ is the first Mg-based Heusler-type compound to exhibit superconductivity. The number of valence electrons for $MgPd_2Sb$ (VEC=27) falls exactly at the maximum of the proposed T_c vs. VEC [6]. For $LiPd_2Ge$ and $LiPd_2Si$ the number of valence electrons is 2 lower, and for the other two Li-based superconductors ($LiGa_2Rh$, $LiGa_2Ir$) VEC=16. While the last two materials are type-II superconductors, $LiPd_2Ge$ and $LiPd_2Si$ are rare cases of the intermetallic compounds for which type-I superconductivity is observed.

Extending our search to the arsenic-containing new Heusler-type compounds, we found superconductivity in an unreported ternary arsenide with T_c=5.5 K. Details of the synthesis process as well as physical properties will be discussed.

[1] M.J. Winiarski, et al., *PRB* **103**, 214501 (2021).
[2] K. Górnicka, et al., *PRB* **102**, 024507 (2020).
[3] K. Górnicka, et al., *Chem. Mat*. in print
[4] E. Carnicom, et al., *Sci. Adv.* 2018, 4, eaar7969 (2018).
[5] K. Górnicka, et al., *Sci. Rep.* **11**, 16517 (2021).
[6] T. Klimczuk, et al., *PRB* **85**, 174505 (2012).
[7] H. Świątek, et al., *in prep.*

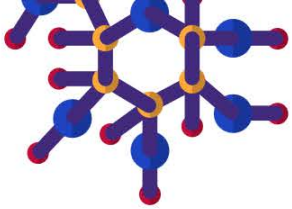

o29

Crystallochemistry, thermodynamic and physical properties of the novel $Cu_{3-x}(As_ySb_{1-y})$ intermetallic compound

Marianne Mödlinger[1], Alessia Provino[1], Pavlo Solokha[1], Serena De Negri[1], Federico Caglieris[1,2], Michele Ceccardi[1], Manish K. Kashyap[3], Cristina Bernini[2], Pietro Manfrinetti[1,2]

[1]University of Genoa, Genoa, Italy. [2]Institute SPIN-CNR, Genoa, Italy. [3]Jawaharlal Nehru University, New Delhi, India

During the investigation of the Cu-As-Sb ternary system, we identified the new ternary intermetallic with stoichiometry $Cu_{3-x}(As_ySb_{1-y})$. Its crystal structure was determined by single crystal and powder X-ray diffraction. While the binary Cu_3As and Cu_3Sb phases crystallize in the hexagonal Cu_3P-type (*hP*24, *P*6$_3$*cm*) and cubic anti-BiF_3-type (*cF*16, *Fm*-3*m*), respectively, $Cu_{3-x}(As_ySb_{1-y})$ adopts the cubic $Cu_{9.1}(TeSb)_3$-type (*cP*32, *Pm*-3*n*), a ternary derivative of the Cr_3Si-type. $Cu_{3-x}(As_ySb_{1-y})$ is the first isotypic representative of this prototype. SEM-EDS analyses reveal a compositional range of 71.1-73.9-at.% Cu, 5.8-24.5 at.% As and 2.1-23.1 at.% Sb for this compound, corresponding to $Cu_{2.84-2.96}As_{0.23-0.98}Sb_{0.23-0.92}$. The lattice parameter increases while increasing the Sb/As compositional ratio from a = 7.479(5) Å (for $Cu_{3-x}As_{0.75}Sb_{0.25}$) to a = 7.652(5) Å (for $Cu_{3-x}As_{0.25}Sb_{0.75}$). $Cu_{3-x}(As_ySb_{1-y})$ forms congruently for Sb-rich compositions and peritectically for As-rich compositions. The melting temperature values decrease as a function of the Sb/As compositional ratio (691°C for $Cu_{72}As_{14}Sb_{14}$, 676°C for $Cu_{72}As_7Sb_{21}$ and 628°C - peritectic - for $Cu_{72}As_{21}Sb_7$). Physical properties (electrical resistivity and magnetic susceptibility) indicate that $Cu_{3-x}(As_ySb_{1-y})$ behaves as a good metal with electrical resistivity decreasing as the Sb/As-concentration increases. DFT calculations have been performed to shed light on the thermodynamic stability along the Sb/As solid solution.

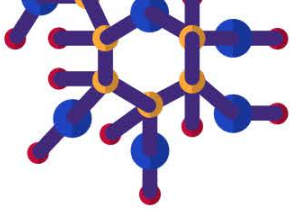

o30

Electronic structure and local magnetic properties of uranium compounds probed with XANES and XMCD.

Fabrice Wilhelm, Andrei Rogalev

ESRF, Grenoble, France

In these last years actinides and actinide compounds, mainly Uranium based compounds, have been the subject of increasing interest due to their very different magnetic and electronic properties, such as Pauli paramagnetism, localized and itinerant magnetism, and superconductivity. The element specific X-ray absorption Near Edge Structure (XANES) and X-ray Magnetic Circular Dichroism (XMCD) spectroscopy techniques have been proven over more than three decades to be the best suitable technique to probe the 5*f* electron occupancy as well as the orbital and spin magnetism offering a possibility to disentangle these contributions using the magneto-optical sum-rules. XANES and XMCD experiments have been reported for a great number of uranium compounds and have permitted to determine the 5*f* ground state. It has also revealed differences between localized and itinerant systems that is still a matter of controversy. This talk reviews recent advances in use of polarized X-rays to study local magnetic properties and electronic structure of various uranium based compounds, like UGe_2 and UTe_2, and their changes with pressure.

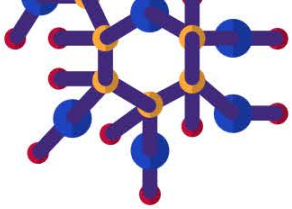

o31

Complex magnetic behaviours in $U_6T_4Al_{43}$ (T = V, Nb, Ta, Cr, Mo, W) with isolated U-dumbells

Mathieu Pasturel[1], Maria Szlawska[2], Adam Pikul[2]

[1]Institut des Sciences Chimiques de Rennes, Rennes, France. [2]Institute of Low Temperature and Structure Research, Polish Academy of Sciences, Wroclaw, Poland

The hexagonal $Ho_6Mo_4Al_{43}$ structure-type is characterized by the formation of dimers of magnetic *f*-element with *f-f* distance of about 3.4-3.5 Å, separated the ones from the others by more than 5 Å in all directions. Accordingly, competing magnetic interactions and frustration may occur between strong intra-dimer coupling and much weaker inter-dimer ones.

If rare earth-based members of this family have been intensively studied these last years, only few reports are available on uranium isostructural aluminides. Polycrystalline samples of $U_6Nb_4Al_{43}$ undergo at least two magnetic transitions with a broad maximum at about 12 K and a Brillouin-like anomaly at 7 K, hinting at a ferromagnetic contribution [1]. $U_6W_4Al_{43}$ remains paramagnetic in the whole investigated temperature range [2]. This difference of magnetic behavior and the lack of data in this isostructural family motivated its investigation.

Multiple transitions are observed for $U_6T_4Al_{43}$ (*T* = V, Cr, Mo) polycristalline samples. Moreover, mm-sized $U_6Nb_4Al_{43}$ single crystals exhibit at least 2 magnetic transitions, an AFM-like at 12 K, and a 1st order one at about 7 K, confirmed by magnetic and specific heat measurements.

A summary of the main results of our investigation will be presented, starting from the 6-4-43 phase formation, to the crystallographic and physical properties of the different compounds.

[1] C. Moussa *et al*., *J. Alloys Compd.* **691**, 893 (2017).
[2] K. Huang *et al*., *J. Phys.:Cond. Matter* **31**, 165601 (2019).

o32

Electrical resistivity of the Zintl phase UCu_2P_2

Volodymyr Buturlim[1,2], Eteri Svanidze[3], Dariusz Kaczorowski[4], Fuminori Honda[5,6], Silvie Mašková-Černá[1], Ladislav Havela[1]

[1]Charles University, Faculty of Mathematics and Physics, Prague, Czech Republic. [2]Glenn T. Seaborg Institute, Idaho National Laboratory, Idaho Falls, USA. [3]Max Planck Institute for Chemical Physics of Solids, Dresden, Germany. [4]Institute of Low Temperatures and Structural Research, Polish Academy of Sciences, Wroclaw, Poland. [5]Central Institute of Radioisotope Science and Safety, Kyushu University, Fukuoka, Japan. [6]Institute for Materials Research, Tohoku University, Oarai, Japan

UCu_2P_2 belongs to the layered Zintl phases with the trigonal structure of the $CaAl_2Si_2$ type (*P*-3*m*), formed by alternating cationic (Ca) and anionic (Al-Si) layers. The ferromagnetic state has relatively high Curie temperature T_C = 216 K.

Electrical resistivity was measured both on single crystal and on sample in the form of microdevice. UCu_2P_2 has a strongly anisotropic electrical resistivity. While the resistivity is smaller for *i* // [001] than for [100] at low temperatures, the situation is reversed in the paramagnetic state. The maximum resistivity is reached at T_C, where the high-temperature paramagnetic regime with negative slope ($dr/dT < 0$) suddenly changes in a precipitous drop in the ferromagnetic range. Reaching 5 or 10 mΩcm (depending on the *i* direction), the absolute resistivity values are by far too high for a conventional metallic system. Such values point to a semi-metallic nature, corroborated by negligible *γ*-value seen in the heat capacity data.

One can also speculate about the origin of the broad shoulder around 150 K for *i* // [100] which is actually more pronounced in the microdevice data, where the current within the basal plane was not constrained to [100]. This indicates an anisotropy within the basal plane.

Possible frameworks of understanding of such behavior will be discussed.

o33

Exploration of the exceptional curie temperatures in Uranium-based UCu_2P_2 ferromagnet using dilatometry

Volodymyr Buturlim[1], Petr Doležal[2], Oleksandra Koloskova[3], Jiří Prchal[3], Ilja Turek[3], Fuminori Honda[4], Martin Divis[3], Dariusz Kaczorowski[5], Krzysztof Gofryk[6], Ladislav Havela[3]

[1]Idaho National Laboratory, Idaho Falls, Idaho, USA. [2]Technical University Vienna, Vienna, Austria. [3]Charles University, Prague, Czech Republic. [4]Kyushu University, Fukuoka, Japan. [5]Polish Academy of Sciences, Wroclaw, Poland. [6]Idaho National Laboratory, Idaho Falls, ID, USA

UCu_2P_2, identified as a Zintl phase possessing the trigonal $CaAl_2Si_2$ structure, emerges as a distinctive 5f ferromagnet showcasing an unprecedented Curie temperature (T_C = 216 K) among uranium compounds.[1]. While the size of the magnetic moment 2.0 μ_B/U is not surprising due to U-U spacing exceeding the Hill limit, the reasons for the high T_C are less understood. Ab-initio calculations reveal only very weak hybridization of the U-5*f* states with the 6*d* states as well as with electronic states of Cu and P. It seems that a transfer of U-6*d* states to the P-3*p* states is an important ingredient, which was highlighted by a rapid increase of T_C under hydrostatic pressure so that a room-temperature 5*f* ferromagnetism could be demonstrated. Besides magnetization, transport, and heat capacity studies on single crystals we performed also characterization of a polycrystalline material, which has T_C = 219 K. Thermal expansion study revealed a moderate increase of both lattice parameters just below T_C, so we can exclude that the pressure enhancement of T_C is driven simply by thermodynamics (via the Ehrenfest relation). Hence the reasons have to be attributed to the enhancement of specific U-U couplings upon compression. Indeed, ab initio calculations probing the energy enhancement upon moments reversal gave a semi-quantitative account of the observed tendency of T_C.

*V. B. acknowledges the support from Idaho National Laboratory's Laboratory Directed Research and Development (LDRD) program under DOE Idaho Operations Office Contract DE-AC07-05ID14517. K. G. acknowledges support from the Division of Materials Science and Engineering, Office of Basic Energy Sciences, Office of Science of the U. S. Department of Energy (U. S. DOE).

[1] D. Kaczorowski, R. Troc, Magnetic and transport properties of a strongly anisotropic ferromagnet UCu_2P_2, J. Phys. Condens. Matter, 1990, 2, 4185.

o34

High-pressure investigation of the crystal structure of UCu_2P_2

Alexandre Kolomiets[1,2], Jiri Prchal[2], Itzhak Halevy[3], Ladisla Havela[2], Volodymyr Buturlim[4]

[1]Lviv Polytechnic National University, Lviv, Ukraine. [2]Charles University, Prague, Czech Republic. [3]Ben Gurion university, Be'er Sheva, Israel. [4]Glenn T. Seaborg Institute, Idaho National Laboratory, idaho, USA

The crystal structure of the Zintl phase UCu_2P_2 has been investigated by the X-ray diffraction in a diamond anvil cell up to the pressure of 23GPa. The original trigonal structure (space group *P*-3*m*1) persists till at least 12GPa. Between 12GPa and 16GPa the structural transformation takes place, and from 16GPa till 23GPa the new crystal structure is observed, which is likely a result of the distortion of the original original trigonal structure. The structural transition is at least partly reversible as indicated by the XRD data collected upon pressure decrease after reaching 23GPa .

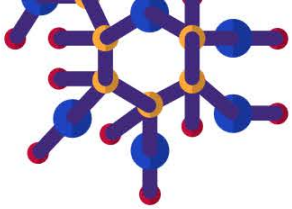

o35

New ternary arsenide of Ytterbium and Iron – a novel ferromagnetic material

Oksana Karychort[1], Mitja Krnel[2], Yuri Prots[2], Nazar Zaremba[2], Lev Akselrud[1], Yurii Grin[2], Olga Zhak[1], Eteri Svanidze[2]

[1]Ivan Franko National University of Lviv, Lviv, Ukraine. [2]Max Planck Institute for Chemical Physics of Solids, Dresden, Germany

Iron-based pnictides of rare earth metals are known for their superconductivity and magnetic properties [1]. In particular, superconductors with various stoichiometries have been previously reported, such as LiFeAs (18 K), and $K_{0.6}Ba_{0.4}Fe_2As_2$ (38 K). Superconductivity of the arsenides $SrFe_2As_2$ and $BaFe_2As_2$ has been induced by pressure with Tc = 27 and 29 K, respectively. A complex magnetic phase diagram with several ferromagnetic-type phase transitions at 56, 38, and 152 K has been observed for $GdFe_4As_{12}$, $TbFe_4As_{12}$, and $EuFe_4As_{12}$, respectively. Transition to ferromagnetic order was observed for compounds $La_{12}Fe_{57.5}As_{41}$ and $Ce_{12}Fe_{57.5}As_{41}$ at 125 and 95 K, respectively. Pronounced transition closely coinciding with the ferromagnetic ordering temperature was observed in electrical resistivity measurements on single crystals of $Ce_{12}Fe_{57.5}As_{41}$. The skutterudite $SmFe_4As_{12}$ shows a ferrimagnetic transition at 29 K. Surprisingly, very few ternary rare earth-based analogs of iron arsenides have been reported so far. Moreover, no ternary arsenides were synthesized in the Yb-Fe-As system, however, Yb is a promising intervalence element, and in the closely related Yb-Ni-As system, five ternary arsenides have been obtained and investigated. In this work, we revisit the Yb-Fe-As ternary system. We were able to obtain the new ytterbium and iron arsenide which crystalizes in *P*21/*m* space group, with the refined lattice parameters: *a* = 9.66188(3) Å, *b* = 3.78719(2) Å, *c* = 7.18491(2) Å; *b* =100.651(1); R_I = 0.0598, R_P = 0.1057, wR_I = 0.2196. The magnetic study of the physical properties of new arsenide revealed magnetic ordering below 130 K with more in-depth investigations currently underway.

[1] Villars P., Cenzual K., Eds. Pearson's Crystal Data: Crystal Structure Database for Inorganic Compounds (Release 2019/20); ASM International®: Materials Park, Ohio (USA), 2019.

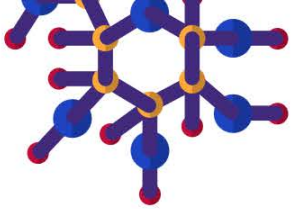

o36

Synthesis and characterization of a new ferrimagnetic $SmFe_5As_3$ pnictide

Mitja Krnel, Oksana Karychort, Nazar Zaremba, Lev Akselrud, Yuri Grin, Berit Goodge, Walter Schnelle, Eteri Svanidze

Max Planck Institute for Chemical Physics of Solids, Dresden, Germany

Pnictides based on transition metals and lanthanides/actinides are known to exhibit interesting physical and chemical features such as high temperature superconductivity [1],[2], thermoelectric properties [3], as well as peculiar crystallographic motifs [4]. We were able to synthesize single crystals of a new ternary pnictide $SmFe_5As_3$ in the form of tiny needles by using Bi as flux. The compound crystallizes in the monoclinic, UCr_5P_3-type crystal structure (space group $P2_1/m$, Pearson symbol $mP18$, with lattice parameters a = 7.1848(8) Å, b = 3.8531(4) Å, c = 9.7103(12) Å, β = 100.55(1)°). The crystal structure can be represented by a 3D Fe-As network, where the building blocks are straight »shamrock« chains. Single crystal diffraction reveals twinning, similar to other isostructural compounds [4]. Magnetization $M(T)$ measurements show a ferrimagnetic (FIM) like transition at T_C = 80 K and an anomaly at T = 30 K, while the field-dependent magnetization $M(H)$ shows several metamagnetic transitions. The inverse susceptibility data fitted with Curie-Weiss law reveals antiferromagnetic coupling between ions with Θ = -29 K. The magnetization measured along the H || [010] and H ⊥ [010] directions as well as magnetoresistance show clear anisotropy.

[1] J. M. Cameron *et al.*: *Chem. Soc. Rev.* **40**, 4099-4118, (2011).
[2] Z. Ren *et al.*: *Chin. Phys. Lett.* **25**, 2215, (2008).
[3] B. C. Sales *et al.*:: Science **272**, 1325, (1996).
[4] N. Zaremba *et al.*: *Inorg. Chem.* **accepted** (2024).

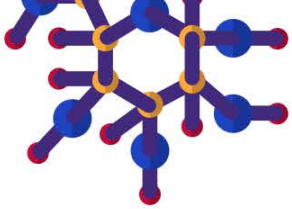

o37

Functionalization of selected 2D materials with π-conjugated bis-hydrazone coordination complex

Piotr Zabierowski[1], Lukáš Děkanovský[1], Vlastimil Mazánek[1], Rui Gusmão[1], Maciej Hodorowicz[2], Zdeněk Sofer[1]

[1]Department of Inorganic Chemistry, University of Chemistry and Technology Prague, Prague, Czech Republic. [2]Faculty of Chemistry, Jagiellonian University, Kraków, Poland

Functionalization of 2D materials corresponds to a deliberate modification of the surface of the material either in a covalent or non-covalent manner with the use of reactive agents, usually organic or organometallic composition. As a result, the properties of the 2D material are modified (e.g. catalytical properties) or their stability at ambient conditions is prolonged. In this study, we present the result of functionalization of selected 2D materials (graphite, thermally reduced graphene oxide (TRGO) and $Ti_3C_2T_x$) with a new bis-hydrazone copper(I) nitrate salt $[Cu_2L_2][NO_3]_2$ (where L denotes, 1,2-di[[2-(pyridin-2-yl)hydrazin-1-ylidene]methyl]benzene), soluble in common organic solvents and maintaining copper(I) oxidation state upon solvothermal functionalization under basic conditions. The functionalization treatment resulted in a striking 328% increase in BET specific surface area for graphite (374 m^2/g), whereas the TRGO surface area remained unchanged. The complex also uniformly coats $Ti_3C_2T_x$ phase, accounting for prolonged stabilization of MXene in ambient conditions. The results of characterization of the materials with XRD, Raman, FTIR, NMR, UV-VIS, PL, HRMS, XPS, FE-SEM, EDX and N_2 adsorption are presented and discussed, together with DFT quantum chemical calculations corroborating interpretation of the spectra (UV-VIS, IR, Raman).

o38

Magnetically soft CoFeNi-based high-entropy alloys

Primož Koželj[1,2], Jože Luzar[1], Stanislav Vrtnik[1], Andreja Jelen[1], Darja Gačnik[1], Peter Mihor[1], Mitja Krnel[1], Bojan Ambrožič[1], Pavol Priputen[3], Marián Drienovský[3], Magdalena Wencka[4,1], Goran Dražić[5], Anton Meden[6], Suomyadipta Maiti[7], Walter Steurer[7], Janez Dolinšek[1,2]

[1]Jožef Stefan Institute, Ljubljana, Slovenia. [2]Faculty of Mathematics and Physics, University of Ljubljana, Ljubljana, Slovenia. [3]Faculty of Materials Science and Technology in Trnava, Slovak University of Technology in Bratislava, Trnava, Slovakia. [4]Institute of Molecular Physics, Polish Academy of Sciences, Poznań, Poland. [5]National Institute of Chemistry, Ljubljana, Slovenia. [6]Faculty of Chemistry and Chemical Technology, University of Ljubljana, Ljubljana, Slovenia. [7]ETH Zurich, Zürich, Switzerland

Many high-entropy alloys (HEAs) – metallic systems composed of 4, 5 or more elements in equimolar or near-equimolar concentrations – are based around the magnetic 3*d* transition elements Co, Fe and Ni. Dependent on the other elements and heat treatment, such systems might be academic curriosities (e.g. spin glasses) or potentially useful soft magnetic materials, e.g. for making transformer cores.

Properly heat-treated FeCoNiPdCu [1] has a narrow hysteresis loop with coercivity of only 115 A/m, a reasonable magnetic saturation polarization of 1.3 T and maximum relative permeability ≈ 3600. Additionally, the material has a high electrical resistivity (reducing eddy current losses) and a high Curie temperature. HAADF STEM and EDS analysis indicate that the material is composed of magnetic FeCoNi-rich nanodomains separated by nonmagnetic PdCu spacers, leading to the conclusion that the mechanism behind the magnetic softness of the HEA is exhange averaging of magnetic anisotropy.

The $AlCoFeNiCu_x$ series of HEAs [2] exhibit besides a nanostructure also a multiphase microstructure. The x = 2.0 alloy has a low coercivity of 650 A/m, a decent saturation polarization of 0.55 T, as well as zero magnetostriction. This zero magnetostriction is a consequence of the three phase microstructure and could lead to supersilent magnetic materials for AC applications.

[1] P. Koželj, *et al.* Adv. Eng. Mater. **21**, 1801055 (2019).
[2]] J. Luzar, *et al.*, Adv. Mater. Interfaces **9**, 2201535 (2022).

o39

Effect of sputtering power on the structural, optical and electrical properties of aluminum-doped zinc oxide thin film

Chonthicha Wannasiri, Patcharin Chintasin, Watcharee Rattanasakulthong

Kasetsart University, Bangkhen, Bangkok, Thailand

Aluminum-doped zinc oxide (AZO) film with different sputtering powers of 140, 160, 180, 200 and 220 W was deposited on a glass substrate by radio frequency sputtering. The average thickness of as-deposited films calculated from SEM images was increased from 53 nm to 111 nm with increasing deposited power. XRD results confirmed that all films displayed the main peak of the AZO phase in the (002) plane. The peak intensity strongly depends on sputtering power. The highest and lowest intensities were observed on 180W and 220W film. Furthermore, the (004) plane was clearly observed on the 140W and 180W film, whereas the (101) and (100) planes were only observed on a 220W film. The average optical transmission of all films is about 80%, with a tiny decrease in a wavelength range of 350-800 nm. The results showed that the 200W film exhibited a regular columnar structure with the highest surface roughness, energy bandgap, figure of merit, and the lowest resistivity. Additionally, the 200W film possessed the highest heat generated by a film due to the Joule heating effect at a temperature of 57°C when a voltage of 14 V was applied. The results confirmed that sputtering power strongly affected the phase structure of the AZO films.

Keywords: AZO thin film, sputtering power, phase structure, optical transmission, roughness.

o40

Transition temperature enhancement in superconducting high entropy alloy films through nitrogen addition

Karol Flachbart[1], Gabriel Pristáš[1], Georg Gruber[2], Matúš Orendáč[1], Július Bačkai[1], Jozef Kačmarčík[1], Filip Košuth[1], Slavomír Gabáni[1], Pavol Szabó[1], Christian Mitterer[2]

[1]Institute of Experimental Physics, Slovak Academy of Sciences, Košice, Slovakia. [2]Montanuniversität, Leoben, Austria

We report about the influence of nitrogen addition on the superconducting transition temperature T_C of TiNbMoTaW high entropy alloy (HEA) films deposited by magnetron sputtering. By measuring the temperature dependence of resistivity of (TiNbMoTaW)N_x nitrides, we observe a considerable increase of T_C, from 0.62 K for x = 0 up to 5.02 K for x = 0.74, with further increase of x, T_C is decreasing to 1.08 K for x = 0.97. The eight fold T_C enhancement seems to be associated with the incorporation of light N atoms into the face-centred cubic lattice and with the simultaneous x-dependent enhancement of the electron-phonon interaction, which may be related to the high configuration entropy in HEA. Additional heat capacity and point contact spectroscopy measurements show that the superconductivity in these about 1 mm thick films is bulk in nature, consistent with conventional BCS weak-coupling phonon mediated superconductivity. Further experiments will be needed, especially on HEA nitrides that have different configuration entropies, a higher starting T_C and exist in the form of bulk crystalline samples, to be able to determine exactly how the electronic density of states, the phonon modes and the electron-phonon interaction develop with N addition [1].

[1] G. Pristáš et al., Multiple transition temperature enhancement in superconducting TiNbMoTaW high entropy alloy films through tailored N incorporation, Acta Mater. 262 (2024) 119428.

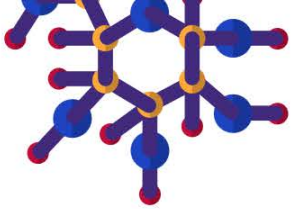

pl06

PLENARY: Towards the metal age of thermoelectricity: High thermoelectric performance in metallic materials via interband scattering

Andrej Pustogow

TU Wien, Vienna, Austria

Thermoelectric (TE) materials directly transform thermal into electrical energy and vice versa, making them promising for a plethora of applications in refrigeration or power generation. However, state-of-the-art semiconductors in the focus of current TE research did not make the leap into broad applications due to their low power density and poor mechanical properties. Metallic systems would be superior in this regard, but remained largely neglected by the TE community over the past decades due to their small Seebeck coefficient S.

Here we realize high TE performance in metals via tuning of electronic interband scattering. Using this paradigm, we discovered record-high power factors up to 34 $mWm^{-1}K^{-2}$ in binary NiAu alloys, exceeding previous benchmark values by several times [1]. The unusually high S in this metallic system, yielding the largest figure of merit $zT \approx 0.5$ in metals reported so far, results from strongly electron-hole asymmetric charge transport. In the highly conductive s-band of NiAu the mobility of holes is selectively reduced by interband scattering from localized Ni d states below the Fermi energy. Our concept is generally applicable to various metallic compounds and alloys – also without expensive elements like Au.

This new paradigm towards scattering-tuned ultrahigh TE performance in metals is cardinally different from tuning zT in semiconductors. Crucially, phonon heat transport is irrelevant in metallic systems due to the Wiedemann-Franz law, which confines the multi-parameter optimization problem of zT to a sole increase of S (in metals $zT = S^2/L$; L is the Lorenz number). Finally, we present a roadmap of systematic electronic tuning of TE properties in metals via high-throughput computational materials screening.

[1] F. Garmroudi, M. Parzer, A. Riss, C. Bourgès, S. Khmelevskyi, T. Mori, E. Bauer, and A. Pustogow, High thermoelectric performance in metallic NiAu alloys via interband scattering, *Sci. Adv.* **9**, eadj1611, (2023)

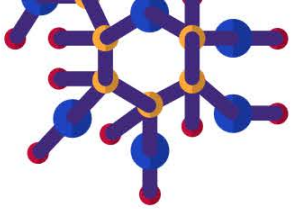

pl07

PLENARY: Geometrically frustrated Ytterbium-oxides for milli-Kelvin adiabatic demagnetization refrigeration

Philipp Gegenwart

University of Augsburg, Augsburg, Germany

Adiabatic demagnetization refrigeration (ADR) is a classical cooling technique with renewed recent attention as alternative to costly and elaborate $^{3}He/^{4}He$ dilution refrigeration. Established water containing ADR salts suffer from chemical instability which requires delicate treatment to avoid degradation and ensure good thermal contact.

In the talk, geometrically frustrated Ytterbium oxides will be discussed as suitable alternatives. They offer minimal ADR temperatures well below 50 mK, in combination with larger volumetric entropy density compared to hydrated paramagnetic salts for similar end temperatures. Most importantly, their chemical stability enables a much simpler ADR pill design and also allows ultra-high-vacuum applications.

We also discuss the impact of geometrical frustration and structural randomness on ADR performance and demonstrate the tunability of cooling power and operating temperature by choosing different materials and chemical substitutions.

Work in collaboration with Y. Tokiwa, S. Bachus, Kavita, A. Jesche, A.A. Tsirlin, N. Oefele, F. Hirschberger, A. Bellon, D.D. Sarma and U. Arjun.

o41

Mechanisms to inhibit thermal conductivity and enhance thermoelectric performance

Takao Mori

National Institute for Materials Science (NIMS), Tsukuba, Japan

Thermoelectric (TE) materials are of interest for energy saving and IoT power sources [1]. For high TE performance, mechanisms to circumvent the traditional tradeoffs between the physical properties are necessary [2]. I will focus on recent mechanisms to effectively lower lattice thermal conductivity k, while not overly degrading electrical conductivity. By nanostructuring, ZT has been enhanced via nanopores, defect engineering [2] and recently higher ordering of nanostructures [3]. Intrinsic mechanisms based on crystal structure are also effective [2]. Partial occupancy was demonstrated as an indicator to identify a low k material catalogue [4]. Particular doping into SnTe was shown to lead to red shift of Raman spectra indicating softening of the lattice and a dramatic reduction of k [5]. Interstitial doping in Mg_3Sb_2 radically lowered the phonon group velocity, leading to exceptional high performance rivalling long-time champion Bi_2Te_3 [6]. Finally, the heterogeneous bonding in mixed anion compounds has been shown to result in exceptional low k [7]. Future outlooks will also be discussed.

[1] *Sci. Tech. Adv. Mater.* **19**, 836 (2018)
[2] *Small* 13, 1702013 (2017), *Energies*, **15**, 7307 (2022)
[3] *Sci. Adv.* 9, eadh0713 (2023), *Adv. Energy Mater.* **13**, 2301667 (2023)
[4] *Energy Environ. Sci.* **14**, 3579-3587 (2021)
[5] *Adv. Energy Mater.* **11**, 2101122 (2021)
[6] *Joule* 5, 1196-1208 (2021), *Nature Commun.* **13**, 1120 (2022)
[7] *J. Mater. Chem. A* 9, 22660 (2021), *J. Mater. Chem. A* **11**, 10213 (2023) *Hot Paper*

o42

Thermoelectric properties of new transition metal chalcogenides and phosphides

David Berthebaud[1,2], Sylvain Le Tonquesse[1,3], Hugo Bouteiller[1,3], Bruno Fontaine[4,5], Takao Mori[6], Jean-François Halet[1,5]

[1]CNRS–Saint-Gobain–NIMS, IRL 3629, Laboratory for Innovative Key Materials and Structures (LINK), National Institute for Materials Science (NIMS), Tsukuba, Japan. [2]Nantes Université, CNRS, Institut des Matériaux de Nantes Jean Rouxel, IMN, Nantes, France. [3]Laboratoire CRISMAT, ENSICAEN, UNICAEN, CNRS, Normandie Univ. (UMR 6508), Caen, France. [4]Saint-Cyr Coëtquidan Military Academy, CReC, Guer, France. [5]Univ Rennes, CNRS, Ecole Nationale Supérieure de Chimie de Rennes (ENSCR), Institut des Sciences Chimiques de Rennes (ISCR), UMR 6226, Rennes, France. [6]Research Center for Materials Nanoarchitectonics (MANA), National Institute for Materials Science (NIMS), Tsukuba, Japan

Here, we will present findings on unexplored compositions of transition metal-based chalcogenides and phosphides. Our focus is on compositions exhibiting promising features for thermoelectric applications. For instance, the low-dimensional pseudo-hollandite $A_xCr_5Se_8$ (A = Tl, Ba, Rb...) demonstrates intrinsic low thermal conductivity and semiconducting behavior owing to the intricate and chemically flexible nature of its structure. Additionally, we will discuss another group of materials, namely copper phosphides, which are notable for their abundance of elements and reported low gravimetric density. These materials, which can be conveniently doped n or p-type, exhibit large power factors and hold significant promise in terms of figures of merit.

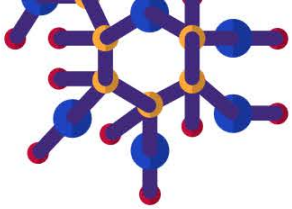

o43

Is the presence of Sn^{2+} a crucial factor for the generation of low thermal conductivity in tin-based sulphides?

Florentine Guiot[1], Carmelo Prestipino[2], Emmanuel Guilmeau[2], Bernard Raveau[2], Susumu Fujii[3,4], Vincent Dorcet[5], Bernard Malaman[6], Thierry Schweitzer[6], Erik Elkaïm[7], Masato Yoshiya[3,4], Pierric Lemoine[6]

[1]Institut des Sciences Chimiques de Rennes, Rennes, France. [2]CRISMAT, Caen, France. [3]Division of Materials and Manufacturing Science, Osaka, Japan. [4]Nanostructures Research Laboratory, Nagoya, Japan. [5]Institut des Sciences Chimiques de Rennes, rennes, France. [6]Institut Jean Lamour, Nancy, France. [7]Synchrotron SOLEIL, Gif-sur-Yvette, France

The design and optimization of thermoelectric (TE) materials rely on the intricate balance between thermopower S, electrical resistivity ρ and thermal conductivity κ. Perfecting such a balance is the key to reach high TE performances determined by the dimensionless figure of merit $ZT=S^2T/\rho\kappa$.[1] Among the most promising TE materials at medium temperature, complex copper-based sulphides are of interest as they are usually made of eco-friendly and low-cost elements [2] and exhibit intrinsically low thermal conductivity.[3] However, the use of copper-based sulphides in TE devices is limited by the performances of the *n*-type materials compared to *p*-types.[4] It therefore necessary to develop more performant n-type sulphide materials. In this presentation I will report a complex crystal structure and physical properties of $Cr_2Sn_3S_7$, a *n*-type magnetic semiconductor with low energy band gap and low thermal conductivity. I will demonstrate experimentally and theoretically that the high structural complexity and the presence of lone pair electrons cations (Sn^{2+}) are responsible of the low thermal conductivity of the material but, unfortunately, also affect drastically the electrical conductivity, avoiding to reach interesting thermoelectric properties without further optimization.

[1] Hébert, S et al. *J. Phys.: Condens. Matter* **2016**
[2] Caballero-Calero et al. M. *Adv. Sustainable Syst.* **2021**
[3] Powell, A. V. J. Appl. Phys. **2019**
[4] Guélou G et al. *J. Mater. Chem. C* **2021**

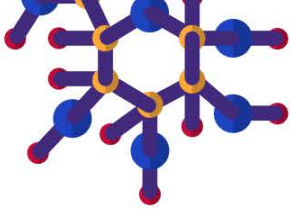

o44

Room temperature giant magnetocaloric materials $(MnFe)_{1.9}(PSi)$ Fe-rich compounds for heat pump application

Hang Hanggai

Faculty of Applied Sciences, Delft University of Technology, Delft, Netherlands

First-order magnetic transitions involve structural, magnetic and electronic changes that are relatively well described at the scale of a unit cell. They have established spectacular consequences on bulk physical properties such as magnetization, transport or thermal properties, which form the basis of their applications. In this work, simultaneous substitutions of Mn for Fe and Si for P on structure, magnetic property and magnetocaloric effects of Fe-rich $Mn_xFe_{1.90-x}P_{1-y}Si_y$ compounds are studied. The transition temperature of the compounds increases linearly with simultaneously increasing Mn and Si content, from 295 K to 332 K. This fulfils one important application requirements of MCMs that the transition temperature can be adjusted continuously over the temperature range relevant for the heat pump application. The maximum isothermal magnetic entropy change ($-\Delta S_m$) increases from 12 $Jkg^{-1}K^{-1}$ (x = 0.60, y = 0.34) to 16 $Jkg^{-1}K^{-1}$ (x = 0.68, y = 0.38) for a field change 2 T. The demonstration of heat capacity measurement with commercial semi-adiabatic option implemented in Versalab. The maximum magnetic entropy change ($-\Delta S_m$) is obtained for Mn=0.66/Si=0.37, and ΔT_{ad} of the compound can reach to 4.2 K in field of 3 T. The *n*-value is used to define the type of magnetic phase transition. The magnetic entropy change scales with the magnetic field as $\Delta S_M \propto H^n$ in the vicinity of the phase transition. The index of the magnetic field can be expressed as $n = d\ ln(|\Delta S_M|)/\ d\ ln(H)$ generally shows a significant variation near the transition temperature. In particular, $n > 2$ was proposed for materials characterized by a first-order magnetic phase transitions (FOPT). With the simultaneous changing of the Mn/Fe and P/Si content, the maximum value of *n* near the phase transition is found to be greater than 2 for all samples.

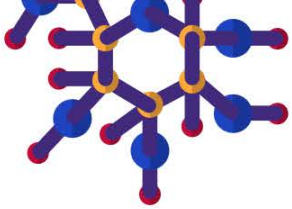

o45

Accelerating material synthesis optimization with Bayesian Optimization: Investigating the magnesioreduction synthesis of magnetocaloric $Mn_{5-x}Fe_xSi_3$

Sylvain Le Tonquesse

CRISMAT, Caen, France

The development of high-performance materials with specific properties necessitates precise control over synthesis parameters and chemical compositions. Conventional approaches based on trial and error can be slow in complex systems due to the intricate relationships among synthesis parameters. In response to these challenges, this study adopts Bayesian Optimization (BO) as an advanced strategy to refine the magnesioreduction synthesis of magnetocaloric $Mn_{5-x}Fe_xSi_3$, a material that is both free from rare earth elements and non-toxic. Magnesioreduction synthesis is an ideal case study for this optimization approach, given the critical need to optimize multiple experimental parameters which significantly influence the reaction outcome. On the contrary of traditional machine learning approaches that necessitate large, noise-sensitive datasets, BO capitalizes on a more compact dataset enriched with prior knowledge. Implementing BO through the use of the GpyTorch and BoTorch open-source libraries, our methodology emphasizes minimizing reaction durations while simultaneously ensuring the material's high purity and optimizing its magnetocaloric effect near ambient temperatures through chemical composition adjustments. This talk will cover the applied methodology, key findings, and the extensive implications of leveraging BO for the synthesis of materials, highlighting its role in diminishing laboratory time and resource consumption.

o46

Discovery of inorganic solids with desired structure motifs guided by Machine Learning

Volodymyr Gvozdetskyi[1], Bryan Owens-Baird[2], Allison Thomé[1], Arka Sarkar[2], Balaranjan Selvaratnam[1], Mohammed Jomaa[1], Kirill Kovnir[2], Arthur Mar[1]

[1]University of Alberta, Edmonton, Alberta, Canada. [2]Iowa State University, Ames, Iowa, USA

High-throughput approaches are helpful to guide the efficient search of composition space to screen for target materials, but their structures may still be unknown. Physical properties are often associated with particular structural features; for example, good thermoelectric materials can be found when lattice thermal conductivity is lower in clathrate structures containing atoms that rattle inside large cages. We hypothesize that machine learning models can be trained on existing phases to identify new compounds exhibiting desired structural motifs, such as channels in Li-containing silicides or layers in alkali-metal-containing antimonides. Such models, of course, have merit only if they can be tested through experimental synthesis and characterization.

o47

What is the true ground-state of intermetallic compound Fe_3Al?

Monika Vsianska[1], Martin Friak[2], Mojmir Sob[1,2]

[1]Masaryk University, Brno, Czech Republic. [2]Institute of Physics of Materials, Academy of Sciences of the Czech Republic, Brno, Czech Republic

We discuss recent doubts about the true ground-state (GS) structure of the intermetallic compound Fe_3Al. It seems that it should be the $D0_3$ structure (observed experimentally), but there are some considerations that, perhaps, $D0_3$ might be a high-temperature (> 400 K) structure and the GS at 0 K might be the $L1_2$ structure because there might be a high energy barrier between both structures and, when the temperature is lowered, the system is not able to transform into the lower-energy $L1_2$ structure. To elucidate this problem, we performed extended ab initio electronic structure calculations with the help of the VASP code using various exchange-correlation energies within the generalized gradient approximation (GGA). Regrettably, some calculations provide the $L1_2$ and some of them $D0_3$ as the GS structure.

To resolve this question, we performed further calculations testing 6 most popular metaGGAs, such as SCAN(-L), rSCAN(-L) and r2SCAN(-L) representing a higher rung of the Jacob ladder. In all cases, the $L1_2$ was favored over the $D0_3$ structure but the calculated magnetic moments increased to unphysically high values. As shown also in earlier papers, the present metaGGAs are not able to treat magnetic materials correctly and, therefore, cannot help here.

Thus, the present results represent the very first step on the way to understand the energetics of the Fe_3Al compound and its ground state. We hope they may motivate future theoretical and experimental work in this direction.

o48

Predictive theory of the spontaneous volume magnetostriction in Fe-Ni alloys: bond repopulation model of Invar effect.

Sergii Khmelevskyi

VSC Reseach Center, Technical Univesity of Viennan, Vienna, Austria

The Invar anomaly in the canonical INVAR alloys Fe-Ni has been investigated on the first-principal basis with inclusion of the longitudinal spin fluctuations in the paramagnetic region. We obtaine almost perfect quantitative descrition of the spontaneous volume magnetestostrictions in their dependence on the alloy chemical composition. With an increase of the Ni concentration the Invar anomaly vanishes. All this features are readily reproduced in our calculations by taking into the account longitudinal spin fluctuations (LSF) that increase a local atomic moment as temperature increases. We demonstrate that the mechanism of the Invar anomaly is rooted in the repopulation of anti-bonding states in the majority spin band and bonding states in the minority spin band at the Fermi level. This repopulation occurs due to thermal magnetic disorder effects that reduce the local atomic moments compare to their values in the ferromagnetic ground state due to itinerant character of the magnetism. We provide evidence that such repopulation of majority and minority spin states occurs with change of their bonding character in Fe-Ni alloys due to special position of the Fermi level in the metallic d-band. We visualize the bonding/anti-bonding character of electronic states in Fe-Ni alloy at the Fermi level using first-principle based Crystal Orbital Hamiltonian Population (COHP) analyses.

o49

Self-consistent renormalization theory of anisotropic spin fluctuations in nearly antiferromagnetic metals

Rikio Konno

Kindai University Technical College, Nabari-shi, Mie, Japan

Self-consistent renormalization theory of anisotropic spin fluctuations in nearly antiferromagnetic metals was composed. Although Moriya et. al. made the self-consistent renormalization theory of isotropic spin fluctuations [1-6], anisotropic spin fluctuations were not considered. The temperature dependence of the inverse of the staggered magnetic susceptibility, the one of the nuclear magnetic relaxation rate, and the T-linearcoefficient of the specific heat were investigated within this theory. At low temperatures the inverse of the staggered magnetic susceptibility shows T^2-linear dependence. In elevated temperatures, it shows T-linear dependence. It has the anisotropy. The nuclear magnetic relaxation rate has T-linear dependence at low temperatures. It has $T^{1/2}$-linear dependence in elevated temperatures. It also has the anisotropy.

* This work is supported by the Kindai University Technical College Grants.

[1] T Moriya, Spin Fluctuations in Itinerant Electron Magnetism, (1985), and references therein.
[2] T Moriya, Physics of Magnetism, (2006) in Japanese and references therein.
[3] K Ueda, Introduction to Magnetism, (2011) in Japanese and references therein.
[4] K .Ueda, Basic Concepts of Magnetism, (2021) in Japanese and references therein.
[5] Y Takahashi, Spin Fluctuation Theory of Itinerant Magnetism, (Springer, 2013) and references therein.
[6] K Yosida, Theory of Magnetism, (Springer, 1996) and references therein.

o50

Intrinsic spin currents in noncentrosymmetric ferromagnets

Ilja Turek

Institute of Physics of Materials, Czech Academy of Sciences, Brno, Czech Republic

Spin-orbit interaction in systems lacking inversion symmetry gives rise to nonzero electron spin currents even in the absence of external electric fields [1, 2]. In noncentrosymmetric systems with dominating ferromagnetic exchange coupling of local magnetic moments, the weak Dzyaloshinskii-Moriya interaction (DMI) leads to a contribution to the micromagnetic energy density that is linear in the gradient of the magnetization direction. This contribution can quantitatively be described in terms of the DMI-tensor which has phenomenologically been related to the intrinsic spin current in the reference ferromagnet [2]. In the present study, we have developed a microscopic theory which connects explicitly the DMI-tensor to the spin current. The theory is applied on an ab initio level to a few selected transition-metal based systems, such as B20 compounds (FeGe) and quaternary Heusler alloys (CoMnFeSi); concentration trends in random ferromagnetic alloys will be discussed as well.

[1] E. I. Rashba, Phys. Rev. B **68** (2003) 241315(R).
[2] T. Kikuchi et al., Phys. Rev. Lett. **116** (2016) 247201.

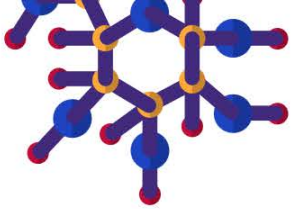

o51

Two-fluid model analysis of the terahertz conductivity of YBaCuO samples: optimally doped, underdoped and overdoped cases

Christelle Kadlec[1], Michal Šindler[1], Wen-Yen Tzeng[2], Jiunn-Yuan Lin[3], Chih-Wei Luo[3,4,5]

[1]FZU - Institute of Physics of the Czech Academy of Sciences, Prague, Czech Republic. [2]Department of Electronic Engineering, National Formosa University,, Yunlin, Taiwan. [3]Institute of Physics, National Yang Ming Chiao Tung University, Hsinchu, Taiwan. [4]Department of Electrophysics, National Yang Ming Chiao Tung University, Hsinchu, Taiwan. [5]National Synchrotron Radiation Research Center, Hsinchu, Taiwan

The most studied high-temperature superconductor is undoubtedly $YBa_2Cu_3O_{7-\delta}$ (YBCO). The exact stoichiometry of oxygen is crucial as it determines the hole doping and it governs the properties of YBCO.

In this work*, time-domain terahertz (THz) spectroscopy was used to measure the complex conductivity of YBCO thin films representing the optimally doped, the underdoped and the overdoped stoichiometry. In the normal state, the frequency dependence of the THz conductivity is described by the Drude model. Below the critical temperature T_c, the two-fluid model (describing the appearance of a superconducting fraction in the normal state) was successfully employed to fit all the THz spectra, from 5 K up to T_c. The temperature behaviour of fundamental parameters such as the scattering time, the superfluid fraction and the conductivity was investigated at selected frequencies. The real part of the conductivity $\sigma_1(T)$ exhibits a peak at low frequencies, which slightly shifts with increasing frequency whereas its height decreases. It can be observed for all three stoichiometries and its exact shape depends on the quality of the sample. A further analysis shows that this peak is a consequence of the competition between the scattering time $\tau(T)$ and the superfluid fraction $f_s(T)$.

The decrease of the superfluid fraction towards T_c depends on the temperature with a power law close to 2, suggesting a dirty d-wave superconductor case for all levels of doping.

* submitted to Physical Review B.

o52

Effect of hydrogenation on the crystal structure and magnetism of Nd_2Ni_2Sn

Khrystyna Miliyanchuk[1], Nazar Saidov[1], Volodymyr Buturlim[2], Lev Akselrud[1], Ladislav Havela[2], Roman Gladyshevskii[1]

[1]Ivan Franko National University of Lviv, Lviv, Ukraine. [2]Charles University, Prague, Czech Republic

Nd_2Ni_2Sn belongs to the orthorhombic structure type W_2CoB_2 (*Immm*) and is characterized by a complex magnetic structure with multiple magnetic phase transitions at T = 17 K and T = 21 K due to competing antiferromagnetic and ferromagnetic exchange interactions [1]. The hydride $Nd_2Ni_2SnH_{4.5}$ was synthesized by interaction of a Nd_2Ni_2Sn alloy, previously activated by heating in vacuum up to 523 K, with hydrogen gas under a pressure of 865 mbar heated up to 393 K. The X-ray diffraction analysis revealed an anisotropic cell volume expansion ($\Delta V/V$ = 15.7%) and monoclinic deformation of the crystal lattice ($C2/m$). The hydride partially decomposed in air over 2 months, resulting in the formation of a hydride with lower hydrogen content ($\Delta V/V$ = 12.0%) and recovery of the original orthorhombic symmetry. Hydrogenation leads to weakening of the magnetic exchange interactions; the hydride $Nd_2Ni_2SnH_{4.5}$ orders magnetically at T = 5 K. The *S*-shape of the magnetization curve at 2 K and negative value of the paramagnetic Curie temperature indicate a dominating role of antiferromagnetic coupling. Nd_2Ni_2Sn continues a series of W_2CoB_2-type compounds forming hydrides but is the first representative demonstrating a structural phase transition upon hydrogenation accompanied by symmetry decrease. The impact of hydrogenation on the magnetism of Nd_2Ni_2Sn will be discussed in terms of the symmetry change and variations of the atomic environments.

[1] P. Kumar at al, *Phys. Rev. B* **77** (2008) 184411.

o53

Phase stability of solid solution $La_{1-x}R_xRh_3B$ (R = Gd, Lu and Sc)with anti-perovskite cubic type structure

Kunio Yubuta[1], Akiko Nomura[2], Takao Mori[3], Shigeru Okada[4], Toetsu Shishido[2]

[1]Department of Applied Quantum Physics and Nuclear Engineering, Kyushu University, Fukuoka, Japan. [2]Institute for Materials Research, Tohoku University, Sendai, Japan. [3]National Institute for Materials Science, Tsukuba, Japan. [4]Department of Science and Engineering, Kokushikan University, Tokyo, Japan

We have investigated a solid solution range of a single phase with an anti-perovskite cubic type structure, and behaviors of lattice parameters, hardness, and thermogravimetry–differential thermal analysis (TG-DTA) in the anti-perovskite cubic type $La_{1-x}R_xRh_3B$ (R = Gd, Lu and Sc) compounds. The anti-perovskite cubic phase exists over the entire composition range x from 0.0 to 1.0 for all La-Gd, La-Lu and La-Sc systems. Both the lattice parameter and the hardness exhibit a linear dependence on the substitution x. The results of TG-DTA measurements indicate that the oxidation of the compounds in air starts at about 500-600 K. The mixed phases of RBO_3, R_2O_3 and Rh are identified as oxidized products around x = 0.5. The oxidation onset temperature, and weight gains due to the oxidation depend on substitution x.

o54

Unveiling exotic magnetic phase diagram of a non-Heisenberg quasicrystal approximant

Farid Labib[1], Kazuhiro Nawa[2], Shintaro Suzuki[3], Hung-Cheng Wu[2], Asuka Ishikawa[1], Kazuki Inagaki[4], Takenori Fujii[5], Katsuki Kinjo[2], Taku J. Sato[2], Ryuji Tamura[4]

[1]Research Institute of Science and Technology, Tokyo University of Science, Tokyo, Japan. [2]Institute of Multidisciplinary Research for Advanced Materials (IMRAM), Tohoku University, Sendai, Japan. [3]Department of Physical Science, Aoyama Gakuin University, Kanagawa, Japan. [4]Department of Materials Science and Technology, Tokyo University of Science, Tokyo, Japan. [5]Cryogenic Research Center, The University of Tokyo, Tokyo, Japan

A magnetic phase diagram of the non-Heisenberg Tsai-type 1/1 Au-Ga-Tb approximant crystal (AC) has been established across a wide electron-per-atom (e/a) range via magnetization and powder neutron diffraction measurements. The diagram revealed exotic ferromagnetic (FM) and antiferromagnetic (AFM) orders that originate from the unique local spin icosahedron common to icosahedral quasicrystals (iQCs) and ACs; The noncoplanar whirling AFM order is stabilized as the ground state at the e/a of 1.72 or less whereas a noncoplanar whirling FM order was found at the larger e/a of 1.80, with magnetic moments tangential to the Tb icosahedron in both cases. Moreover, the FM/AFM phase selection rule was unveiled in terms of the nearest neighbour (J1) and next nearest neighbour (J2) interactions by numerical calculations on a non-Heisenberg single icosahedron. The present findings will pave the way for understanding the intriguing magnetic orders of not only non-Heisenberg FM/AFM ACs but also non-Heisenberg FM/AFM iQCs, the latter of which are yet to be discovered

o55

Revisiting the $RE_2Pd_3Si_5$ series: flux growth, crystal structure and chemical bonding

Riccardo Freccero, Pavlo Solokha, Serena De Negri

Department of Chemistry and Industrial Chemistry, University of Genoa, Genoa, Italy

Ternary $RE_2M_3X_5$ intermetallics (*RE* = rare earth metal/actinide; *M* = transition metal; *X* = *p*-block element) have attracted attention over the last decades, as recently acknowledged by a dedicated chapter in the Handbook on the Physics and Chemistry of Rare Earths[1]. More than 200 $RE_2M_3X_5$ compounds, crystallizing with eight structure types, have been reported so far, with some representatives displaying intriguing and exotic properties. Over the last ten years, our attention was devoted to the $RE_2Pd_3Ge_5$ series, integrating, and revising literature data with accurate crystal structure solutions, physical properties measurements and bonding analysis[2]. As a natural consequence of these studies, we recently targeted the $RE_2Pd_3Si_5$ series. Although compounds with *RE* = La – Pr, Sm, Eu were already reported, their *oI*40-$U_2Co_3Si_5$ (*Ibam*; № 72) crystal structure was often assigned based on powder data. To ensure the growth of high-quality crystals, a recrystallization in Sn flux was also applied. While the orthorhombic structure was confirmed for the La and Ce analogues, $Pr_2Pd_3Si_5$ and $Nd_2Pd_3Si_5$ were found to crystallize with an *mP*20 ($P2_1/m$; № 12) structure, being a new structure type. Contrary to the *oI*40 compounds containing (2*b*) and (0*b*)Si species, formally obeying the Zintl formalism, the *mP*20 features (1*b*), (2*b*), and (3*b*)Si, hinting toward different bonding scenarios.

[1] Brown, W. K. et al. *Handb. Phys. Chem. Rare Earths* **2023**.
[2] Freccero, R.; et al. *Inorg. Chem.* **2021**, *60*, 3345–3354.

o56

The new $PrNi_6Si_6$ intermetallic: crystal structure, thermal and electrical transport properties in the temperature range 2 - 900 K

Alessia Provino[1,2], Saurabh Singh[3], Ilaria Pallecchi[2], Federico Caglieris[2,4], Marianne Mödlinger[1], Paolo Mele[5], Giovanna Latronico[5], Tsunehiro Takeuchi[3], Pietro Manfrinetti[1,2]

[1]Department of Chemistry, University of Genova, Genova, Italy. [2]Institute SPIN-CNR, Genova, Italy. [3]Toyota Technological Institute - Energy Materials Laboratory, Nagoya, Japan. [4]Department of Physics, University of Genova, Genova, Italy. [5]Shibaura Institute of Technology, Saitama, Japan

We investigated the ternary rare earth intermetallic $PrNi_6Si_6$, a new member of the RNi_6Si_6 series (R=rare earth). This compound crystallizes in the tetragonal YNi_6Si_6-type (*tP*52, *P*-4*b*2), with lattice parameters a = 7.7846(1) Å, c = 11.2144(1) Å, and unit cell volume V_{cell} = 679.58(2) Å^3. This prototype is a tetragonal ordered derivative of the cubic $NaZn_{13}$-type structure.

Magnetization measurements reveal $PrNi_6Si_6$ orders antiferromagnetically with a Néel temperature $T_N \approx$ 9 K. The temperature dependence of the inverse magnetic susceptibility follows the Curie-Weiss law with values of effective magnetic moment (μ_{eff}) and Weiss temperature (Θ_{pm}) of 3.55 μ_B and –4.5 K, respectively. The observed μ_{eff} is close to the theoretical value 3.58 μ_B for the free Pr^{3+} ions, while the negative value of Θ_{pm} corroborates the antiferromagnetic interactions in $PrNi_6Si_6$.

Electrical and thermoelectric transport data indicate that $PrNi_6Si_6$ exhibits metallic behavior across the entire temperature range 2 - 900 K. Thermal conductivity, k, is as low as 6 W K^{-1} m^{-1} at room temperature, which is due to either scattering of phonons, or complex crystal structure and weak Pr chemical bonds. The specific heat, C_P, above room temperature is ≈ 0.42 J K^{-1} g^{-1}, which is consistent with the high number of atoms per unit cell. The peculiar combination of metallic conductivity and low thermal conductivity of this material makes it promising for applications in systems where thermal insulation must be maintained.

o57

An ab-initio theory of vibrational inelastic tunneling spectrum of magnetic molecules adsorbed on superconductors

Athanasios Koliogiorgos, Richard Korytár

Charles University, Prague, Czech Republic

We present an efficient method of calculating the vibrational spectrum of a magnetic molecule adsorbed on a superconductor, directly related to the first derivative of the tunneling IV curve. The work is motivated by a recent scanning-tunneling spectroscopy of lead phthalocyanine (PbPc) on superconducting Pb(100), showing a wealth of vibrational excitations, the number of which highly exceeds molecular vibrations typically encountered on normal metals [1]. We design a minimal model which represents the inelastic transitions by the spectral function of a frontier orbital of the molecule in isolation. In this way, the initially intractable interacting electron-vibrational problem allows for an exact solution. The model parameters are supplied from an ab-initio calculation, where the presence of the surface on the deformation of molecular geometry can be taken into account. The spectral function of the highest-occupied molecular orbital of the anionic $PbPc^{1-}$ shows the best agreement with the experimental reference among other molecular charge states and orbitaldsa.

[1] Homberg, J.; Weismann, A.; Markussen, T.; Berndt, R. Phys. Rev. Lett. 2022, 129, 116801.

o58

Large magnetostriction and anisotropy energy in FePt and Fe_5Ta_2

Dominik Legut[1,2], Tengfei Xu[3], Zhiyang Zheng[3], Ruifeng Zhang[3]

[1]Charles University, Prague, Czech Republic. [2]VSB Technical University of Ostrava, Ostrava, Czech Republic. [3]Beihang University, Beijing, China

Magneto-crystalline anisotropy is one of the fundamental quantities for permanent magnets, but not only. We have carefully analyzed its origin, i.e. for Fe_5Ta_2[1]. However, there are other magnetic properties related to it e.g. magnetostriction and magnetoelasticity. Utilizing the in-house developed approach[2] the origin of the anisotropic magnetocrystalline energy (MAE) guided by the spin-orbit coupling (SOC) in the ordered L10 -FePt phase is analyzed and discussed by means of theoretical calculations showing excellent agreement with the known experimental studies. A systematic analysis of the MAE, magnetostriction,and magnetoelasticity by means of first-principles plane-wave calculations and post-processing of calculated eigenvalues (orbital energies) and functions (orbital occupancies) are done to establish their correlations. Our study includes the convolution of the projected wave function (density of states) of each orbital of the Fe and Pt sub-lattices into orbital energies. The current novel technique shows the orbital contributions to MAE and magnetoelasticity in accordance with the plane-wave total energies including SOC, which have not been discussed earlier. We also explore the complete anisotropic magnetostriction of this material, finding a significant magnetostrictive (λ) performance of the order about $\lambda \sim 10{-}4 - 10{-}3$ in some particular crystallographic directions of the ordered crystal model, also known in the experiment. However, the poly-crystalline model of L10-FePt based on the uniform stress approximation, leads to a sharp decline in the overall magnetostrictive behavior due to the linear combination of the single crystal magnetostrictive coefficients in the standard numerical techniques, leaving us with an explanation of the lower magnetostriction for polycrystalline thin-films as known also in the latest laboratory research[3-4].

[1] S. Arapan, P. Nieves. H. C. Herper, D. Legut, Computational screening of Fe-Ta hard magnetic phases, **Phys. Rev. B 101**, 014426 (2020).
[2] P. Nieves, S. Arapan, S.H. Zhang, A.P. Kądzielawa, R.F. Zhang, D. Legut, Automated calculations of exchange magnetostriction, *Computational Materials Science* **224** (2023) 112158.
[3] D. Legut, T. Das, P. Nieves, Origin of Larger Magnetostriction and Anisotropy Energy in L10-FePt, *International Journal of Engineering Science* (under review)
[4] P. Nieves, D. Legut, Influence of grain morphology and orientation on saturation magnetostriction of polycrystalline Terfenol-D, *Solid State Communications* **352** (2022) 114825.
[5] P. Nieves, S. Arapan, A. P. Kądzielawa, D. Legut, MAELASviewer: An Online Tool to Visualize Magnetostriction, *Sensors* **20**, (2020) 6436

o59

Phonons and superconductivity of high entropy alloys

Sylwia Gutowska[1], Bartlomiej Wiendlocha[2]

[1]University of Vienna, Vienna, Austria. [2]AGH UST in Krakow, Krakow, Poland

In this study, we employ first-principles calculations to investigate the phonons of superconducting High Entropy Alloys (HEAs) for the first time.

HEAs are metallic alloys consisting of at least five elements, typically in equiatomic or near-equiatomic proportions, which contributes to their high configurational entropy. They exhibit various properties such as enhanced strength, hardness, corrosion resistance, and superconductivity. While the electronic structure of a few superconducting HEAs has been studied, their phonon structure remains unknown, hindering a comprehensive exploration of their superconducting properties.

We focus on a superconducting HEAs composed of Nb, Ta, Hf, Zr, and Ti, with a critical temperature of approximately 7.5 K. Previous studies have indicated that its electronic structure is not significantly influenced by chemical disorder, likely due to the similar chemical nature of its constituents. However, it have remained unclear whether the same holds true for phonons.

Through density functional theory simulations employing the VASP software and the supercell method, we investigate the electronic structure, phonon spectra, and electron-phonon coupling mechanisms of these HEAs. Our results reveal that phonons are much more sensitive to chemical disorder, providing new insights into the influence of chemical disorder on superconductivity in these complex systems.

o60

Lattice dynamical properties and its thermal conductivity in two-dimensional Boron Nitride (BN) and Graphene

Svitlana Pastukh[1,2], Dominik Legut[1]

[1]IT4Innovations, VSB - Technical University of Ostrava, 708 00 Ostrava, Czech Republic, Ostrava, Czech Republic. [2]The Henryk Niewodniczański Institute of Nuclear Physics Polish Academy of Sciences 31-342, Kraków, Poland

Two-dimensional (2D) materials, particularly boron nitride (BN) and graphene, have garnered substantial attention owing to their distinctive characteristics and promising applications. This contribution presents a comparative analysis of the lattice dynamical properties with respect to the thermal conductivity of these materials. Utilizing first-principles computational methods based on density functional theory and its determination of atomic forces we are able to capture the atomic vibrations in quasi-harmonic approximation as well as if and how strong the anharmonicity is presented. Anharmonic effects are meticulously considered using the temperature-dependent effective potential approach, offering valuable insights into the ramifications of non-ideal vibrational behavior on thermal transport. The findings unveil discernible traits in the dynamical properties of BN and graphene, elucidating the influence of factors such as LO-TO splitting and anharmonic corrections of various orders. Additionally, the thermal conductivity of BN undergoes comprehensive scrutiny, showcasing commendable congruence with experimental observations. We comment on the heat capacity of single vibration modes, the group velocities, as well as for the lifetime of phonon-phonon interactions pointing to the distinctive behavior between graphene and BN.

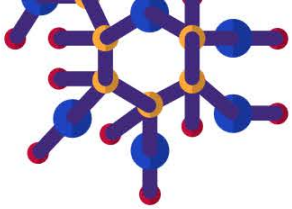

pl08

PLENARY: Mass renormalisation and superconductivity in quantum materials

Malte Grosche

Cavendish Laboratory, University of Cambridge, Cambridge, United Kingdom

Correlated electron systems often display enhanced effective masses of the charge carriers as well as a tendency towards long-range order. Where a continuous phase transition into a magnetically ordered state is suppressed to zero, near a magnetic quantum critical point, anomalous low temperature transport or thermodynamic properties are frequently observed, sometimes accompanied by unconventional superconductivity. This talk will discuss the combination of base-line mass enhancement caused by local interactions and the emergence of long-range interactions near a quantum critical point with the help of recent examples in NiS_2 [1], YFe_2Ge_2 [2], $CeSb_2$ [3], and UTe_2 [4].

[1] Semeniuk, K. *et al,* PNAS e2301456120 (2023)
[2] Baglo, J. *et al,* Phys. Rev. Lett. **129,** 046402 (2022)
[3] Squire, O.P. *et al,* Phys. Rev. Lett. **131,** 026001 (2023)
[4] Eaton, A. G. *et al,* Nature Comm. **15**:223 (2024)

pl09

PLENARY: Optical detection of symmetry breakings in ferroic and multiferroic materials

Tsuyoshi Kimura

University of Tokyo, Bynkyo-ku, Tokyo, Japan

The symmetry breaking ascribed to the evolution of an order parameter is one of the most important concepts in materials physics. Representative examples are symmetry breakings in “ferroic” materials such as the symmetry breaking of time reversal in ferro-magnets and that of space inversion in ferro-electrics. Thus, one can find that this concept contributes to not only fundamental science but also materials’ functionalities available for device applications. Furthermore, recent research developments of “multiferroic” materials have triggered extensive studies on unconventional ferroic materials such as “ferro-toroidic” and “ferro-axial” materials.

In this presentation, I show optical phenomena induced by symmetry breakings in various ferroic and multiferroic materials. The phenomena include nonreciprocal directional dichroism and nonreciprocal rotation of reflected light in multiferroic materials and electrogyration and electric-field-induced magneto-chiral dichroism in ferro-axial materials. Furthermore, in general, ferroic materials bear “domain” structures, that is, spatial distributions of order parameters. Here, I also show ways to spatially resolve domain structures in these ferroic and multiferroic materials by using the abovementioned optical phenomena.

This work has been done in collaboration with T. Hayashida, K. Arakawa, and K. Kimura.

o62

Metal hydridoborates, novel energy storage materials

Radovan Černý

University of Geneva, Geneva, Geneva, Switzerland

Sodium salts of large-cage hydridoborates $[B_xH_x]^{2-}$ (x = 10,12), and their C-derivatives $[CB_{x-1}H_x]^-$ have proven to be promising Na-based solid-state electrolytes [1]. Fast cationic motion generally occurs after a polymorphic transition towards higher-symmetry phases. This order-disorder phase transition provides structures with more free sites for the cations, improved conduction pathways as well as increased rotational energy of the anion cages, which enhances the cation motion. However, such phase transition usually occurs above room temperature (*rt*), thus hampering practical applications. Lowering the temperature of phase transition has been made possible by chemical tuning, i.e. mixing anionic hydridoborate clusters and by physical or mechanical treatment [2-3].

The 3*d* transition metal and magnesium hydridoborates $M^{x+}(B_{12}H_{12})_x$ have been studied as electrodes with the idea of identical chemistry on the interface with the electrolyte [4,5]. More chemical research is needed to stabilize the compounds with the transition metal in a higher oxidation state.

[1] Černý R., Brighi M., Murgia F., *Chemistry* (Easton). **2020**, *2*, 805
[2] Brighi M., Murgia F., Černý R., *Cell Press Phys Sci*. **2020**, *1*, 100217
[3] Murgia F. *et al*., *Appl. Materials Interfaces*. **2021**, *13*, 61346
[4] Didelot E., Sadikin Y., Łodziana Z. and Černý R., *Solid State Sciences* **2019**, *90*, 86-94
[5] Didelot E., Łodziana Z., Murgia F. and Černý R., *Crystals* **2019**, *9*(7), 372

o63

H_2 production and storage: New active and stable Ni_xFe_y catalysts supported on conductive ball-milling prepared titanium oxides for OER in alkaline medium and design of light HEA's for H_2 storage.

Victor RAUD[1,2], Claudia GOMES DE MORAIS[1], Aurélien HABRIOUX[1], Jean-Louis BOBET[2], Laurence PIRAULT-ROY[1]

[1]IC2MP, Poitiers, France. [2]ICMCB, Bordeaux, France

In order to boost decarbonisation of industries, H_2 can be used as an energy carrier in the future energetic grid as it can be produced by water electrolysis, assisted by renewable energies leading to low CO_2 emissions. Water electrolysis in alkaline medium is attractive because it aims to use new electrocatalysts based on "low-cost" transition elements. Thus, the design of catalysts able to decrease the cell tension especially for Oxygen Evolution Reaction (OER) requires to develop new active phase supported on oxides exhibiting high conductivity, specific surface and corrosion resistance properties. This study is focused on the development of conductive TiO_x species using ball milling as an activation energy source to produce a support for metallic active phases in alkaline medium OER. Ni and Fe were then deposited onto this support by a simple wet impregnation process and a soft thermal reduction to target the following formula $Ni_{1-x}Fe_x$. The XRD analysis of the catalysts points out the formation of conductive Ti_2O_3 after the active phase addition. Afterwards, the Ni-Fe loading influence and the Ni/Fe ratio were investigated. The 30% $Ni_{0.5}Fe_{0.5}$ appears to be the best catalyst with a potential, close to the target value, of only 1.54 V *vs.* RHE to reach a current density of 10 mA cm^{-2}. Long term stability and post-mortem characterizations were carried out to check the stability of the catalysts under harsh conditions.

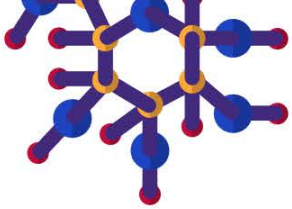

o64

Light elements (H, O, F) insertion into the RScSi (R = La, Nd, Pr) intermetallics: Structural studies and a gateway to catalysis applications

Khaled Alabd, Etienne Gaudin, Sophie Tencé

CNRS, Univ. Bordeaux, Bordeaux INP, ICMCB, UMR 5026, Bordeaux, France

Research involving applications of the intermetallics of the RTX type (R = rare earth, T = Transition metal, X = metalloids) has been rapidly growing. In ammonia synthesis, RTX were used as Ru catalyst support [1]. Especially intermetallics of the CeFeSi and CeScSi structure types. The main player in the catalysis applications are their empty crystallographic sites, mainly the R_4 tetrahedral for CeFeSi and R_4 tetrahedral and Sc_4R_2 octahedral for CeScSi.

Recently, our group insert light elements like F and O in the R_4 site of LaFeSi by topotactic routes. F was inserted in LaFeSi using C_4F_8 while O was inserted by heating it under air leading to the formation of $LaFeSiO_{1-x}$ and $LaFeSiF_{1-x,}$ both of them were superconductors [2].

When we extended our study to CeScSi structures, we discovered that F can be inserted in the Sc_4R_2 site while the R_4 site remains empty. When RScSi materials were heated under air at 350°C, neutron diffraction experiments showed that O was inserted into the Sc_4R_2 site while H was inserted into R_4 site simultaneously, leading to compositions like $LaScSiO_{0.36(1)}H_{0.89(2)}$ and $PrScSiO_{0.28(1)}H_{0.36(1)}$. Pure oxygen gas was also used to insert only oxygen into LaScSi at 350°C, making it a possible catalyst for the ORR in fuel cells. The new materials showed interesting magnetic properties like the ferromagnetic $PrScSiO_{0.28(1)}H_{0.36(1)}$ with T_c = 72 K.

[1] Croisé, C. *et al.,* ChemCatChem **e202201172** (2023)
[2] Vaney, J. B. *et al.,* Nature Communications **13**, (2022)

o65

Collinear magnetic structures induced by ferroelectric distortion in multiferroic quadruple perovskites $BiM_3Cr_4O_{12}$ and $BiMn_7O_{12}$

Stanislav Kamba[1], André Maia[1], Rui Vilarinho[2], Joaquim Agostinho Moreira[2], Christelle Kadlec[1], Petr Proschek[3], Alexei A. Belik[4]

[1]Institute of Physics of the Czech Academy of Sciences, Prague 8, Czech Republic. [2]University of Porto, Porto, Portugal. [3]Charles University, Prague, Czech Republic. [4]Research Center for Materials Nanoarchitectonics (WPI-MANA), National Institute for Materials Science (NIMS), Tsukuba, Japan

Multiferroic materials are divided into type I multiferroics, where magnetic and ferroelectric ordering occurs independently at different temperatures, and type II multiferroics, where spin interactions in the magnetic phase induce weak ferroelectric polarization. In the former case (e.g. $BiFeO_3$), although the ferroelectric polarization is strong, the magnetoelectric coupling is weak. In the second case (e.g. $TbMnO_3$) the magnetoelectric coupling is very strong, but critical Tc are usually low.

We report a new type of multiferroics where a displacive ferroelectric phase transition triggers the antiferromagnetic ordering of Cr spins in $BiMn_3Cr_4O_{12}$. Both ferroelectric and magnetic phase transitions occur at the same temperature of 125 K. The Mn spins are further antiferromagnetically ordered at 50 K. [1]

In the case of $BiMn_7O_{12}$, a series of three structural (including two displacive ferroelectric) phase transitions above room temperature and three magnetic phase transitions below 60 K occur.[2] Recent NPD studies revealed that polar distortion in the ferroelectric phase stabilizes the collinear magnetic structure due to trilinear coupling of order parameters.[3]

In our talk we will show the results of magnetic and pyroelectric measurements together with lattice dynamics studied by THz, IR and Raman spectroscopy.

[1] A. Maia *et al.* J. Eur. Ceram. Soc. **43**, 2479 (2023)
[2] A. Maia *et al.* arXiv:**2401.02808**
[3] D. Behr *et al.* PRB **107**, L140402 (2023)

o66

$RuIn_6Sn_6O_{16}$, $Ru_4In_2Sn_{20}O_{21}$ and $Ir_3In_3Sn_{12}O_{14}$ - Synthesis and structural characterization of novel transition metal oxide clusters

Mohammed Abdelbassit[1], Samuel Yick[1,2], Tilo Söhnel[1,2]

[1]University of Auckland, Auckland, New Zealand. [2]MacDiarmid Institute for Advanced Materials and Nanotechnology, Wellington, New Zealand

A key structural feature across the stannate clusters is the formation of MSn_6-octahedra filled with different transition metals, forming isolated or one-dimensional endless chains through shared corners and edges of the $[MSn_6]$-octahedra [1]. Compounds like $RuSn_6[MO_4]O_4$ (M = Si, Al, Mn, Fe, Co, Zn, Mg) and $(M, M')_4X_2Sn_7O_{16}$ (M,M' = Fe, Mn; X = Si, Ge), where $[MSn_6]$-octahedra do not condense, have been found [1-4].

A group of novel cluster compounds $Ir_3In_3Sn_{12}O_{14}$, $RuIn_6Sn_6O_{16}$ and $Ru_4In_2Sn_{20}O_{21}$ have recently been discovered, which exhibit new types of structures with proposed In+ and In3+ sites in addition to the possible oxidation states of Sn^{2+} and Sn^{1+}. Out of the three cluster compounds, only $RuIn_6Sn_6O_{16}$ contains highly ordered Sn/In sites with alternating discrete $RuSn_6$ octahedra encapsulated in an indium oxide 3D-substructure substructure. $Ru_4In_2Sn_{20}O_{21}$ shows the formation of isolated and condensed $RuSn_6$ clusters in the same compound for the first time. So far, only isolated or condensed clusters could be found in a compound. $Ru_4In_2Sn_{20}O_{21}$ could be seen as a combination of $Ru_3Sn_{15}O_{14}$ and a (hypothetical) $RuSn_6[SnO_4]O_4$. $Ir_3In_3Sn_{12}O_{14}$ crystallises in the $Ru_3Sn_{15}O_{14}$ structure type.

[1] Reichelt W., Söhnel T. *et al.*, Angew. Chem. Int. Ed. 1995, 34, 2113; Söhnel, T., *et al.* Z. Anorg. Allg. Chem. 2000, **626**, 223; Anorg. Allg. Chem. 2008, 634, 2082; Z. Anorg. Allg. Chem., 624, 708-714, 1998.
[2] Allison MC, *et al.* Chem. Mater. 2020, 34, 1369.

o67

Sliding ferroelectricity in bulk misfit layered compound $(BiS)_{1.24}CrS_2$

Jiří Volný[1], Kateřina Tetalová[1], Klára Uhlířová[1], Cinthia Correa[2,1], Tim Verhagen[2,1]

[1]Charles University, Prague, Czech Republic. [2]Institute of Physics, Prague, Czech Republic

Sliding ferroelectricity exists only in 2D materials where the out-of-plane polarization is switched by in-plane interlayer sliding and thus breaking the inversion symmetry [1]. So far, sliding ferroelectrics have been mostly observed in artificially created van der Waals multilayers, where manually exfoliated 2D layers are stacked on top of each other with a small twist angle between the individual layers [2]. Misfit layer compounds (MLC) are naturally grown heterostructures consisting of alternating layers of two different 2D materials forming an ordered superstructure. Recently, sliding ferroelectricity has been observed in bulk misfit layered compound $(PbS)_{1.12}VS_2$[3] where the mutual interaction between the two subsystem introduces twins with a small mutual twist, breaking the inversion symmetry.In this work we focus on another MLC compound $(BiS)_{1.24}CrS_2$ formed by alternating layers of transition metal monochalcogenide BiS and transition metal dichalcogenide CrS_2. Bulk $(BiS)_{1.24}CrS_2$ is stable at ambient conditions and exhibits sliding ferroelectric behaviour. Ferroelectric domains of sizes varying between tens of nm up to tens of µm were observed using scanning electron microscopy and scanning probe microscopy. We show that ferroelectric domains of arbitrary shape can be written using focused electron beam.

[1] L. Li and M. Wu, ACS Nano **11**, 6382 (2018)
[2] A. Weston *et al*, Nature nanotechnology **17**, 390 (2022)
[3] C. A. Correa *et al*, **arXiv:2306.14446** (2023)

o68

Structure and bonding of compounds in the Sc-rich part of the Sc-{Mn,Fe,Co,Ni,Pd,Pt}-Ga systems

V.V. Romaka[1,2], G. Rogl[1], J. Bursik[3], A. Grytsiv[1], G. Giester[4], P. Rogl[1]

[1]Institute of Materials Chemistry, University of Vienna, Vienna, Austria. [2]Leibniz Institute for Solid State and Materials Research Dresden (IFW Dresden), Dresden, Germany. [3]Institute of Physics of Materials, Czech Academy of Sciences, Brno, Czech Republic. [4]Institute of Mineralogy and Crystallography, University of Vienna, Vienna, Austria

Although Sc shows outstanding technological potential in scandium-reinforced light alloys with good corrosion resistance, the Sc-containing systems with transition elements and gallium still lack information on the formation, structure, bonding, and properties of the corresponding Sc-rich ternary phases [1].

Our recent investigation of the Sc-{Mn,Fe,Co,Ni,Pd,Pt}-Ga systems revealed the formation of a series of homologous compounds $Sc_{54}\{M,Ga\}_{17}$ for M = Mn, Fe, Co, Pd, and Pt, which appeared to be isotypic with the $Hf_{54}Os_{17}$-type structure (space group *Immm*). Most of these phases have limited homogeneity regions, while $Sc_{54}(Pt_{1-x}Ga_x)_{17}$ exhibits at 850°C a large homogeneity region ($0<x<0.28$) extending from Ga-rich $Sc_{76}Pt_{17.5}Ga_{6.8} \equiv Sc_{54}(Pt_{0.72}Ga_{0.28})_{17}$ to novel binary $Sc_{54}Pt_{17}$. However, we observe an opposite effect against the usual trend of solid solution hardening, which is less pronounced for $Sc_{54}(Pd_{1-x}Ga_x)_{17}$ than for $Sc_{54}(Pt_{1-x}Ga_x)_{17}$. In addition to the detailed structural analysis of the two new compounds in the Sc-Co-Ga system: $Sc_{50}Co_{13}Ga_3$ (space group *F*-3*m*), ε-$Mg_{26-x}Ag_{7+x}$ type, and $Sc_6Co_{1.73+x+y}Ga_{1-x}$ (space group *Immm;* x=0.43; y=0.14), Ho_6Co_2Ga derivative type, we present a detailed DFT study of chemical bonding, band structure, thermodynamic and elastic properties for all studied compounds and related kappa phases.

[1] B.Ya. Kotur, E. Gratz, "Handbook on the Physics and Chemistry of Rare Earths (ed. K.A. Gschneidner, L.R. Eyring), NH, vol. 27, 339-533 (1999).

o69

Lattice, magnetic, and in-gap optical states in van der Waals antiferromagnet VCl_3

Dávid Hovančík[1], Amit Pawbake[2], Fedir Borodavka[3], Jan Dzian[4], Martin Veis[4], Milan Orlita[2], Clement Faugeras[2], Stanislav Kamba[3], Vladimír Sechovský[1], Jiří Pospíšil[1]

[1]Charles University, Faculty of Mathematics and Physics, Prague, Czech Republic. [2]LNCMI, CNRS, EMFL, Université Grenoble Alpes, Grenoble, France. [3]Institute of Physics, Czech Academy of Sciences, Prague, Czech Republic. [4]Institute of Physics of Charles University, Prague, Czech Republic

A recently proposed picture of Mott-Hubbart insulator VCl_3 hosting 2D magnetic polarons has attracted more interest in the material and stimulated further studies as such states are less explored. We used magneto-spectroscopy methods (Raman scattering and photoluminescence) to probe the lattice, magnetic and electronic properties of VCl_3. Temperature-dependent Raman scattering shows the change (splitting, activation, energy trend change) of the k=0 phonon modes spectra just below 100 K, which we ascribe to a structural transition. At around 25 K we detected additional changes in the phonon spectra accompanied by the appearance of a broad spectral weight at low wavenumbers associated with the antiferromagnetic (AFM) order (T_N = 21K). The field-dependent Raman data (out-of-plane field) revealed that the fundamental magnon gap is split at zero field, pointing to a biaxial magnetic anisotropy. In addition, we discovered another excitation at higher energies susceptible to magnetic field resembling magnon behavior. Photoluminescence measurements in the near-infrared range exhibit multiple in-gap excitations at around 1.1 eV below T_N, with one of the excitations showing clear splitting in the applied magnetic field. Our unique findings provide insight into the structure and magnetic state evolution of VCl_3. Likewise, the data set indicates a possible correlation between emitted photons and spins in a layered AFM state, providing a path for studying magneto-optics in 2D materials.

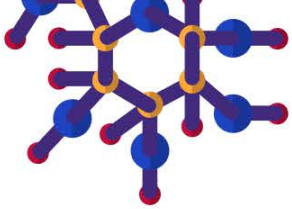

o70

Unconventional magnetic and magneto-transport properties of tetragonal $RbCo_2As_2$

Abhishek Pandey

Materials Physics Research Institute, School of Physics, University of the Witwatersrand, Johannesburg, Gauteng, South Africa

ACo_2As_2 (*A* = alkali metal/alkaline earth metal) compounds that crystallize in the $ThCr_2Si_2$-type tetragonal structure present a classic example of the role played by structural parameters and resultant interatomic bondings in governing the electronic as well as the magnetic ground state of a material [1-4]. The investigations performed so far establish that several properties of these compounds delicately depend upon the interlayer As-As distance, which regulates the oxidation state of the Co-ions by controlling the extent of interlayer As-As bonds [4]. In this work, we present an investigation of structural, thermal, electrical, magneto-electrical, and magnetic properties of the single crystals of a novel compound $RbCo_2As_2$. Consistent with the previous studies on ACo_2As_2 compounds, our results establish the decisive role played by interlayer bondings in realizing the rather unusual magnetic and electronic properties of $RbCo_2As_2$. Further, we report on the observation of an unusual and anisotropic magnetoresistance in this compound which attains extremely high values at low temperatures in magnetic fields of a few Tesla. To our knowledge, this is the first instance where this kind of unusual anisotropic magnetoresistance behavior is observed in any $ThCr_2Si_2$-type material.

o71

Comparative study of magnetocaloric effect in the $RE_5T_2In_4$ (RE = Gd–Tm, T – transition metals = Pt, Pd, Rh) compounds

Altifani Rizky Hayyu[1,2], Stanisław Baran[2], Andrzej Szytuła[2]

[1]Jagiellonian University, Doctoral School of Exact and Natural Sciences, Faculty of Physics, Astronomy and Applied Computer Science, Kraków, Poland. [2]M. Smoluchowski Institute of Physics, Jagiellonian University, Kraków, Poland

The $RE_5T_2In_4$ (RE = Gd–Tm, T – transition metals = Pt, Pd, Rh) rare earth intermetallic compounds crystallize in an orthorhombic crystal structure of the $Lu_5Ni_2In_4$-type (*Pbam* space group, No. 55) with the rare earth occupying with three different Wyckoff positions. The compounds have been investigated using X-ray diffraction, as well as by DC and AC magnetometric measurements. Based on this experimental research, the maximum magnetic entropy change, the temperature averaged entropy change (TEC), relative cooling power (RCP), and refrigerant capacity (RC) values have been determined and compared to those of the isostructural $RE_5Ni_2In_4$ as well as to those of other rare earth intermetallics with good magnetocaloric performance [1-3]. The $RE_5T_2In_4$ compounds show quite good magnetocaloric performance at low temperatures with magnetic entropy change exceeding 10 $J \cdot kg^{-1} \cdot K^{-1}$ under magnetic flux density change of 0–7 T for selected chemical compositions. Such a performance makes the investigated compounds good candidates for application in low-temperature magnetic refrigeration, especially in cascade cooling systems.

[1] A. R. Hayyu *et al.*, arXiv cond-mat.mtrl-sci, 2212.0717 (2022)
[2] S. Baran *et al.*, Journal of Alloys and Compounds, **877**, 160171 (2021)
[3] Z. Zhang *et al.*, Intermetallics, **100**, 136-141 (2018)

o72

Magnetic properties at ambient and under high pressure in Ho_3Co

Srikanta Goswami[1,2], M. S. Henriques[1], V. Petříček[1], P. D. Babu[2]

[1]Institute of Physics of the Czech Academy of Sciences, Prague, Czech Republic. [2]UGC-DAE Consortium for Scientific Research, Mumbai Centre, Mumbai, India

The rare earth rich intermetallic compounds of type R_3T (R = rare earth and T = transition metals) exhibit various interesting magnetic properties emerging out of their complex magnetic structures. Among this family, Ho_3Co is an interesting case that has been studied in the present experimental work in terms of dc magnetization, specific heat, ac-susceptibility and neutron powder diffraction measurements. Bulk magnetic measurements at ambient condition predominantly suggest that the magnetic structure below the Néel temperature at T_N (= 21 K) changes continuously until another antiferromagnetic (AFM) transition occurs at T_t (= 9 K). The incommensurate modulated magnetic structures were solved by magnetic superpace formalism. The magnetic superspace group describing the spin configuration realized in Ho_3Co explains the evolution of the structures with temperature and supports the speculations drawn from the bulk magnetic measurements. Below T_t, the magnetic modulation is anharmonic. Further, frequency dependent experiments reveal the coexistence of spin glass like states with non-collinear AFM order at low temperature. Externally applied pressure wipes out the low temperature magnetic transition at T_t. The AFM interactions are strengthened with increasing pressure at low temperature while the weak signature of spin glass like state remains up to 1.10 GPa.

o73

Misfit layered compounds, a route towards natural morié lattices

Klara Uhlirova[1], Cinthia Antunes Corrêa[1], Jiri Volny[1], Katerina Tetalova[1], Vaclav Petricek[2], Tim Verhagen[1]

[1]Charles University, Faculty of Mathematics and Physics, Prague, Czech Republic. [2]Institute of Physics of the Czech Academy of Sciences, Prague, Czech Republic

Moiré lattices of van der Waals materials are under intense study for engineering interfacial states, leading to various phenomena such as sliding ferroelectricity, superconductivity, or moiré excitons [1-3]. For low angles between adjacent van der Waals layers, the atomic scale lattice reconstruction lowers the energy of the stacks, leading to atomic scale reconstruction into microscopic domains with different stacking orders.

Misfit layered compounds (MLCs)are natural van der Waals superlattices formed by MX and TX layers (where T = Ti, V, Cr or Ta and M = Sn, Sb, Pb or Bi or even rare earth, X = S or Se), alternately stacked along the *c*-axis. Within the basal plane, the MX and TX_2 are incommensurate due to the different lattice parameters of each layer. Using a $(PbS)_{1.11}VS_2$ as a representative, we have demonstrated that MLCs create reconstructed moiré lattices. Single crystal x-diffraction and high-resolution transmission electron microscopy have shown that single crystals of MLCs are naturally mosaic with many twins. The moiré reconstructed domains, being ferroelectric or ferroelastic, were imaged by scanning electron microscopy using secondary electron channeling contrast, atomic force and electric force microscopy, and photoemission electron microscopy. The domains have triangular or lamellar shapes with sizes from hundreds of nanometers to tens of micrometers, suggesting various twist angles ranging from 1 to 0. 01°, respectively. MLCs, therefore, bring possibilities for studies of interface-clean moiré systems without the complex fabrication of twisted artificial van der Waals latices.

[1] K.F. Mak & J. Shan, *Nature Nanotechnology* **17**, 390 (2022)
[2] C. Wang et al., *Nature Materials* **22**, pages 542–552 (2023)
[3] A. Weston et al., *Nature Nanotechnology* **17**, 390 (2022)
[4] C.A. Correa et al., *arXiv*:**2306.14446** (2023)

o74

Physics and chemistry of UTe_2

Eteri Svanidze

MPI CPfS, Dresden, Germany

Unconventional superconductor UTe_2 has attracted much attention since its discovery in 2019.[1,2] Still, many questions remain regarding the intrinsic crystal structure and its affect on the physical properties. In particular, it has been shown that the crystals of UTe_2 can be grown in several different ways – Te-flux,[1] chemical vapour transport,[3,4] and salt flux.[5] While previous reports [3,6–8] have related the differences between T_c, residual resistivity ratio, shape and height of the specific heat anomaly to the particular features of the synthesis route, the complete understanding of underlying chemical features that cause these differences remains unknown. I will discuss a comprehensive review on the sample-dependence of UTe_2 and provide microscopic insight into the origin of differences, reported so far for this peculiar system.

[1] Ran, S. *et al. Science* **365**, 684–687 (2019).
[2] Aoki, D. *et al. J. Phys. Condens. Matter* **34**, 243002 (2022).
[3] Cairns, L. P. *et al. J. Phys. Condens. Matter* **32**, 415602-1–6 (2020).
[4] Yao, S. *et al. CrystEngComm* **24**, 6262–6268 (2022).
[5] Sakai, H. *et al. Phys. Rev. Mater.* **6**, (2022).
[6] Thomas, S. M. *et al. Phys. Rev. B* **104**, 224501 (2021).
[7] Ikeda, S. *et al. J. Phys. Soc. Japan* **75**, 116–118 (2006).
[8] Haga, Y. *et al. J. Phys. Condens. Matter* **34**, 7 (2022).

o75

Lattice dynamics of UTe_2 in high magnetic fields studied by ultrasound

Michal Vališka[1], Tetiana Haidamak[1], Andrej Cabala[1], Jiří Pospíšil[1], Gaël Bastien[1], Tatsuya Yanagisawa[2], Petr Opletal[3], Hironori Sakai[3], Yoshinori Haga[3], Atsuhiko Miyata[4], Sergei Zherlitsyn[4], Vladimír Sechovský[1], Jan Prokleška[1]

[1]Charles University, Prague, Czech Republic. [2]Hokkaido University, Sapporo, Japan. [3]Japan Atomic Energy Agency, Tokai, Japan. [4]Helmholtz-Zentrum Dresden-Rossendorf, Dresden, Germany

We present a study of high-quality single crystals of UTe_2 with $T_c \approx 2$ K employing ultrasound and magnetostriction measurements performed in high magnetic pulse fields up to 60 T and down to 0.4 K [1]. Careful analysis of the data for four different accessible modes C_{33}, C_{44}, C_{55}, and C_{66} allowed us to reveal the dramatic softening at the Critical End-Point (CEP) found in UTe_2. It is the finite phase region where the first-order metamagnetic transition placed at 35 T for the field applied along the *b* axis changes to a broad cross-over transition to the field-polarized paramagnetic state at an elevated temperature of around 8 K. This is in agreement with the previous high-field studies of magnetoresistance and magnetization [2,3] where CEP was also detected. We follow the similar softening of the elastic constants at CEP in another itinerant f-electron system where the applied magnetic field induces the metamagnetic transition - UCoAl. We further traced the signatures of changes in the selected elastic constants C_{ij} of UTe_2 connected to the entering of the superconducting state at a low temperature below T_c and a magnetic field below H_{c2}. Comparative ultrasound measurements of the elastic constants were performed with the magnetic field applied in the *b-c* plane tilted by 30° to see the imprint of the high-field-induced superconducting phase which exists confined in the polarized paramagnetic state. These results bring further information to the magnetic field phase diagram of UTe_2 and the possible symmetries of its superconducting phases.

[1] M. Vališka, *arXiv:***2307.01884** (2023)
[2] A. Miyake et al., *J. Phys. Soc. Jpn.* **88** (2019) 063706
[3] W. Knafo et al., *J. Phys. Soc. Jpn.* **88** (2019) 063705

o76

Evolution of electronic structure across the U-Te series of compositions

Evgenia Tereshina-Chitrova[1], Ladislav Havela[2], Martin Diviš[2], Oleksandr Romanyuk[1], Oleksandra Koloskova[2], Sonu George Alex[1], Thomas Gouder[3]

[1]Institute of Physics of the Czech Academy of Sciences, Prague, Czech Republic. [2]Faculty of Mathematics and Physics, Charles University, Prague, Czech Republic. [3]European Commission, Joint Research Centre (JRC), Karlsruhe, Germany

Uranium tellurides exhibit a wide range of phenomena that span magnetism [1] to unconventional superconductivity [2]. Of particular interest is understanding the behaviour of 5*f* electrons across diverse U-Te compositions. Relativistic effects, strong electron correlations, and ligand hybridization contribute to the complexity of observed effects. In this study, we conduct photoemission experiments on freshly prepared surfaces of U_xTe_y thin films under ultra-high vacuum (UHV) conditions (10^{-11} mbar), which eliminates concerns related to surface contamination. By comparing the evolution of experimental U-4*f* core-level X-ray Photoelectron Spectroscopy (XPS) spectra with valence band spectra assessed by Ultraviolet Spectroscopy (UPS), we aim to elucidate changes in electronic structures across various uranium telluride stoichiometries. Our objective is to integrate our understanding of these compounds' magnetism with photoemission spectra to establish systematic trends across the U-Te series.

[1] Suski et al., *Phys. Stat. Sol. (a)* **14**, K157 (1972).
[2] S. Ran et al., *Science* **365**, 684 (2019).

o77

New uranium-based arsenides: A small review

Nazar Zaremba, Mitja Krnel, Yuri Prots, Marcus König, Lev Akselrud, Yuri Grin, Eteri Svanidze

Max-Planck-Institut für Chemische Physik fester Stoffe, Dresden, Germany

Iron-based high-temperature superconductors still pose many open questions even after nearly two decades of intense research. While small energy scales of analogous actinide- and lanthanide-based materials likely prohibit the existence of similarly high-temperature superconductivity, it is certainly fruitful to investigate what happens when 4*f* and 5*f* orbitals are introduced into these structures. In this talk, I will showcase some of our recent work on iron and cobalt-based arsenides. We will revisit the U-Fe-As, U-Co-As, and U-Rh-As ternary systems, in which five compounds have been reported to exist so far – U*M*As_2 (*M* = Fe and Co) (*P*4/*nmm* space group), $U_2Co_{12}As_7$ (*P*-6 space group), $URh_{1.55}As_{1.91}$ (*I*4*cm* space group) and $URh_{1.51}As_{1.78}$ (*P*4/*nmm* space group). By implementing flux synthesis, we were able to grow large single crystals of several new phases [1,2]. Their chemical and physical were studied in detail, revealing anti- and ferromagnetic orders.

[1] N. Zaremba, M. Krnel, Yu. Prots, M. König, L. Akselrud, Yu. Grin, and E. Svanidze, *Inorg. Chem.,* accepted (2024)
[2] N. Zaremba, M. Krnel, Yu. Prots, M. König, L. Akselrud, Yu. Grin, and E. Svanidze, in preparation (2024)

o78

System Thorium - Boron - Carbon, revisited

Peter Rogl[1], Raimund Podloucky[1], Henri Noel[2], Gerald Giester[1]

[1]Universitaet Wien, Wien, Austria. [2]University of Rennes, Rennes, France

As generation IV nuclear fuels include actinoid carbides in combination with B_4C control rods, interest has been revived in the corresponding phase relations for the Th-B-C system. Secondly, the study of topological states in condensed-matter systems has recently also focused on thorium boron carbides.

In the present paper we have studied the thermodynamic stabilities via DFT heat of formation data along two sections, which involve all the ternary thorium boron carbides: ThB_4 - ThC_2 and B - ThC. A similar analysis has been made for the corresponding U-sections.

DFT calculations by application of VASP were made for all thorium boron carbides as well as for the homologous uranium boron carbides (including also isotypic CeB_2C). For the exchange correlation functional the general gradient approximation was utilized. Optimized structural parameters were in good agreement with the experimental values. Relativistic calculations by including spin-orbit coupling for the electronic structure were performed. Atomic volumes and charges were computed by the concept of Bader yielding the ionic charges and the charge transfer among the atoms.

Based on metastable ThB_2 and a new structure determination of $ThB_{\sim 60}$ (former ThB_{66}) we have revised the phase relations for the Th-B-C system.

o79

Revisiting the Strontium-Mercury phase diagram

Rachel Nixon[1,2], Yurii Prots[1], Mitja Krnel[1], Nazar Zaremba[1], Marcus Schmidt[1], Yuri Grin[1], Eteri Svanidze[1]

[1]Max Planck Institute for Chemical Physics of Solids, Dresden, Saxony, Germany. [2]University of St Andrews, St Andrews, Fife, United Kingdom

Mercury-based materials and their applications have been of interest for decades[1-3]. The first Sr-amalgam was reported in 1954[4], with the first study on a binary phase diagram in 1974[5]. Over fifty years the binary was developed and revised, with focus on the Hg-rich region[6-8]. Efforts were aimed at understanding crystallographic features, with work on physical properties unfeasible. Similar to other Hg-based systems, these compounds are air-sensitive, requiring special laboratory conditions for synthesis and characterization[9-11]. We have synthesised large, single crystals of two Sr-Hg phases showing conventional superconductivity at low temperatures. By comparing crystallographic features of these new systems with other Sr-Hg compounds and alkali-based amalgams, we aim to uncover connections between chemical features and resultant ground states.

[1] Sappl, J. *et al. Crystals* **7**, (2017).
[2] Pelloquin, D. *et al*. *Phys. C Supercond. its Appl.* **216**, 257–263 (1993).
[3] König, M. *et al. Science* **318**, 766–770 (2007).
[4] Ferro, R. *Acta Cryst.* **7**, 781 (1954).
[5] Bruzzone, G. & Merlo, F. *J. Less-Common Met.* **35**, 153–157 (1974).
[6] Tkachuk, A. V. & Mar, A. *Inorg. Chem.* **47**, 1313–1318 (2008).
[7] Tkachuk, A. V. & Mar, A. *Dalt. Trans.* **39**, 7132–7135 (2010).
[8] Wendorff, M. & Röhr, C. *Z Kristallogr. Cryst. Mater.* **233**, 515–529 (2018).
[9] Prots, Y. *et al. Inorg. Chem.* **61**, 15444-15451 (2022).
[10] Witthaut, K. *et al. ACS Org. Inorg.* **3**, 143–150 (2023).
[11] Prots, Y. *et al. Phys. Rev. B* **106**, L060412 (2022).

o80

From industry to lab: Pioneering automated sample preparation

Tomáš Červeň, David Sviták, Damian Wałoszek, Štěpán Venclík, Nikolaos Biniskos, Petr Čermák

Charles University, Prague, Czech Republic

In the modern era, there is a significant emphasis on transferring knowledge from basic research to applied research and, subsequently, to its industrial application. This represents a challenging task, as the worlds of industry and science operate on different principles. However, isn't it time for science to instead learn from the knowledge and techniques utilized in industrial sectors?

New technologies that have been gradually transforming the industry for several years are now also making their way into the field of solid-state materials physics. We will demonstrate how neural networks are predicting physical models, how big data are uncovering new materials, how Bayesian optimization is accelerating demanding experiments and contributing to environmental conservation. The integration of robots and automation processes, familiar in large-scale factories, into sample preparation (e.g. [1]) not only makes the entire process more efficient and faster but also renders the sample preparation process (especially for monocrystals) fully reproducible through precise measurement of hundreds of parameters.

We will be presenting the Automatic Laue Sample Aligner (ALSA) prototype [2], which fully automates the process of arranging monocrystals using X-ray Laue diffraction, robotic manipulators, real-time camera recognition, and specialized artificial intelligence-based software for analyzing crystal placement. The ALSA device represents a revolutionary change in the field of sample preparation, as it drastically speeds up the process and significantly increases the precision of arrangement.

This talk aims to provide a comprehensive overview of the evolution of automated sample preparation and its pivotal role in enhancing the capacity for scientific inquiry and innovation.

[1] Szymanski, N.J., Rendy, B., Fei, Y. *et al. Nature* **624**, 86–91 (2023).
[2] https://mambaproject.cz/alsa

o81

Elevating cancer treatment with advanced dosimeters and crystal precision

Cristiana Rodrigues[1,2,3], António Pereira Gonçalves[1], João Gentil Saraiva[2], Luís Peralta[2,4]

[1]Centro de Ciências e Tecnologias Nucleares (C2TN), Departamento de Engenharia e Ciências Nucleares (DECN), Instituto Superior Técnico (IST), Universidade de Lisboa, Lisbon, Portugal. [2]Laboratório de Instrumentação e Física Experimental de Partículas (LIP), Lisbon, Portugal. [3]Faculdade de Ciências, Universidade de Lisboa, Lisbon, Portugal. [4]Faculdade de Ciências da Universidade de Lisboa, Lisbon, Portugal

Understanding the intricate effects of radiation at the microscale is pivotal for advancing cancer treatment strategies. This study focuses on the development of cutting-edge passive dosimeters that are able to achieve microscale sensitivity and improve such description. Corundum (Al_2O_3) single crystals were grown isothermally by the flux method, with a Li_2O–MoO_3 flux system. Herein, we report the effect of preparation conditions on crystal quality, which influences the overall performance of the detector. Li_2O concentration ranged from 2% to 15% mol of the total flux. Crystal growth occurred by heating a mixture of Al_2O_3 and the flux at 1150°C for 72 hours. Crystal transparency improved with increasing amount of Li_2O, possibly due to more controlled nucleation related to the slower flux evaporation. The most suitable flux composition to grow high-quality transparent Al_2O_3 single crystals was found to be 15% mol Li2O – 85% mol MoO_3. Subsequently, to achieve the standard composition for the Fluorescent Nuclear Tracking Detector, carbon and magnesium doped Al_2O_3 will be produced. To further enhance the detectors' efficiency (i.e., improved signal-to-noise ratios and heightened detection accuracy) and sensitivity to low-mass particles, novel doping combinations including transition metals, such as copper, zinc, nickel and chromium, will be explored.

o82

Elastic and inelastic neutron scattering studies in ternary boride $YbPt_5B_2$

Leonid Salamakha[1], Oksana sologub[1], Herwig Michor[1], Dmitry Khalyavin[2], Manh Duc Le[2], Devashibhai Adroja[2], Ernst Bauer[1]

[1]TU Wien, Wien, Austria. [2]ISIS Neutron and Muon Facility, Chilton, United Kingdom

Ternary compounds $YbPt_5B_2$ and $LuPt_5B_2$ have been characterized quite recently [1]. $YbPt_5B_2$ exhibits two magnetic phase transitions at T_{mag1} ~ 8 K and T_{mag2} ~ 4 K. To resolve the magnetic structure of $YbPt_5B_2$ and crystalline electric field (CEF) features, elastic and inelastic neutron studies have been carried out at ISIS.

Elastic neutron studies essentially confirmed the previous bulk measurements, revealing antiferromagnetic (AFM) transitions at T_{N1} ~ 8 K and T_{N2} ~ 4 K. While simple AFM was obtained for $T < T_{N2}$ with a propagation vector k_{com} = (0,0,0) and Yb-magnetic-moments as large as 3.04 μ_B (T = 1.5 K), k dramatically modifies for $T_{N2} < T < T_{N1}$, revealing an incommensurate structure k_{incom} = (0.1938725, 0, -0.0446576), with a temperature dependent variation of the respective (hkl) values. Modifications of the magnetic structure and the respective magnetic moments owing the application of external fields were derived from these studies, too.

In order to explain temperature dependent quantities, such as the specific heat or the magnetic susceptibility of $YbPt_5B_2$, the knowledge of the CEF is indispensable. The present inelastic neutron studies allowed to derive the CEF scheme and associated magnetic moments. A doublet as ground state with a predominant |7/2> ground state explains the magnetic moments at low temperature. The respective level scheme with excited CEF levels at 11, 25 and 34 meV excellently accounts for the almost constant magnetic entropy below 100 K.

[1] L. Salamakha, et al., *PRB* **105**, 205112 (2022).

o83

Angle-resolved magnetoresistance in the strongly anisotropic quantum magnet TmB_4

Slavomír Gabáni[1], Július Bačkai[1,2], Gabriel Pristáš[1], Matúš Orendáč[1], Karol Flachbart[1], Kirill Krasikov[3], Nikolay Sluchanko[3], Konrad Siemensmeyer[4], Natalya Shitsevalova[5]

[1]Institute of Experimental Physics, Slovak Academy of Sciences, Košice, Slovakia. [2]Faculty of Electrical Engineering and Informatics, Technical University, Košice, Slovakia. [3]Prokhorov General Physics Institute, Russian Academy of Sciences, Moscow, Russian Federation. [4]Helmholtz-Zentrum Berlin, Berlin, Germany. [5]Institute for Problems of Materials Science, National Academy of Sciences of Ukraine, Kiev, Ukraine

Precise angle-resolved magnetoresistance (ARMR) measurements in various magnetic fields enabled us to create illustrative distributions of $\Delta\rho/\rho(\phi, H)$ in TmB_4, where ϕ is the angle between the sample c axis and applied magnetic field H. These distributions reveal the charge transport anisotropy in this strongly Ising anisotropic quantum antiferromagnet with a geometrically frustrated Shastry-Sutherland lattice exhibiting fractional magnetization plateaus. While in the paramagnetic region $\Delta\rho/\rho(\phi, H)$ reaches its maxima for $H \perp c$, below the Néel temperature $T_N = 11.7$ K the situation is different. Here the main MR features appear for H // c, i.e., along the easy axis of magnetic anisotropy, and correspond to magnetic phases and phase transitions between them. It is interesting that all the above features (maxima) related with the scattering of conduction electrons on spin magnetic structure are related with fractional magnetization plateaus. Above the field of magnetic saturation, moreover, significant MR maxima have been observed at certain angles which correspond to specific directions in the crystal lattice, pointing to field directions in which the scattering of conduction electrons on the magnetic structure is the highest. Thus, ARMR appears to be a sensitive experimental tool reflecting the angular dependence of the interplay between charge carriers and magnetic structure as a function of temperature and applied magnetic field.

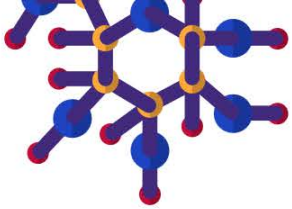

pl10

PLENARY: Antiferromagnetism, ferrimagnetism, magnetization reversal and linear magnetoelectricity in $A_4Nb_2O_9$ where A=3d (Mn,Fe,Co,Ni) magnetic elements

Antoine Maignan, Christine Martin

CNRS, Caen, France

Honeycomb (HC) antiferromagnets (AF) are candidates for showing quantum critical points and for AF based spintronic. Searching for large magnetoelectric (ME) coupling, the Linear ME AF compounds form a third class of multiferroics: upon magnetic field application a polarization P proportional to H is induced, α-Cr_2O_3 (*P*$\bar{3}$*c*1) being its prototype. This motivated the study of the *P*$\bar{3}$*c*1 LME $M_4Nb(Ta)_2O_9$ "429" [1], with structures made of two HC layers.

Considering the existence of several $M_{4-x}M''_xM'_2O_9$ solid solutions, the M'' dilution was exploited to generate LME properties in $Fe_2Co_2(Nb/Ta)_2O_9$ and $Fe_3NiNb_2O_9$ [2-4] overpassing those of the limit members. $Ni_4Nb_2O_9$ is a ferrimagnetic 429 (*Pbcn* structure). It exhibits an anisotropic magnetization switching [5, 6], and Zn for Ni in $Ni_4Nb_2O_9$ allowed to enhance its magnetization reversal [7,8].

In this presentation, selected examples of substitution by 3d cations in 429 will be chosen to illustrate their properties richness.

[1] E. F. Bertaut et al., *J. Phys. Chem. Solids* **21**, 234 (1961).
[2] A. Maignan et al, *J. Mater. Chem. C* **9**, 14236 (2021).
[3] A. Maignan et al,, *Z. Anorg. Allg. Chem.* **648**, e202200011 (2022).
[4] A. Maignan et al, *Solid State Sci.* **125**, 106821 (2022).
[5] B. Meng, et al, *J. Low Temp. Phys.* **207**, 115-126 (2022).
[6] C. Martin, et al, *J. Phys.: Condens. Mater* (in press)
[7] J.P. Bolletta, et al, *J. Appl. Phys*. **132**, 153901 (2022).
[8] E. Rufeil Fiori, et al, *J. Phys.: Condens. Matter* **36**, 015801 (2024).

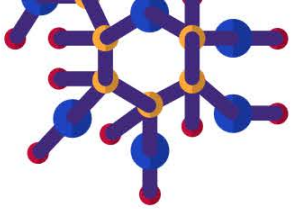

p01

High-field magnetoacoustics of a $Dy_2Fe_{14}Si_3$ single crystal

A.V. Andreev[1], D.I. Gorbunov[2], T. Nomura[2], S. Zherlitsyn[2]

[1]Institute of Physics ASCR, Na Slovance 2, 18221, Prague, Czech Republic. [2]Hochfeld-Magnetlabor Dresden, Helmholtz-Zentrum Dresden-Rossendorf, 01328, Dresden, Germany

Magnetic properties of rare-earth intermetallic compound $Dy_2Fe_{14}Si_3$ are determined by 4f electrons of Dy, 3d electrons of Fe and their intersublattice interactions. It is a highly-anisotropic ferrimagnet with M_s = 8 m_B and T_C = 500 K. The large magnetic anisotropy is of the easy-plane type with the [100] axis is an easy magnetization direction. Large anisotropy is observed also within the basal plane. In magnetic fields applied along the easy [100] axis, the magnetization jump is observed in 33 T (at 2 K). The transition has a 3 T hysteresis confirmed its first-order type. The critical field of the transition increases with temperature. The field-induced transition of the second-order type is observed in field 41 T (at 2 K) along the [120] axis.

Both transitions are accompanied by pronounced anomalies in acoustic properties - relative changes of sound velocity and changes of sound attenuation. Along the [100] axis, $\Delta v/v$ jumps up at low temperatures. In field applied along the [120] axis, $\Delta v/v$ has a deep minimum at the transition. Effect in the sound attenuation $\Delta\alpha$ is a sharp maximum along the both axes.

An additional acoustic effect $\Delta v/v$ was observed in field applied along the [120], the hard axis within the basal plane, starting at 100 K up to 160 K where the anisotropy field within the basal plane, $H_a^{[120]}$, becomes considerably lower than at low temperatures where the $M(H)$ curve is determined first of all by field-induced non-collinearity of the sublattices. Similar effect decorated anisotropy field at elevated temperatures (above 200 K) was observed also in fields applied along the hardest axis [001]. In both cases no anomaly was observed in the sound attenuation.

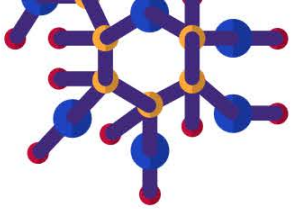

p02

Enhanced superconducting critical parameters in a new high-entropy alloy $Nb_{0.34}Ti_{0.33}Zr_{0.14}Ta_{0.11}Hf_{0.08}$

Rafał Idczak[1], Wojciech Nowak[1,2], Bartosz Rusin[1], Rafał Topolnicki[1,3], Tomasz Ossowski[1], Michał Babij[2], Adam Pikul[2]

[1]Institute of Experimental Physics, University of Wrocław, Wrocław, Poland. [2]Institute of Low Temperature and Structural Reaseach, Polish Academy of Sciences, Wrocław, Poland. [3]Dioscuri Center in Topological Data Analysis, Institute of Mathematics, Polish Academy of Sciences, Wrocław, Poland

High entropy alloys (HEAs) are defined as a homogeneous mixture of five or more elements, each with an atomic content between 5% and 35%. The compositions of HEAs result in distinct physical properties that cannot be explained by simply adding the properties of the individual components. In particulars, such alloys are known for their exceptional mechanical properties, thermal stability, and corrosion resistance. Therefore, they are considered materials with high potential for applications such as high-durability mechanical devices or magnets. Moreover, the discovery of the first superconducting high-entropy alloy $Ta_{0.34}Nb_{0.33}Hf_{0.08}Zr_{0.14}Ti_{0.11}$ (Koželj *et al.* 2014) has opened up new possibilities for their use as mechanically durable superconductors.

This contribution reports on the formation and physical properties of a new high-entropy alloy $Nb_{0.34}Ti_{0.33}Zr_{0.14}Ta_{0.11}Hf_{0.08}$. The alloy has a simple body-centered cubic (bcc) structure, and compositional analysis reveals a homogeneous distribution of alloying elements in the studied sample. The physical properties of the alloy suggest that it exhibits a conventional type II superconductivity, with a critical temperature of T_c = 7.5 K and an upper critical field of $\mu_0 H_{c2}$ = 12.2(1) T. Electronic structure calculations, performed within Density Functional Theory (DFT), support the experimental results. The discussion compares the obtained results with corresponding data reported for other HEA superconductors.

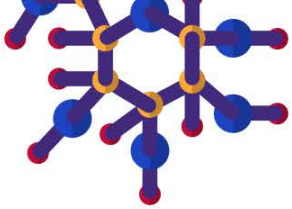

p03

Possible realization of the Majumdar-Ghosh point in the mineral szenicsite

Adam Berlie[1], Ian Terry[2]

[1]ISIS Neutron and Muon Source, Didcot, Oxfordshire, United Kingdom. [2]Durham University, Durham, Co. Durham, United Kingdom

The Majumder-Ghosh (MG) point is a point in parameter space for a 1D frustrated system where $\alpha = J_1/J_2 = 0.5$ and the ground state has been shown to be a superposition of singlet states. This leads to no magnetic order, instead the ground state is dominated by electronic dynamics. Szenicsite ($Cu_3(MoO_4)OH)_4$) is a natural mineral, that has central 1D chains of Cu^{2+} ions, with side chains of Cu^{2+} ion that dimerise and antiferromagentically order. The resultant ground state is dominated by the magnetism of the isolated 1D chains. In this work we have used muon spin spectroscopy to demonstrate that szenicsite does not magnetically order down to 100 mK, and there is an absence of a spin gap, with 1D magnetic excitations dominating [1], commensurate with the system being on the MG point.

[1] Adam Berlie and Ian Terry. *Phys. Rev. B*, **105**, L220404 (2022)

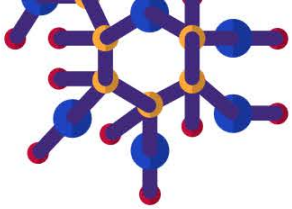

p04

Investigation of vacuum cryodeposited water films capturing carbon monoxide on an optical surface

Yevgeniy Korshikov, Abdurakhman Aldiyarov, Assel Nurmukan, Dmitriy Sokolov

Al Farabi Kazakh National University, Almaty, Kazakhstan

In recent years, many researchers have focused their attention on studying interstellar dust and astrophysical ices. These objects are of particular interest because they are key components of the interstellar medium and play an important role in the formation of stars and planets. The following feature of studying the properties of vacuum cryodeposited films expands modern knowledge about the processes of formation of clathrates and hydrates in mixtures of CO and H_2O, their physical characteristics, as well as the appearance of certain features depending on the method of formation. Capturing and storing carbon monoxide molecules is one of the most promising strategies to combat global warming, a potential environmental disaster.

The purpose of this work is to study the IR spectra of thin films of a mixture of carbon monoxide and water, obtained by vapor deposition, in the temperature range 11–180 K. Based on the analysis of the spectra, the formation of hydrates and clathrates, which are of interest for modern condensed matter physics, was studied. To carry out the research, methods of IR spectroscopy, Mass spectroscopy and optical analysis of the resulting thin films were used. During the experiments, CO hydrate and gas hydrate structures formed in the mixture. In this case, the sublimation temperature of CO molecules bound into hydrate structures becomes much higher than the equilibrium values. For the selected concentration of CO (25%) – H_2O (75%), changes in the observed spectra and data obtained using mass spectroscopy indicate incomplete hydration of the mixture. Some CO molecules remain unbound and sublimate earlier. The results obtained expand modern knowledge about the processes of formation of clathrates and hydrates in mixtures of CO and H_2O, their physical characteristics, as well as the appearance of certain features depending on the method of formation.

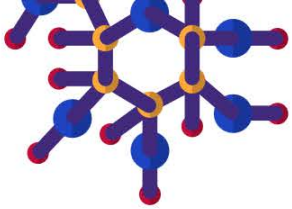

p09

In situ diffraction study of the phase transformations occurring in the thermoelectric colusite $Cu_{26}V_2Sn_6S_{32}$

Florentine Guiot[1], Abdelhamid Bourhim[2], Gabin Guélou[2], Catherine Dejoie[3], Andy Fitch[4], Emmanuel Guilmeau[2], Pierric Lemoine[5], Carmelo Prestipino[2]
[1]Institut des Sciences Chimiques de Rennes, Rennes, France. [2]CRISMAT, Caen, France. [3]ESRF, Grenoble, Estonia. [4]ESRF, Grenoble, France. [5]Institut Jean Lamour, Nancy, France

Interest in thermoelectric (TE) technology has been continuously growing in the last decade driven to the necessity to limiting waste heat during energy transformation. Derivatives of the natural mineral colusite, with general formula $Cu_{26}A_2E_6S_{32}$, (A=V,Nb,Ta,Cr,Mo,W;E=Ge,Sn,As,Sb), are an emerging class of excellent thermoelectric materials.[1] As example, the ZT value of the colusite $Cu_{26}V_2Sn_6S_{32}$ rises to near unity at 675K, making this material one of the best p-type TE in this temperature region.[2] Its performances are mainly related to the coexistence of an ordered (*P*-43*n*) and a disordered (*F*-43*m*) forms obtained after sintering at 1023K (i.e. sample H), leading to a very low thermal conductivity.[3] In addition, colusite V-Sn is known to exhibit an intrinsic exsolution phenomenon.[4]In this study, we investigated by *in-situ* synchrotron powder diffraction the solid-state phase equilibrium as function of the temperature between the ordered and disordered forms of colusite V-Sn. The use of high-resolution setup revealed a complex behavior with several phase transformations, probably related to a mutual interaction and kinetic effects.

[1]G. Guélou,et al., Applied Materials Today **22**, 100948 (2021).
[2] C. Bourgès, et al. J. Am. Chem. Soc. **140**, 2186 (2018).
[3]C. Candolfi,et al. Phys. Rev. Materials **4**, 025404 (2020).
[4] K. Suekuni,et al., Appl. Phys. Lett. **105**, 132107 (2014).

p10

Thickness dependence on the properties of sputtered-AZO thin film on flexible substrate for transparent heater

Thimada Woraporntassana, Kanchanee Niyom, Watcharee Rattanasakulthong

Kasetsart University, Bangkok, Thailand

Aluminum-doped ZnO film with different thicknesses of 87, 136, 181, 252 and 310 nm on a flexible substrate was prepared using the RF-sputtering technique. The major peak of the AZO phase in the (002) plane and the minor peaks of (103) and (004) planes were observed except on the 87 nm film. The peak intensities were increased with increasing thickness. The films thicker than 100 nm showed that the surface roughness was increased, and the surface morphology consisted of a columnar-like structure with a different size distribution with increasing thickness. Alternatively, a continuous grain surface with a lower surface roughness was found on the 87 nm film. The electrical resistance was decreased with increasing film thickness. The average optical transmission of all AZO films was about 80% in a 550-1100 nm wavelength range and kept constant with a tiny wave pattern in a 600-1100 nm wavelength range. The Joule heating effect measurement found that the film temperature was increased with the applied voltage, and the 310 nm film showed a maximum temperature of 49°C when a voltage of 14 V was applied with the highest roughness, bandgap, figure of merit, and the lowest resistivity. The results indicated that thickness manipulated the structure and surface morphology, affecting the optical and electrical properties, and was strongly related to the heat released from the AZO films.

p11

Strong electron-phonon coupling and superconducting gap in Heusler-type superconductor $ScAu_2Al$

Gabriel Kuderowicz, Bartłomiej Wiendlocha

Faculty of Physics and Applied Computer Science, AGH University of Kraków, Kraków, Poland

Heusler compounds is a large family of intermetallics with over a thousand systems. They remain a very active field of research because of plethora of physical properties which can be easily tuned by chemical substitution and pressure. To our knowledge, superconductivity was reported in less than 50 Heusler compounds to date. These materials are low temperature superconductors, with transition temperature T_c below 6 K, and the pairing is the electron-phonon interaction. Recently characterized $ScAu_2Al$ was reported to have T_c=5.1 K [1] which is one of the highest among Heusler compounds. To better understand superconductivity in $ScAu_2Al$ we performed ab initio calculations [2]. We examined the electronic-structure, phonons and electron-phonon coupling using Quantum Espresso [3,4] and we calculated the superconducting gap with Superconducting Toolkit [5]. In the electronic structure a van Hove singularity appears 10 meV below the Fermi level. The electron-phonon coupling constant λ=1.25 is the highest among Heusler compounds and it classifies $ScAu_2Al$ in a strong coupling regime. Obtained T_c=5.4 K is in a good agreement with the experiment. The spin-orbit coupling significantly changes the electronic structure and phonons. With removed degeneracy the flat electronic bands move away form the Fermi level and acoustic phonon modes are strongly softened. The calculated superconducting gap exhibits moderate anisotropy.

Acknowledgements

This work was supported by the National Science Centre (Poland), Project No. 2017/26/E/ST3/00119 and in part by the PL-Grid infrastructure.

[1] B. Bag et al., *J.Phys.: Condens.Matter* **34**, 195403 (2022).
[2] G. Kuderowicz et al., *Phys. Rev. B* **108**, 224501 (2023).
[2] P. Giannozzi et al., *J.Phys.: Condens.Matter* **21**, 395502 (2009).
[3] P. Giannozzi et al., *J.Phys.: Condens.Matter* **29**, 465901 (2017).
[4] M. Kawamura et al., *Phys. Rev. B* **95**, 054506 (2017).

p12

Superconductivity in medium- and high-entropy alloy thin films

Gabriel Pristáš[1], Július Bačkai[1,2], Matúš Orendáč[1], Slavomír Gabáni[1], Filip Košuth[1,3], Marek Kuzmiak[1,2], Pavol Szabó[1], Emil Gažo[1], Robert Franz[4], Sabrina Hirn[4], Georg C. Gruber[4], Christian Mitterer[4], Serhii Vorobiov[3], Karol Flachbart[1]

[1]Institute of Experimental Physics, Slovak Academy of Sciences, Košice, Slovakia. [2]Faculty of Electrical Engineering and Informatics, Technical University, Košice, Slovakia. [3]Institute of Physics, P.J. Šafárik University, Košice, Slovakia. [4]Department of Material Science, Montanuniversität Leoben, Leoben, Austria

We have prepared and investigated superconducting $Nb_{67}Hf_{11}Ti_{11}Zr_{11}$ and $Nb_{35}Ta_{35}Hf_{10}Ti_{10}Zr_{10}$ medium and high-entropy alloys in form of thin films with thicknesses of 600, 100, and 30 nm, and compared theirproperties with bulk counterparts. We have shown that the superconducting transition temperature T_c as well as the upper critical magnetic field $B_{c2(0)}$ decrease with decreasing thickness. Application of hydrostatic pressure up to 33 kbar on the 600-nm $Nb_{35}Ta_{35}Hf_{10}Ti_{10}Zr_{10}$ film shows a decrease of T_c with pressure, which differs from that observed on bulk sample. Moreover, we performed point-contact spectroscopy measurements on the 600-nm $Nb_{67}Hf_{11}Ti_{11}Zr_{11}$ and $Nb_{35}Ta_{35}Hf_{10}Ti_{10}Zr_{10}$ films and were able to observe directly the temperature development of the superconducting energy gap $\Delta(T)$ and determine the superconducting coupling strength $2\Delta/k_BT_c = 3.54$ and $2\Delta/k_BT_c = 4.21$, respectively, which is consistent with that of conventional *s*-wave phonon-mediated Bardeen-Cooper-Schrieffer superconductors [1].

[1] G. Pristáš et al., *Physical Review B* **107**, 024505 (2023).

p13

Exploring a new method in the field of metal hydrides

Christohe CONA

CNRS icmcb, Bordeaux, France

Nowadays the world depends mainly on fossil fuels and this dependence leads to significant CO_2 emissions which has a significant impact on our environment.

The challenge ahead is therefore to find clean and renewable energy. Hydrogen appears to be an energy vector meeting current criteria. It has the advantage of being more energetic than oil and only releases water when it burns. However, it is difficult to store and produce (at low cost and without CO_2 emissions). There are different methods for storing and producing hydrogen. The aim of this work was to develop a new method based on the use of microwaves.

We already have demonstrated that microwaves have the capacity, in a very short time, to desorb hydrogen from binary hydrides such as TiH_2 or MgH_2. In fact, heating a material by microwave is quick and more efficient than conventional heating.

We were interested in the influence on the desorption kinetics of certain parameters such as the microwave irradiation time, the applied power, the quantity of material, the size of the particles (depending on the type and time grinding). Nevertheless, it is necessary to mix with carbon so that the hydride can absorb under microwaves exposure.

Although, in the case of the well-known intermetallic $LaNi_5$, we managed to reversibly absorb and desorb hydrogen at room temperature and moderate pressure in a few minutes.

This ensures a new avenue of research and first results on other intermetallics (*e.g.* FeTi,…) will be available very soon.

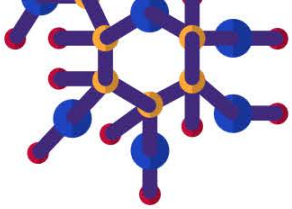

p14

Magnetic Structures of U_nRhIn_{3n+2} Materials

A. Bartha[1], M. Klicpera[1], P. Čermák[1], P. Doležal[1], B. Ouladdiaf[2], J. Custers[1]

[1]Department of Condensed Matter Physics, Charles University, 121 16 Prague, Czech Republic. [2]2Institut Laue Langevin, 71 Avenue des Martyrs, CS 20156, 38042 Grenoble Cedex, France

U-compounds crystallizing in the $HoCoGa_5$-type tetragonal crystal structure (No. 123, P4/*mmm*) exhibit interesting magnetic properties. $UNiGa_5$ orders in the G-type antiferromagnetic (AFM) phase, while $UPdGa_5$ and $UPtGa_5$ show the A-type AFM state. The G-type indicates a three-dimensional Néel state, while A-type refers to a layered AF structure in which spins align ferromagnetically in the *ab* plane and AFM along the c axis [1]. The difference in the two magnetic structures is significant since it implies a sign change of the nearest-neighbor interaction. This comes rather surprising as the U-115 compounds differ only by the substitution of the transition metal ions.

Here we report on synthesis and the magnetic structure determination of $URhIn_5$ and U_2RhIn_8, two new members of the $U_nT_mX_{3n+2m}$ (*T* = transition metal, *X* = In,Ga) family of compounds [2]. Our neutron diffraction experiments on $URhIn_5$ confirmed the magnetic propagation vector being ***k*** = (1/2,1/2,1/2), i.e., G-type, predicted by NMR experiments [3] and a magnetic moment of 1.65 μ_B/U^{3+}. The neutron study on U_2RhIn_8 revealed a propagation vector ***k*** = (1/2,1/2,0), also G-type, and a respective ordered moment of 1.7 μ_B/U^{3+}. We discuss the implication of this result with respect to UIn_3.

[1] A. Bartha *et al.*, J. Magn. Magn. Mater. **381,** 310 (2015)
[2] A. Bartha *et al.*, Acta Phys. Pol. A **127,** 339 (2015)
[3] H. Sakai *et al.* Phys. Rev. B **88,** 045123 (2013)

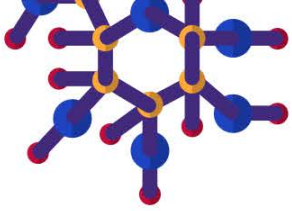

p15

Tailoring the size and shape of actinide compounds

Karin Popa

European Commission, Joint Research Centre (JRC), Karlsruhe, Germany

The JRC-Karlsruhe has broad expertise in the synthesis, processing, and characterization of actinide-containing compounds, including aspects related to the control of powder morphology and microstructure engineering of solid blocks. We summarise here our recent results on (1) production of actinide dioxide nano- and micro-particles and (2) manufacturing of solids with extremely fine or ultra-large grains.

p16

Syntheses and some properties of solid solution Yb(Al,*T*)B_4 (*T*=Fe,Cr,Mo,Mn,W) compounds

Kaoru Kouzu[1], Shigeru Okada[2], Takeshi Hagiwara[2], Akiko Nomura[3], Kunio Yubuta[4], Takao Mori[5,6], Toetsu Shishido[3], Akira Yoshikawa[3]

[1]Kokushikan University, Tokyo, Japan. [2]Kanagawa University, Yokohama, Japan. [3]Tohoku University, Sendai, Japan. [4]Kyushu University, Fukuoka, Japan. [5]National Institute for Materials Science, Tsukuba, Japan. [6]International Center for Materials Nanoarchitectonics, Tsukuba, Japan

RAlB_4 (*R*=rare earth) have attracted increasing attention with recent reports of interesting structural, chemical and physical properties [1]. The authors developed and synthesized of the $YCrB_4$-type solid solution *R*(Al_xT_{1-x})B_4 (*T*=Fe,Cr,Mn,Mo) using the Al flux method. From the result of XRD patterns, Tm($Al_{1-x}Mo_x$)B_4 were obtained as a single phase from the $Al_{1-x}Mo_x$ flux (x=0.005~0.010) [2].

In this study, we investigated the formation of the solid solution Yb($Al_{0.995}T_{0.005}$)B_4 (*T*=Fe,Cr,Mo, Mn,W) compounds in which the Al position of $YbAlB_4$ is substituted with *T* atoms. The resulting crystals were examined for lattice constants and chemical composition, in addition, hardness values by micro-Vickers hardness and oxidation resistance by heating in air with a DTA-TG apparatus.

Comparing the lattice constants of $YbAlB_4$ and Yb($Al_{0.995}T_{0.005}$)B_4, the lattice constant becomes smaller when Cr, Fe, and Mn are included. When Mo and W were included, the values tended to increase. The hardness values of Yb($Al_{0.995}T_{0.005}$)B_4 was within the range of 11.0 (±0.7) to 15.7 (±1.9) GPa. Comparing the hardness of $YbAlB_4$ and solid solution compounds, the hardness tended to be slightly higher when Fe and W were dissolved in solid solution, and slightly lower when Cr, Mo, and Mn were dissolved in solid solution. We discuss oxidation resistance due to heating in air.

[1] T. Mori, *J. Solid State Chem.*, **275**, 70-82 (2019).
[2] S. Okada et al., *Solid State Phenomena*, Vol. **289**, 65-70 (2019).

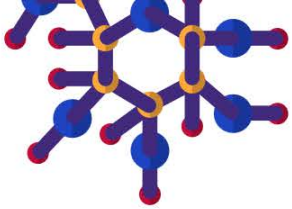

p17

Exploring magnetic transition metal sulfides and their thermoelectric properties

Laura Agnarelli, Antoine Maignan, Denis Pelloquin, Sylvie Hébert

CRISMAT, Caen, France

In the search for environmentally friendly and economical thermoelectric (TE) materials, our research has focused on transition metal sulfides, driven by the abundance and low cost of the constituting elements.[1] Sulfides have garnered attention due to their potential in exhibiting high thermoelectric power factors ($PF=S^2/\rho$; S=Seebeck coefficient and ρ = electrical resistivity), positioning them as viable candidates for sustainable thermoelectric applications. A significant aspect of our study delves into magnetic sulfides, motivated by the influence of magnetism on the transport properties. Specifically, the application of a magnetic field can modulate the figure of merit, *ZT*, through alterations in band structure and the induction of extra entropic terms, consequently affecting thermopower. [2-5] Our presentation shows results on pyrite-derived materials, in particular $Co_{1-x}Fe_xS_2$ ($x \leq 0.30$), highlighting the synergy between their magnetic properties and TE performance. Some preliminary results will be presented for x > 0.30, focusing on the challenges associated with the synthesis of such materials and offering insights into how different Fe concentrations influence the thermoelectric and magnetic behaviors of the materials.

[1] A. V. Powell, J. Appl. Phys. **2019**, 126, 100901
[2] A. Maignan *et al.* Phys. Cond. Matter **2003**, 15, 2711
[3] Y. Wang *et al.* Nature **2003**, 423, 425
[4] S. Hébert *et al.* ZAAC 2022 **2022**, 648, e202200045
[5] S. Hébert *et al.* ZAAC **2023**, 649, e202200324

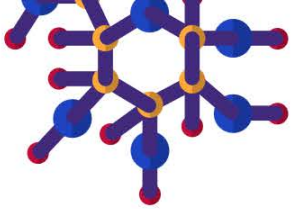

p18

Coupled magnetic-crystallographic transition and associated multi-functional properties in $La_{0.9}Ce_{0.1}Fe_{12}B_6$

Léopold Diop[1], Tom Faske[2], Mehdi Amara[3], Wolfgang Donner[2], Olivier Isnard[3]

[1]Institut Jean Lamour, UMR 7198 CNRS & Université de Lorraine, Nancy, France. [2]Institute of Materials Science, Technical University of Darmstadt, Darmstadt, Germany. [3]Institut Néel, UPR2940 CNRS & Université Grenoble Alpes, Grenoble, France

Magnetoelastic coupling, structural, magnetic, electronic transport, and magnetotransport properties of $La_{0.9}Ce_{0.1}Fe_{12}B_6$ are investigated by means of temperature- and magnetic-field-dependent XRD, magnetization, electrical resistivity, and magnetostriction measurements. The intermetallic compound $La_{0.9}Ce_{0.1}Fe_{12}B_6$ crystallizes in the rhombohedral $SrNi_{12}B_6$ structure type and exhibits multiple magnetic transitions, antiferromagnetic-ferromagnetic [AFM-FM] and ferromagnetic-paramagnetic [FM-PM], driven by changes in both temperature and magnetic field. At low temperatures, the field-induced first-order AFM-FM metamagnetic transition is discontinuous and manifests itself by sharp jumps, giving rise to a unique and unusual avalanche-like behaviour. XRD data reveal a magnetic-field-induced structural phase transition associated with the AFM-FM and PM-FM transformations. The lattice distortion is driven by magnetoelastic coupling and converts the crystal structure from rhombohedral (*R-3m*) to monoclinic (*C2/m*). The AFM and PM states are related to the rhombohedral structure, whereas the FM order develops in the monoclinic symmetry. A huge volume magnetostriction of ~1% accompanies this field-induced symmetry-lowering crystallographic distortion. A highly anisotropic lattice expansion as well as giant negative thermal expansion [NTE] with a volumetric NTE coefficient of −200 ppm/K are observed. Furthermore, a remarkably large negative magnetoresistance [MR] of −78% is discovered.

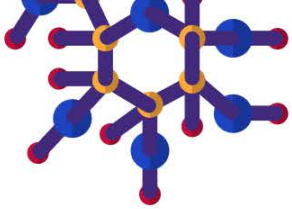

p19

Magnetic field-induced phase transition and weak ferromagnetism in the underdoped PrBCO cuprate

Mahieddine Lahoubi[1], Shengli Pu[2], Weinan Liu[2], Zhe Yang[2]

[1]Badji Mokhtar Annaba University, Annaba, Algeria. [2]University of Shanghai for Science and Technology, Shanghai, China

The magnetic properties of an underdoped $PrBa_2Cu_3O_{6.44}$ ceramic of cuprate family are characterized with magnetization M experiments in low and high dc magnetic fields H. Significant field effects are observed in the derivative $dM(T)/dT$ versus T in the region of $T_{cr} \sim 4.5$ K, $T_2 \sim 6.5$ K and $T_N = 9$ K, which are respectively, the low-critical point, the spin reorientation phase transition temperature, and the Néel temperature of the AFM ordering of the Pr^{3+} sublattice [1]. Using Arrott plot analysis, we identified at 1.35 K weak field-induced phase transitions at two critical fields, $H_{cr1} \sim 3.3$ T and $H_{cr2} \sim 7.5$ T, whose associated transition lines appear to emerge from T_N. Below T_N, the derivatives $dM(H)/dH$ versus H show an increase for H_S in the range of 0.7-1.2 T, where H_S is considered as the specific field above which the weak ferromagnetic (WFM) part settles in both Pr and Cu(2) AFM regimes with the occurrence for metamagnetic-like phase transitions at a threshold-field. From the equation $M(H) = M_S(T) + \chi_d(T)H$ for $H_S < H < 2$ T, we deduced the spontaneous magnetization $M_S(T)$ which decreases as $1/T$, with a shape change when crossing T_N. Whereas the differential magnetic susceptibility $\chi_d(T)$ shows a shape change at T_{cr}, T_2, and T_N. These results are taken as evidence for an additional WFM-like behavior and show that the Pr-Cu(2) magnetic coupling [2] continues well above T_N.

[1] M. Lahoubi, *Physica B* **536** (2018) 12.
[2] A. T. Boothroyd et al., *phys. Rev. Lett.*, **78** (1997] 130.

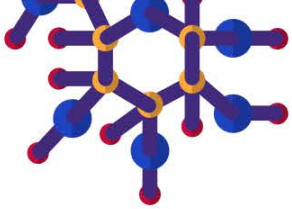

p20

Magnetization Study of the Low Temperature Anomalies in the Substituted Dysprosium-Yttrium Iron Garnets

Mahieddine Lahoubi

Badji Mokhtar Annaba University, Annaba, Algeria

Recently, the $Dy_xY_{3-x}IG$ system ($0 \le x \le 3$) was used as tri-layer heterostructure films for spintronic devices [1]. Based on the study of the anomalous magnetic properties of DyIG due to the appearance of the Belov point $T_B \sim 42$ K [2, 3] predicted earlier for ferrimagnets [4], our attention focused on the T_B anomalies which have been less investigated in this $Dy_xY_{3-x}IG$ system. We report magnetization experiments obtained in the 2-300 K range in high dc magnetic fields H applied on single crystals which have a $T_{comp}(x)$ point. Between $T_{comp}(x)$ and $T_{SR} = 14.62$ K [5] which is the transition temperature of the spin reorientation <111>↔<uuw>, anomalies with minima and maxima are observed at $T_B \sim 42$ K in the temperature variations of some pertinent parameters, independently of x or the three main crystallographic axes. Considering the anisotropy of the crystal field and exchange interactions based on a strong contribution from the spin S, a modified T_B formula is proposed. All results are discussed in connection with the magnetodielectric effect revealed in DyIG [6], together with some concomitant effects due to the Schottky anomaly [2, 3].

[1] M. J. Gross et al., *J. Magn. Magn. Mater.*, **564** (2022) 170043.
[2] A. Boutaba et al., *J. Magn. Magn. Mater.*, **476** (2019) 551.
[3] A. Boutaba et al., *J. Superconduct. Novel Magn.*, **32** (2019) 3087.
[4] K. P. Belov, *Phys. Usp.* **39** (1996) 623.
[5] T. Zhu et al., *AIP Advances* B (2019) 035326.
[6] T. D. Kang et al., *Phys. Rev., B* **86** (2012) 144112.

p22

Quantum Spin Liquid vs. Spin-glass: $S_{(eff)}$ = ½ Pyrochlore Fluoride Antiferromagnets $NaCdCu_2F_7$ & $NaCdCo_2F_7$

Andrej Kancko[1], Gerald Giester[2], Cinthia Antunes Correa[3], Petr Proschek[1], Hironori Sakai[4], Yo Tokunaga[4], Ross Harvey Colman[1]

[1]Charles University, Prague, Czech Republic. [2]Universität Wien, Vienna, Austria. [3]Czech Academy of Sciences, Prague, Czech Republic. [4]Japan Atomic Energy Agency, Tokai, Ibaraki, Japan

The true ground-state of the S = ½ Heisenberg pyrochlore antiferromagnet remains a challenging problem in modern theoretical physics. The system's complexity leads to method-dependent predictions, ranging from dimer singlet phases to chiral spin liquids. [1-3]. Few materials exist to validate these predictions, making ideal realizations highly sought after.

The $NaAM_2F_7$ pyrochlore fluorides (A = Sr^{2+}, Ca^{2+} or Cd^{2+} and M = magnetic transition metal 2+ ion) are a family of near-ideal model materials which, however, suffer from a small magnetic-bond-disorder due to random mixing between Na^+ and A^{2+} ions on the pyrochlore A-site.

We present a magnetic-ground-state characterization of two new additions to this family: $NaCdCu_2F_7$ (S = ½) and $NaCdCo_2F_7$ (S_{eff} = ½). [4] While structurally similar, they exhibit different magnetic-ground-state properties. $NaCdCo_2F_7$ undergoes a spin-freezing transition below T_f = 4 K, while $NaCdCu_2F_7$ shows no magnetic transition down to 100 mK, suggesting it could be an ideal S = ½ Heisenberg pyrochlore antiferromagnet with a quantum spin liquid ground-state.

[1] H. Tsunetsugu, *Phys. Rev. B*, vol. **65**, no. 2 (2002) 1–11
[2] Y. Iqbal et al., *Phys. Rev. X*, vol. **9**, no. 1 (2019) 11005
[3] B. Schneider et al., *Phys. Rev. B* **105** (2022) 125122
[4] A. Kancko et al., *Phys. Scr.*, vol. **98**, no. 7 (2023) 0–11

p23

Fluctuation conductivity and pseudogap in slightly doped $HoBa_2Cu_3O_{7-\delta}$ single crystals

Liudmyla Bludova[1], Eugene Petrenko[1], Ruslan Vovk[2], Andrei Solovjov[1,3]

[1]B.Verkin Institute for Low Temperature Physics and Engineering of NAS of Ukraine, Kharkiv, Ukraine. [2]Physics Department, V. Karazin National University, Kharkiv, Ukraine, Ukraine. [3]Institute for Low Temperatures and Structure Research, Wroclaw, Poland

The effect of annealing at room temperature on the fluctuation conductivity (FLC) $\sigma'(T)$ and pseudogap (PG) $\Delta^*(T)$ in the basal *ab* plane of $ReBa_2Cu_3O_{7-\delta}$ (Re = Ho) single crystals with a lack of oxygen has been studied. It is shown that at all stages of annealing, the FLC near *Tc* can be described by the Aslamazov–Larkin and Maki– Thompson fluctuation theories, demonstrating a 3D–2D crossover with increasing temperature [1]. The crossover temperature T_0 was used to determine the coherence length along the *c* axis, $\xi_c(0) = (2.82 \pm 0.2)$ Å. At the inter-mediate stage of annealing, an anomalous increase in 2D FLC was revealed, which is associated with the influence of uncompensated magnetic moments in $HoBa_2Cu_3O_{7-\delta}$ (HoBCO): $\mu_{eff,\,Ho} = 9.7\mu_B$. For the quenched sample S1, the temperature dependence of the PG has a shape typical of single crystals with a large number of defects. However, $\Delta^*(T)$ has two small additional maxima at high temperature, which is a feature of HoBCO single crystals with pronounced twins and indicates the two-phase nature of the sample. Upon annealing, the shape of $\Delta^*(T)$ noticeably changes, very likely due to an increase in the magnetic interaction (sample S2). More important is the change in the slope of the data at high temperatures, which has become about 3.5 times steeper. The ordering of the oxygen distribution due to the diffusion process during annealing somewhat compensates for the influence of magnetic interaction. But the slope does not change (sample S3).

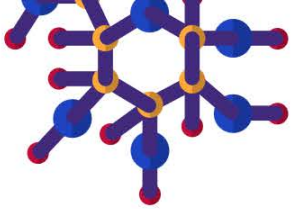

p24

Magnetoelastic properties of UIrGe studied by ultrasound

Tetiana Haidamak[1], Michal Vališka[1], Denis Gorbunov[2], Sergei Zherlitsyn[2], Vladimír Sechovský[1], Jan Prokleška[1]

[1]Charles University, Faculty of Mathematics and Physics, Department of Condensed Matter Physics, Prague, Prague, Czech Republic. [2]Hochfeld-Magnetlabor Dresden (HLD-EMFL), Helmholtz-Zentrum Dresden-Rossendorf, Dresden, Germany

UIrGe is an isostructural and isoelectronic counterpart of the well-known ferromagnetic superconductors UCoGe and URhGe in the family of orthorhombic UTX (*T* = transition metal, *X* = p element) compounds. It is an antiferromagnet with T_N = 16.5 K [1] characterized by complex orthorhombic magnetocrystalline anisotropy [2] and a non-collinear magnetic structure [3]. At temperatures below T_N, it undergoes metamagnetic transitions (MTs) in fields of 21 T and 14 T (at 2 K) applied along the *b*- and *c*-axis, respectively [4]. At low temperatures, the MT is of FOMPT. The observed Ising-like behavior of magnetization is observed despite the metamagnetic states being non-collinear [3]. At higher temperatures up to T_N, the MT is of SOMPT. The FOMPT and SOMPT segments in a magnetic phase diagram are separated by a tricritical point at T_{TCP} [5]. The tricriticality is believed to be a phenomenon present in some Ising collinear antiferromagnets with strong uniaxial anisotropy and competing ferromagnetic and antiferromagnetic exchange interactions. UIrGe represents an exception. We studied magnetoelastic effects of tricriticality in a UIrGe single crystal by measuring elastic constants by ultrasound technique in high pulse magnetic fields up to 50 T at temperatures down to 1.4 K. Two elastic modes: longitudinal C_{22} and transversal C_{66} were investigated with the magnetic field applied along the *b*-axis. Both show the tricritical behavior for sound velocity around 10-12 K and fields around 20 T.

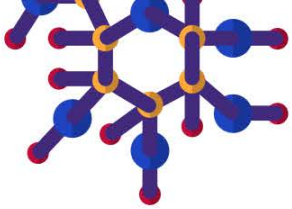

p25

Magnetoelastic coupling in HoB_4

Cinthia Antunes Correa[1,2], Srikanta Goswami[1], Dominik Kriegner[1,2], Denis Gorbunov[3], Oleg Petrenko[4], Margarida Henriques[1], Daniel Brunt[4], Geetha Balakrishnan[4]

[1]Institute of Physics of the Czech Academy of Sciences, Prague, Czech Republic. [2]Faculty of Mathematics and Physics, Charles University, Prague, Czech Republic. [3]Helmholtz-Zentrum Dresden-Rossendorf, Dresden, Germany. [4]University of Warwick, Coventry, United Kingdom

Rare-earth (R) tetraborides are well-known for their interesting magnetic phenomena and rich phase diagrams driven by the competition between multipolar interactions and the geometrically frustrated lattice of the rare-earth ions [1]. In such systems, the resulting ground state strongly depends on perturbations that will lift the frustration such as long-range interactions, quantum fluctuations, or coupling to nonmagnetic degrees of freedom [2].

The compound HoB_4 orders at the Néel temperature T_{N_1}=7.1 K and undergoes a first-order phase transition from an incommensurate to a commensurate magnetic phase at T_{N_2}=5.7 K [3]. The magnetic ordering transitions seem to be coupled to lattice distortions and/or structural transitions [4]. Nevertheless, no detailed description of any of the lattice changes exists. To investigate the crystal structure of HoB_4 below T_{N_1}, a thorough study using X-ray powder diffraction in the temperature range of 3.5 K to 8 K = 7.1 K was performed. It was found that the crystal structure distorts between T_{N_2} and T_{N_1}. Furthermore, below T_{N_2} the unit cell transforms from tetragonal symmetry (*P4/mbm* space group) to a monoclinic symmetry. Thus, at 3.5 K the crystal structure of this tetraboride compound is best described by the space group $P2_1/b$.

[1] D. Brunt, et al., Sci Rep 8, 232 (2018).
[2] M. J. Harris, et al., Phys. Rev. Lett. 79, 2554 (1997).
[2] J. Kim, et al., J. Appl. Phys. 105, 07E116 (2009).
[4] D. Brunt, et al., Phys. Rev. B 95, 024410 (2017).

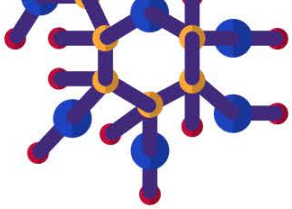

p26

Magnetism and anisotropy of vdW antiferromagnet VCl_3

Ondřej Michal[1], Dávid Hovančík[1], Parvez Ahmed Qureshi[1], Jiří Pospíšil[1], Vladimír Sechovský[1], Tetiana Haidamak[1], Martin Míšek[2], Petr Proschek[1], Jan Prokleška[1], Yurii Skourski[3], Marc Uhlarz[3]

[1]Charles University, Faculty of Mathematics and Physics, Prague, Czech Republic. [2]Czech Academy of Sciences, Institute of Physics, Prague, Czech Republic. [3]Helmholtz-Zentrum Dresden-Rossendorf, Dresden, Germany

The Van der Waals antiferromagnet VCl_3 belongs to the group of 2D transition-metal-trihalide materials [1]. We have grown high-quality VCl_3 single crystals and subjected them to specific heat and magnetization measurements. The specific heat data revealed two transitions: a structure transition from a high-temperature rhombohedral to a monoclinic structure at 104 K and a magnetic transition at 22 K. The system exhibits a signature of a strong magnetocrystalline anisotropy, with a minimal detectable effect of B applied perpendicular to *c*. The magnetic entropy was smaller than theoretically predicted for the pure high spin state (S = 1) of V^{3+} with a value of S_{mag} = 0.23Rln3. This can be attributed to a small B_{int} value, likely a result of orbital coupling partially cancelling the core polarization hyperfine field. The small value of S_{mag} may explain why the magnetization curve observed at 30 K does not correspond to a fully paramagnetic state. The large orbital moment can be deduced from the measured saturated high-field magnetization, with a value of 1.2 μ_B/V^{3+} - considerably below the anticipated 2 μ_B/V^{3+}. A transition from antiferromagnetic to a polarized paramagnetic phase was detected in the field of 25 T applied along *c*. Based on these experimental observations, we suppose an in-plane antiferromagnetism with out-of-plane anisotropy.

[1] D. Mastrippolito et al., *Polaronic and Mott Insulating Phase of Layered Magnetic Vanadium Trihalide VCl_3*, Physical Review B 108, (2023).

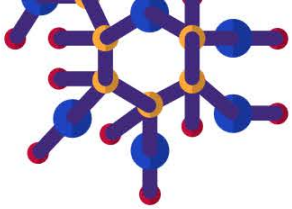

p27

Exploring electrical and magnetical properties of $NiBr_2$

Parvez Ahmed Qureshi, Dávid Hovančík, doc. RNDr. Jiří Pospíšil, Prof. RNDr. Vladimír Sechovský

Faculty of Mathematics and Physics, Charles University, Prague, Prague, Czech Republic

In this work, we studied the structural, electrical, and magnetic properties of a single crystal of NiBr2 compound intending to explore its predicted multiferroic behavior[1]. The single crystals of NiBr2 were grown using the chemical vapour transport method by direct reaction of the stoichiometric amount of elements. The analysis of structural parameters was using powder X-ray diffraction confirmed the trigonal crystal structure (space group R-3m) of NiBr2. The two anomalies observed in specific heat data reveal the magnetic phase transitions in NiBr2. One points to an antiferromagnetic transition at Néel temperature TN = 44 K, and the second signalizes the order-to-order transition at T = 22.5 K to a helical incommensurate antiferromagnetic structure[2, 3]. Microscopic analysis confirmed the hygroscopic behavior of NiBr2 single crystal. A selected suitable single crystal was successfully exfoliated to the nanometer range (confirmed via atomic force microscopy analysis) to study single-layer optical and ferroic properties. The anomalies observed in low-temperature Raman and terahertz spectra and their relation to changes in electrical, magnetic, and lattice properties will be discussed during the presentation.

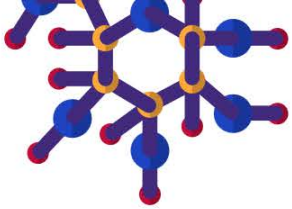

p28

Structural and magnetic properties of R_2Cu_2In intermetallics

Petr Král[1], Martin Diviš[1], Milan Klicpera[1], Ladislav Havela[1], Jiří Kaštil[2], Petr Doležal[1], Vladimir Pomjakushin[3], Jiří Prchal[1]

[1]Charles University, Department of Condensed Matter Physics, Prague, Czech Republic. [2]Institute of Physics of the Czech Academy of Sciences, Prague, Czech Republic. [3]Laboratory for Neutron Scattering and Imaging, Paul Scherrer Institute, Villigen, Switzerland

A broad variety of physical properties may be followed across the R_2T_2X intermetallics (tetragonal *P*4/*mbm* structure), covering superconductors, localized magnets with complex phase diagrams or Kondo lattices, heavy-fermions, and intermediate-valence compounds. Considerable attention is dedicated also to the magnetic frustration arising from the details of crystal structure, analogous to the Shastry-Sutherland lattice.

An interesting realization of magnetism can be observed among the R_2Cu_2In series. We present the results of a systematic (experimental and theoretical) study on R = Ce, Dy, and Tm materials. Non-magnetic La- and Lu-based analogs provide background information. In addition, La_2Cu_2In was found to exhibit superconductivity below 0.93 K. Regarding the magnetic systems, resistivity, magnetization, and specific heat measurements are reported, however, the key method is neutron diffraction providing important insight into the microscopic details of R_2Cu_2In magnetism.

Particularly, we have focused on the Kondo-lattice Ce_2Cu_2In with two successive AFM transitions (5.5 K, 4.8 K) on the light rare-earth side [1]. Among heavy rare earths, Dy_2Cu_2In has been reported as an interesting case, however, with uncertainties concerning its magnetic order [2,3]. Another system of our interest is Tm_2Cu_2In found to exhibit glassy features [4,5].

[1] Physica B 230-232 (1997) 211
[2] JMMM 202 (1999) 1
[3] JALCOM 667 (2016) 130
[4] JMMM 543 (2022) 168599
[5] JMMM 570 (2023) 170527

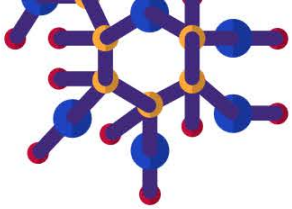

p29

Strong magnetocaloric effect induced by anisotropic ferromagnetism in $EuAl_{12}O_{19}$

Adam Eliáš[1], Quentin Courtade[1], Tetiana Haidamak[1], Petr Proschek[1], Michal Dušek[2], Jan Priessnitz[1,3], Pavel Baláž[2], Ross Colman[1], Gaël Bastien[1]

[1]Charles University, Faculty of Mathematics and Physics, Department of Condensed Matter Physics, Prague, Czech Republic. [2]FZU-Institute of Physics, Czech Academy of Sciences, Prague, Czech Republic. [3]IT4 Innovations, VSB - Technical University of Ostrava, Ostrava-Poruba, Czech Republic

We announce the discovery of a large magnetocaloric effect (MCE) and rotational MCE in $EuAl_{12}O_{19}$. The Eu^{2+} ions with a spin of S=7/2 are arranged in triangular two-dimensional sublattices in the basal plane. These sublattices are separated by large interplanar distances filled with a non-magnetic spinel block. We have measured specific heat and magnetization down to 0.4K, and our research has unveiled a strongly anisotropic ferromagnetic phase with a Curie temperature T_C=1.3K. The strong magnetocaloric effect below 5K in $EuAl_{12}O_{19}$ comes from the ferromagnetic ordering of large spins S=7/2 carried by Eu^{2+} ions. We observe a strong inverse magnetocaloric effect below T_c under magnetic field applied in the basal plane induced by the strong magnetic anisotropy. Interestingly this effect is unusual in ferromagnets and it implies a giant rotational MCE providing the ability to use the material for low-temperature refrigeration to reach temperatures well below T_c=1.3K, with relatively small magnetic fields achievable using commonly available permanent magnets.

p30

Crystal Structure and Magnetic Properties of Uranium-Hafnium Hydrides

Shanmukh Veera Venkata Devanaboina, Oleksandra Koloskova, Silvie Mašková Černá, Ladislav Havela

Department of Condensed Matter Physics, Faculty of Mathematics and Physics, Charles University, Prague, Czech Republic

Uranium hydride (UH_3) belongs to the first known 5*f* materials with ferromagnetic ordering [1]. It exists in two different cubic modifications: a stable *β*-UH_3 phase (complex cubic with *a* = 664 pm), and a metastable *α*-UH_3 (*bcc* cubic with *a* = 414-416 pm). Our prime objective is to explore the role of Hafnium (Hf) in stabilizing the *bcc* α-UH_3 phase and examine its impact on the crystal lattice as well as magnetic and transport properties.

In the present work, the alloys $U_{1-x}Hf_x$ with *x* = 0.10, 0.15, 0.30, and 0.40 were synthesized by arc-melting of pure elements (natural U-2N8, Hf-3N) in an Ar atmosphere. Subsequently, the alloys were hydrogenated by exposure to high pressure of H_2 gas (*p* = 100 bar) for 120 hours at ambient temperature. XRD analysis revealed that β-UH_3 is the prominent phase for 10 at. % Hf, gradually decreasing with increasing Hf concentration up to 40 at%. At this threshold, α-UH_3 becomes the majority phase, with a small peak of β-UH_3 remaining at around $2\vartheta = 33.1^{\circ}$. The determined lattice parameters of the stabilized *α*-UH_3 phase are in good agreement with the literature.

Magnetization measurements confirmed the ferromagnetic phase of $U_{1-x}Hf_x$ hydrides. The incorporation of Hf enhances the Curie temperature of UH_3 from 175 K to 179 K observed at 10 at. % Hf concentration, showing slight variation with further increasing Hf content.

[1] Troc R. and Suski W. *THE DISCOVERY OF THE FERROMAGNETISM IN U(H,D)(3) - 40 YEARS LATER.* J. Alloys Comp. **219**, 1, (1995).

p31

Universal anomalous low-temperature properties of the binary ZnO-P_2O_5 glasses

Vladimír Tkáč[1], Pavlo Baloh[1], Róbert Tarasenko[1], Erik Čižmár[1], Martin Orendáč[1,2], Alžbeta Orendáčová[1], Jana Holubová[3], Eva Černošková[3], Zdeněk Černošek[3], Alexander Feher[1]

[1]Institute of Physics, Faculty of Science, P. J. Šafárik University in Košice, Košice, Slovakia. [2]Department of Solid State Engineering, University of Chemistry and Technology, Praque, Czech Republic. [3]Department of General and Inorganic Chemistry, Faculty of Chemical Technology, University of Pardubice, Pardubice, Czech Republic

The glassy system is characterized by an excess in the vibrational density of the states, which is not present in their crystalline counterparts described by Debye's theory. This property is manifested as boson peak (BP) in the reduced specific heat C_p/T^3 and plateau in the thermal conductivity $k(T)$ [1]. Thermal conductivity and specific heat C_p measurements of the xZnO-(100-x)P_2O_5 (xZP) glasses were performed in a wide range of various (x = 64, 62, 60, 57, 53, and 50) compositions. The $k(T)$ was studied down to T = 2 K, while C_p was investigated down to T = 0.38 K. The BP in C_p/T^3 of ZP glasses depends linearly on sample composition and is in the temperature range between $T \approx 8$ K for 50ZP and $T \approx 14$ K for 64ZP. The structural analysis found potential correlations between the size of the cavities and the amount of ZnO fraction. The $k(T)$ plateau is in the temperature range between $T \approx 8$ K and $T \approx 20$ K. Two types of one-dimensional chains are present in the ZP glasses: the one created from the PO_4 tetrahedra and the second type built from Zn_xO_y polyhedral. The correlation between glassy nanoscopy structure and low-temperature universal anomalous behavior of glass will be discussed.

This work was supported by the APVV-18-0197, APVV-22-0172, APVV-SK-BY-RD-19-0008, APVV-20-0324, and VEGA 1/0132/22.

[1] P. Baloh, V. Tkáč, R. Tarasenko, E. Čižmár, M. Orendáč, A. Orendáčovéa, O. Onufriienko, J. Holubová, E. Černošková, Z. Černošek, A. Feher, *J. Magn. Magn. Mater.* ***588,*** 171415 (2023).

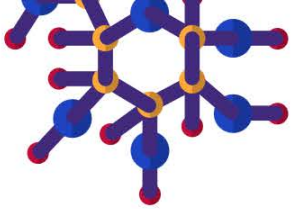

p32

Anomalous Hall effect and chiral anomaly in antiferromagnetic DyPtSb

Snehashish Chatterjee, Abhinav Agarwal, Orest Pavlosiuk, Piotr Wiśniewski, Dariusz Kaczorowski

Institute of Low Temperature and Structure Research, Polish Academy of Sciences, Wroclaw, Poland

We present the results of our transport and magnetic investigation of a frustrated antiferromagnet DyPtSb (T_N = 2.2 K, $-\vartheta_{CW}/T_N \sim 6$). The temperature variation of the electrical resistivity exhibits a prominent broad peak around 30 K, which signals a transition from semiconducting/semimetallic to metallic regime, thus indicating the presence of two parallel conducting channels. Below 20 K, the compound shows unsaturated transverse magnetoresistance in high magnetic fields, while in small fields it is governed by a weak antilocalization effect. The longitudinal magnetoresistance has a strong negative component, and the planar Hall resistivity reaches a very large magnitude. Interestingly, both these features are fingerprints of the chiral magnetic anomaly inherent in Weyl semimetals. At low temperatures, the Hall resistivity of DyPtSb is dominated by anomalous contribution, which probably arises due to a non-zero Berry curvature in the electronic band structure.

This work was supported by National Science Centre (NCN, Poland) under grant No. 2021/40/Q/ST5/00066.

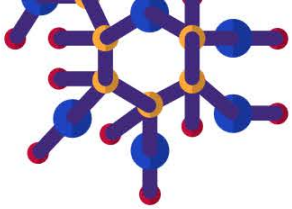

p33

Spin-orbit interactions and magnetism in open *d*-shell oxides: $CdVO_3$ and Ba_2LuMoO_6

Ryszard RADWANSKI, Zofia ROPKA

Center of Solid State Physics, Krakow, Poland

There is a long debate about how *d*-electrons should be described - is a better starting point is their localization or the itinerancy with the wide continuous energy band. By years we advocate for their substantial localization preserving strongly-correlated atomic-like electronic structure. In the localized case one derives a low-energy discrete electronic structure predominantly determined by crystal-field (CEF) and spin-orbit (s-o) interactions. We have noticed that despite of a conceptual simplicity of the CEF and s-o interactions the resulting magnetic and electronic properties can be very complex, insulators or metallics, magnetically ordered or being paramagnetic to the lowest temperatures [1,2,3].

$CdVO_3$ exhibits the ferromagnetic order with T_c=24 K (PRB84(2011)144429). Ba_2LuMoO_6 stays paramagnetic down to 1 K showing a strong violation of the Curie-Weiss law (npjQM **7** (2022)74). In $CdVO_3$ the V ions are formally tetravalent. Mo ions in Ba_2LuMoO_6 are formally as Mo^{5+}. By analysis of magnetic properties we derived the low-energy (< 200meV, excitations close to the Fermi level) discrete electronic structure (originating from the octahedral t_{2g} band) evaluating CEF parameters and spin-orbit coupling.

Reached successful description, with V^{4+} ($3d^1$) and Mo^{5+}($4d^1$) ions, proves that the realized valency is equal to the formal valency confirming the high physical adequacy of the used our Quantum Atomistic Solid-State (QUASST) approach [1,2,3].

We conclude that predominant strong-electron correlations in transition-metal compounds, i.e. compounds containing 3d/4f/5f/4d/5d atoms, are predominantly on-site correlations.

[1] Z. Ropka and R.J. Radwanski, Phys. Rev. B **67** (2003) 172401. email: rjradwanski@gmail.com
[2] R.J. Radwanski and Z. Ropka, *Orbital moment in NiO*, Acta Physica Polonica A **97** (2000) 963.
[3] R.J. Radwanski, Quantum Atomistic Solid-State Theory:$CeRh_2Si_2$, K_2CoF_4, $LaCoO_3$, Sr_2VO_4, Ba_2IrO_4, Acta Phys. Polonica A **143** (2023) 211. DOI: 10.12693/APhysPolA.143.21

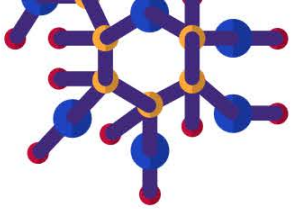

p34

Physical properties of a Kondo lattice oxypnictide $Ce_3Cu_4P_4O_2$

Szymon Królak[1,2], Duygu Yazici[1,2,3], Michał Jerzy Winiarski[1,2], Tomasz Klimczuk[1,2]

[1]Faculty of Applied Physics and Mathematics, Gdansk University of Technology, Gdańsk, Poland. [2]Advanced Materials Centre, Gdansk University of Technology, Gdańsk, Poland. [3]The Scientific and Technological Research Council of Turkey, Ankara, Turkey

Heavy fermion (HF) compounds are intriguing physical systems due to the strong electronic correlations arising from the presence of localized states at the Fermi level. Here, we report the successful synthesis of a layered oxypnictide $Ce_3Cu_4P_4O_2$ and the characterization of its physical properties employing magnetic susceptibility, transport, and heat capacity measurements.

We discuss the physical properties of $Ce_3Cu_4P_4O_2$ as resulting from the Kondo lattice formation. The magnetic contribution to the resistivity $\rho_{mag}(T)$ shows a maximum at $T \approx 230$ K and the low-temperature resistivity $\rho(T)$ shows a knee at $T \approx 3.5$ K, highly susceptible to the magnetic field. In addition, it was observed that the magnetoresistance at $T = 2$ K is negative.

The magnetic susceptibility of $Ce_3Cu_4P_4O_2$ shows the Curie – Weiss behavior at high temperatures and a strong deviation from the localized-moment behavior in the low-temperature range. Importantly, the M(H) data measured at 2 K shows a strongly reduced ($\approx 1/3$ μ_{eff} of Ce^{3+}) magnetic moment value at $\mu_0 H = 9$ T.

From the specific heat data of $Ce_3Cu_4P_4O_2$, we extracted the value of the Sommerfeld coefficient: $\gamma = 100$ mJ mol^{-1} K^{-2}/f. u., which is enhanced in comparison to $La_3Cu_4P_4O_2$ (≈ 10 mJ mol^{-1} K^{-2}/f. u. [1]). To elucidate the character of the HF behavior we calculated the Kadowaki – Woods ratio, $A/\gamma^2 = 1.65 \cdot 10^{-5}$ μΩ cm (mol K mJ^{-1})^2.

[1] S. Królak, M. J. Winiarski, D. Yazici, S. Shin, T. Klimczuk, unpublished

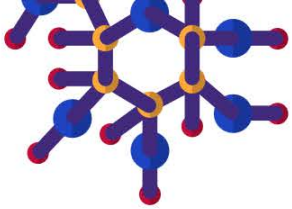

p35

Formation, structure, and properties of R_2Pt_2Sn intermetallics (R = Sc, Y, La-Sm, Gd-Lu)

V.V. Romaka

Leibniz Institute for Solid State and Materials Research Dresden (IFW Dresden), Dresden, Germany

Metallic systems with Shastry-Sutherland lattice based on rare-earth elements have the potential for complex magnetic phase diagrams due to the interplay with conduction electrons. New representatives of such systems are R_2Pt_2Sn compounds that crystallize in the anisotropic Mo_2FeB_2 (space group *P*4/*mbm*) structure type and represent the 2D Shastry-Sutherland lattice with magnetic ions of the R metals. The most intriguing appeared to be the Sm_2Pt_2Sn and Ce_2Pt_2Sn phases, which are characterized by the two-branches homogeneity region similar to those reported for Ce_2Pd_2In [1]. Optimization of the synthesis procedure allowed us to obtain almost single-phase samples of Sm_2Pt_2Sn and Ce_2Pt_2Sn. DFT modeling of the R_2Pt_2Sn compounds showed that their enthalpy of formation is mostly slightly above the tie-line that connects RPtSn and RPt, which is consistent with experimental observations. However, off-stoichiometry could stabilize these phases at higher temperatures, as indicated by DTA measurements. Calculated and measured elastic properties and hardness of R_2Pt_2Sn indicate their ductile behavior. Most investigated compounds reveal a Curie-Weiss behavior with antiferromagnetic ordering at low temperatures.

The work is funded by DFG (project RO 6386/2-1). The author thanks U. Nitzsche for using the ITF/IFW compute cluster.

[1] M. Giovannini, H. Michor, E. Bauer, G. Hilscher, *Physical Review B - Condensed Matter and Materials Physics*. 2000, ***61***, 4044–4053.

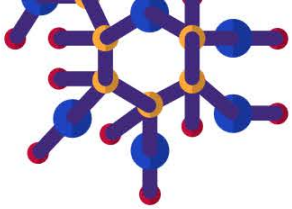

p36

Phase equilibria, crystal structure, physical properties, and DFT study of ternary stannides in Hf-Cu-Sn system

V.V. Romaka[1], L. Romaka[2], Yu. Stadnyk[2], A. Horyn[2]

[1]*Leibniz Institute for Solid State and Materials Research Dresden (IFW Dresden), Dresden, Germany.*
[2]*Inorganic Chemistry Department, Ivan Franko Lviv National University, Lviv, Ukraine*

The interaction of hafnium with copper and tin was studied at 870 K over the whole concentration range using XRD and SEM/EDX methods. At the temperature of investigation, three ternary compounds are realized in the Hf-Cu-Sn system: HfCuSn (LiGaGe-type), $HfCu_5Sn_2$ ($HfCu_5Sn_2$-type), and Hf_5CuSn_3 (Hf_5CuSn_3-type). New $HfCu_5Sn_2$ ternary stannide crystallizes in a hexagonal structure (space group $P6_3/mmc$, a = 0.42959(7) nm, c = 1.54165(4) nm), which is related to the $YbFe_2Sb_{4.5}$ structure type. Differential thermal analysis of the $HfCu_5Sn_2$ phase showed stability up to ~1020 K. The composition of the Hf_5CuSn_3 compound corresponds to the maximum solubility of Cu in the interstitial-type solid solution $Hf_5Cu_xSn_3$ (x = 0.0-1.0) based on the Hf_5Sn_3 binary. The Vicker's hardness measurements show close values for all three ternary compounds: HV(HfCuSn) = 3.46 GPa, HV(Hf_5CuSn_3) = 3.75 GPa, and HV($HfCu_5Sn_2$) = 4.15 GPa and are comparable with those from DFT calculations. Electrical resistivity measurements indicated the metallic conductivity of all studied ternary compounds and are in good agreement with the calculated distributions of the density of electronic states. The $Hf_5Cu_{0.3}Sn_3$ and Hf_5CuSn_3 phases show nearly no magnetoresistance at 4 K under applied magnetic field up to 5 T caused by non-magnetic constituent components. With the increasing Hf content in the studied ternary compounds, the calculated heat of formation decreases almost linearly.

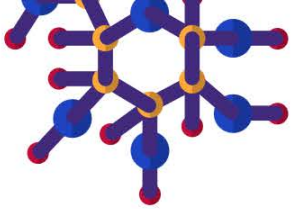

p37

Structure, properties, and DFT study of RCr_6Ge_6 (R = Gd-Lu) compounds with kagome lattice

V.V. Romaka[1], L. Romaka[2], M. Konyk[2], B. Kuzhel[2], Yu. Stadnyk[2], Yu. Yatskiv[2]

[1]*Leibniz Institute for Solid State and Materials Research Dresden (IFW Dresden), Dresden, Germany.*
[2]*Department of Inorganic Chemistry, Ivan Franko National University of Lviv, Lviv, Ukraine*

Electrons in a kagome lattice can form a unique band structure characterized by a flat band, which, if located near the Fermi level, can lead to a large effective electron mass and exotic transport or magnetic properties. Among the candidates for such materials are intermetallic compounds with 1:6:6 stoichiometry and hexagonal structure. Our recent progress in the study of the R-Cr-Ge systems (R - rare-earth of the Yttrium group) led to the discovery of three new representatives: $TmCr_6Ge_6$, $YbCr_6Ge_6$, and $LuCr_6Ge_6$, for which additionally the single crystals were grown. Performed DTA measurements indicated that compounds with Tm and Lu are stable up to 1467 K and 1481 K, respectively. Structural analysis of the RCr_6Ge_6 compounds showed that they crystallize in the $SmMn_6Sn_6$ structure type (space group *P*6/*mmm*) with a small number of vacancies at 1*a* (R) and 2*e* (Ge1) sites and two additional partially occupied 1*b* (R*) and 2*e* (Ge*) crystallographic positions. To explain the factors that govern disorder in the studied compounds, we exploited a Zint-Klemm concept with DFT modeling and the developed three-sublattice model. The electrical resistivity of all studied intermetallics indicates a metallic conductivity and agrees with DFT modeling. Magnetization measurements of $LuCr_6Ge_6$ indicated a Curie-Weiss behavior and a moment of 1.86 μ_B/Cr. The $YbCr_6Ge_6$ compound exhibits antiferromagnetic ordering at 3.3 K.

The authors thank U. Nitzsche for using the ITF/IFW compute cluster.

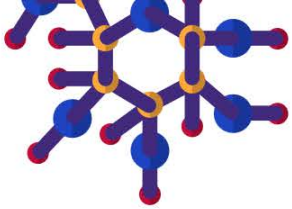

p38

Magnetic anisotropy of $YCo_{12}B_6$ single crystals

Baptiste Vallet-Simond[1], Jiří Pospíšil[2], Léopold V. B. Diop[3], Jérôme Debray[4], Mehdi Amara[1], Olivier Isnard[1]

[1]Université Grenoble-Alpes, Institut Néel - CNRS, Grenoble, France. [2]Faculty of Mathematics and Physics, Charles University, Prague, Czech Republic. [3]Institut Jean Lamour - CNRS, Nancy, France. [4]Institut Néel - CNRS, Grenoble, France

Intrinsic magnetic properties of a trigonal ferromagnet $YCo_{12}B_6$ have been investigated on single crystals by means of temperature- and magnetic field-dependent magnetization measurements in the temperature range from 2 to 200 K. $YCo_{12}B_6$ single crystals were grown by optical furnace with implemented floating zone method and equipped by four halogen bulbs inside a parabolic mirror focusing. The single-crystallinity control and orientation of the grains were performed by back-scattering Laue x-ray diffraction. The crystal structure of $YCo_{12}B_6$ intermetallic compound is well established; it crystallizes in the rhombohedral $SrNi_{12}B_6$-type structure, *R-3m* space group. Magnetization curves were recorded up to 8 T along the principal crystallographic directions in order to probe the anisotropic behaviour. $YCo_{12}B_6$ exhibits a ferromagnetic ground state and orders magnetically below T_C = 155 K. Typical behaviour of easy-plane magnetocrystalline anisotropy is observed; the data measured along the threefold symmetry axis [001] clearly identifies this as the hard magnetization direction. The anisotropy field has been determined, as well as the anisotropy parameters K_1 and K_2 values and their temperature dependence. In addition, magnetostriction measurements have been performed on oriented crystals up to 6 T over a wide temperature range from 300 K down to 2 K, confirming the anisotropic character of this compound.

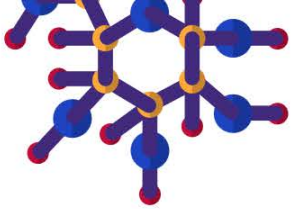

p39

Structural and magnetic properties of the chiral solid solution $La_{1-x}Ce_xRhC_2$

Volodymyr Levytskyi[1], Ulrich Burkhardt[2], Markus König[2], Eteri Svanidze[2], Yuri Grin[2], Roman Gumeniuk[1]

[1]Institut für Experimentelle Physik, TU Bergakademie Freiberg, 09599 Freiberg, Germany. [2]Max-Planck-Institut für Chemische Physik fester Stoffe, 01187 Dresden, Germany

$LaRhC_2$ and $CeRhC_2$ have a tetragonal chiral crystal structure (space groups $P4_1$ or $P4_3$) [1]. The existence of a solid solution between the ternary phases due to the mixed occupation of the rare earth position is observed. To investigate the dependence of properties upon Ce content, we have prepared the series of polycrystalline samples $La_{1-x}Ce_xRhC_2$ ($0 \le x \le 1$, $\Delta x = 0.2$) by arc-melting followed by annealing at 1523 K for 120 h under Ar. Handedness-sensitive EBSD (electron backscatter diffraction) studies [2] on the polished samples showed domains with the common plane parallel to (001) and opposite handedness within individual grains. The assignments of the handedness are confirmed by single-crystal XRD experiments on pieces taken by FIB (focused ion beam) from the enantiopure domains of the $LaRhC_2$ sample. Powder XRD revealed the linear decrease of the unit cell parameters a [3.9704(1)–3.9327(1) Å] and c [15.3325(5)–15.3024(5) Å] with increasing Ce content. Magnetization studies showed $LaRhC_2$ to be diamagnetic, while $CeRhC_2$ to order antiferromagnetically (AF). For $x = 0.2$–1, the estimated paramagnetic moment of Ce remains close to theoretically expected for Ce^{3+}. Magnetic transitions are examined down to 0.35 K by heat capacity measurements. The λ-anomaly indicating a long-range AF ordering is observed in samples with $x = 0.6$, 0.8, and 1 at $T = 0.6(1)$, 1.2(1), and 1.7(1) K, respectively. The magnetic entropy at T_N ($CeRhC_2$) recovers only ~$0.33R\ln 2$ per Ce.

[1] Tsokol A.O. *et al*., *Sov. Phys. Crystallogr*. **31** (1986) 39.
[2] Burkhardt U. *et al*., *Sci. Rep.***10** (2020) 4065.

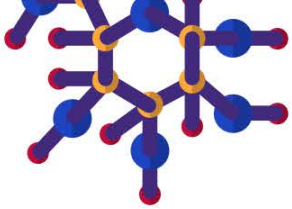

p40

The $NdTIn_{1-x}Al_x$ (T = Ni, Pd) continuous solid solutions

Galyna Nychyporuk[1], Myroslava Horiacha[1,2], Orest Kots[1], Oleh Hudzo[1], Sabine Wurmehl[2], Vasyl Zaremba[1]

[1]Ivan Franko National University of Lviv, Lviv, Ukraine. [2]Leibniz Institute for Solid State and Materials Research (IFW) Dresden, Dresden, Germany

The $NdTIn_{1-x}Al_x$ (T = Ni, Pd) systems were investigated in full concentration range. Samples were synthesized by arc-melting with subsequent annealing for one month at 870 K. Phase analysis was made by means of X-ray powder diffraction (DRON 2.0M, Fe $K\alpha$-radiation and Stoe Stadi P, Mo $K\alpha$-radiation) and energy dispersive X-ray analysis (Tescan Vega 3 LMU and Zeiss-EVO MA 15 scanning electron microscopes).

The existence of the continuous solid solutions with the ZrNiAl-type structure (space group P-62m) were observed and the unit cell parameters for them were refined:
$NdNiIn_{1-0}Al_{0-1}$: a = 0.75204(10)–0.70281(6), c = 0.39339(6)–0.40662(5) nm;
$NdPdIn_{1-0}Al_{0-1}$: a = 0.76821(1)–0.71848(1), c = 0.40012(1)–0.41841(1) nm.

The results of partial substitution of In atoms by Al atoms were confirmed by single crystal X-ray analysis (Super Nova Rigaku Oxford Diffraction, Mo $K\alpha$-radiation, JANA2006). $NdPdIn_{0.55}Al_{0.45}$ phase crystallizes with ZrNiAl-type structure (P-62m, a = 0.75300(2), c = 0.40376(1) nm, $R1$ = 0.0194 for 529 F^2 values, 16 variables), which agrees well with the results of phase analysis and EDX data: Nd : Pd : In : Al – 38.3(2) at. % Nd; 32.1(2) at. % Pd; 15.9(2) at. % In; 13.6(2) at. % Al (Zeiss-EVO MA 15 scanning electron microscope).

Magnetic susceptibility measurements of $NdPdIn_{1-x}Al_x$ (x = 0, 0.1 and 0.2) samples in the temperature range 2–300 K indicates decreasing of ordering temperature with increasing Al content.

M. Horiacha is indebted to Maria Reiche Postdoctoral Fellowship for a research stipend.

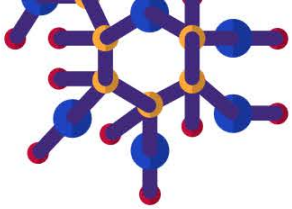

p41

Influence of Ti/Zr-BASED intermetallics on hydrogen storage and generation properties of MgH_2 composites

Ihor Zavaliy[1], Vasyl Berezovets[1], Oleksandr Kononiuk[1], Andriy Kytsya[1], Volodymyr Yartys[2]

[1]Karpenko Physico-Mechanical Institute, NAS of Ukraine, Lviv, Ukraine. [2]Institute for Energy Technology, Kjeller, Norway

Practical use of MgH_2 in hydrogen storage systems is limited due to the several significant disadvantages: high hydrogen sorption-desorption temperatures, low absorption-desorption rates, difficulties of activation, low cyclic stability. Improvement of hydrogen absorption-desorption parameters can be achieved by mechanochemical milling of magnesium with catalytic additives. Another application of MgH_2 is its use in the hydrolysis reaction to obtain hydrogen and supply it to the fuel cells (FC). Noncatalyzed MgH_2 hydrolysis reaction with water is characterized by a low yield of hydrogen and very slow rate of the process. To increase the rate of the reaction and the yield of hydrogen, hydrolysis of MgH_2 with catalytic additives shows a high efficiency when carried out in presence of the acids or salts.

This report will present an overview of our recent works aimed to establish a catalytic effect of the oxygen-stabilized Ti/Zr-based η-phases on the mechanochemical synthesis of the hydride composites, their sorption-desorption properties and H_2 generation efficiency in the hydrolysis reaction. The starting ingredients for the preparation of the hydride composites were two types of magnesium (shavings and high-purity finely dispersed powder), graphite powder, as well as melted in an electric arc furnace and annealed $Zr_3V_3O_{0.6}$, $Ti_4Fe_2O_{0.3}$ and Ti_3Fe_3O alloys. The kinetics of hydrolysis was studied under pseudo-isothermal conditions and the amount of released hydrogen was measured by the volumetric method. Hydrolysis was carried out in deionized water and in aqueous $MgCl_2$ solutions of different concentrations. A strong dependence of the conversion rate on the concentration of $MgCl_2$ was observed. For the concentration range of 0.05…0.1 M $MgCl_2$, a degree of conversion for all composites was in the range 70-90 %. We conclude that the proposed MgH_2–IMC–C composites can be used both in hydrogen storage systems and in the hydrolysis setups for powering FCs.

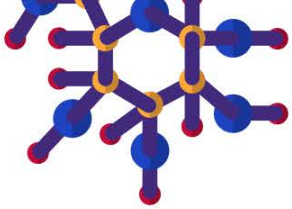

p42

New quaternary compounds $R_2CoAl_4Si_2$

Svitlana Pukas, Kateryna Kravets, Pavlo Demchenko, Nataliya Semuso, Roman Gladyshevskii

Department of Inorganic Chemistry, Ivan Franko National University of Lviv, Lviv, Ukraine

Within a systematic investigation of quaternary systems *R*–*T*–Al–*M* (*R* = rare-earth metal, *T* = 3*d*-element, *M* = Si or Ge) we searched for new compounds with the structure type $Tb_2NiAl_4Ge_2$ (*tI*18, *I*4/*mmm*) [1]. So far, all known representatives of this type were germanides $R_2TAl_4Ge_2$ (*R* = Y, Sm, Gd-Lu, *T* = Fe, Co, Ni) [2,3].

Eight new silicides, $R_2CoAl_4Si_2$ (*R* = Y, Gd-Yb), were synthesized by arc melting, and their crystal structures were studied by X-ray powder diffraction. Compounds with Sm or Lu were not observed under the experimental conditions. The cell parameters of the isotypic $R_2CoAl_4Si_2$ compounds are: a = 4.09338(5), c = 19.3439(3) Å (*R* = Y), a = 4.1144(5), c = 19.432(3) Å (*R* = Gd), a = 4.0899(5), c = 19.321(4) Å (*R* = Tb), a = 4.0831(6), c = 19.286(3) Å (*R* = Dy), a = 4.0802(4), c = 19.268(2) Å (*R* = Ho), a = 4.0726(4), c = 19.227(2) Å (*R* = Er), a = 4.0623(5), c = 19.174(3) Å (*R* = Tm), and a = 4.0687(7), c = 19.195(5) Å (*R* = Yb).

The structure type $Tb_2NiAl_4Ge_2$ is a quaternary variant of the type $Yb_3S_2F_4 \equiv (NiGe_2)Tb_2Al_4$. The structure of $R_2CoAl_4Si_2$ can be described as a packing of monocapped square antiprisms [$SiAl_4R_5$] and cubes [$CoAl_8$].

[1] B. Sieve, P.N. Trikalitis, M.G Kanatzidis, *Z. Anorg. Allg. Chem.* **628** (2002) 1568-1574.
[2] P. Villars, K. Cenzual (Eds.), *Pearson's Crystal Data: Crystal Structure Database for Inorganic Compounds*, Release **2023/24**, ASM International, Materials Park, Ohio, USA.
[3] S. Pukas, N. Semuso, R. Gladyshevskii, *Chem. Met. Alloys* **15** (2022) 17-21.

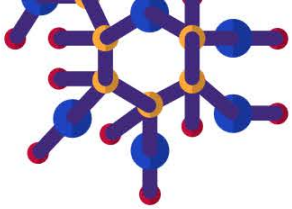

p43

New ternary gallide $Zr_7Pd_7Ga_3$:preparation, crystal and electronic structures

Volodymyr Babizhetskyy[1], Oksana Myakush[2], Bogdan Kotur[3], Chong Zheng[4]

[1]Department of Inorganic Chemistry, Ivan Franko National University of Lviv, Lviv, Ukraine. [2]National University of Forest and Wood Technology of Ukraine, Lviv, Ukraine. [3]Department of Inorganic Chemistry, Lviv, Ukraine. [4]Department of Chemistry and Biochemistry, Northern Illinois University, DeKalb, USA

A part of the isothermal section at 870 K of the Zr–Pd–Ga has been reported. Six ternary compounds have been synthesized and characterized: $Zr_6Pd_xGa_{23-x}$ (6.41<*x*<9.89) (Th_6Mn_{23} type structure), $ZrPd_{0.60}Ga_{2.40}$ ($AuCu_3$), $ZrPd_{0.70}Ga_{13}$ (KHg_2), ZrPdGa (LaNiAl), $ZrPd_2Ga$ ($MnCu_2Al$), and $Zr_{12}Pd_{40-x}Ga_{31+y}$ (*x*=0-1.5, *y*=0-0.5) (original type structure). Recently a new ternary phase of composition ~$Zr_{41}Pd_{41}Ga_{18}$ has been obtained and studied. $Zr_7Pd_7Ga_3$ was prepared by arc melting the initial elements under argon and subsequent annealing the sample at 870 K for 720 h. Single-crystal XRD data revealed $Zr_7Pd_7Ga_3$ to crystallize in Zr_7Ni_{10} type structure: PS *oC*68, SG *Cmce*, *a* = 12.997(3) Å, *b* = 9,6231(17), *c*=9.6302(15) Å. Statistical mixtures of Pd and Ga atoms in ratio of 7:3 *M*(Pd/Ga) occupy three atomic sites of Ni atoms in the binary prototype. Contrary to M-M and Zr-Zr distances which are longer than the sum of metallic radii of atoms the shortest Zr-M distances between 2.729 and 2.780 Å are significantly contracted. These data indicate the covalent bonding between Zr and *M*(Pd/Ga) atoms which is a remarkable feature of the structure. 3D [Pd_7Ga_3] framework consisting of sinusoidal *M* layers (d_{M-M} = 2.763-2.774 Å) along the [100] direction is another feature of the structure. Such layers are stacked along the *b* axis with only slightly longer *M*1-*M*2 (2.858 Å) and *M*3-*M*3 (2.872 Å) interlayer bonds. Differences in electronic structure and chemical bonding between $Zr_7Pd_7Ga_3$ and Zr_7Ni_{10} were examined.

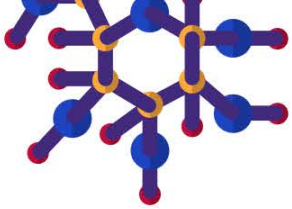

p44

Crystal structure of the $Mg_{5.57}Ni_{16}Ge_{7.43}$ ternary compound

Nazar Pavlyuk, Vasyl Kordan, Grygoriy Dmytriv, Volodymyr Pavlyuk

Ivan Franko National University of Lviv, Lviv, Ukraine

The Mg-based intermetallic compounds are widely investigated now due to their very well hydrogen storage and electrochemical properties. During the systematic study of Mg–Ni-Ge alloys the cubic phase $Mg_{5.57}Ni_{16}Ge_{7.43}$ was detected. The $Mg_{5.57}Ni_{16}Ge_{7.43}$ ternary compound was prepared in a tantalum crucible in a resistance furnace with a thermocouple controller. The single crystal of $Mg_{5.57}Ni_{16}Ge_{7.43}$ was investigated by means Oxford Diffraction Xcalibur3 diffractometer with CCD detector. The crystal structure of $Mg_{5.57}Ni_{16}Ge_{7.43}$ compound was successfully solved by direct methods and refined in space group *Fm*-3*m*. The refined lattice parameters are a= 11.5036 (6) Å, V = 1522.3 (2) Å^3. The starting atomic parameters were taken from an automatic interpretation of direct methods followed by difference Fourier syntheses using SHELX-97 package programs. Finally, all parameters are refined to R_1 = 0.013 and wR_2 = 0.028 using 131 independent reflections with $I > 2\sigma(I)$. The ternary germanide $Mg_{5.57}Ni_{16}Ge_{7.43}$ can be described as three core–shell clusters of $[GeNi_8(Mg/Ge)_6@Ni_{24}@Ni_{32}(Mg/Ge)_{24}]$. The polyhedron $[Ni_{32}(Mg/Ge)_{24}]$ is a new type of convex polyhedron, namely as pentacontatetrahedron with the vertex configuration: 24 ($3^2 5^2$), 24 (345^2) and 8 (5^3). The pentacontatetrahedron is a new representative of Pavlyuk's group of polyhedra based on pentagonal, tetragonal and trigonal faces.

*Research funding: National Research Foundation of Ukraine (2022.01/0064).

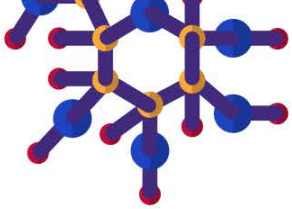

p45

Crystal structure of the new ternary indide $ErCo_2In$

Yuriy Tyvanchuk[1], Volodymyr Babizhetskyy[1], Volodymyr Smetana[2], Mariya Dzevenko[1]

[1]Department of Inorganic Chemistry, Ivan Franko National University of Lviv, Lviv, Ukraine. [2]Department of Biological and Chemical Engineering and iNANO, Aarhus University, Aarhus, Denmark

The new ternary compound $ErCo_2In$ was found during our investigations of the Er-Co-In ternary system.

Polycrystalline samples were synthesized by arc melting of high–purity metals under an argon atmosphere. Intensity data from single crystal, which was extracted from the crushed $Er_{31}Co_{38}In_{31}$ sample, were collected using a Bruker D8 Venture diffractometer with monochromated MoK_α radiation. The crystal structure of the $ErCo_2In$ ($PrCo_2Ga$–type structure, *Pmma,* oP8, a = 4.999(4), b = 4.029(3) and c = 7.078(5) Å) was determined by direct methods using SHELXL-2018 package programs. Refined composition of the compound agrees well with one established using EDX analysis. Based on the 183 independent reflections [$I>2\sigma(I)$], the crystal structure was refined to the reliability factors $R1$ = 0.055 and $wR2$ = 0.120 with anisotropic displacement parameters for all atoms. The shortest distances are: Co–Co (2.467), Er–Co (2.708), Co–In (2.791), and Er–In (3.245 Å).

The lattice parameters of $ErCo_2In$ determined by Rietveld analysis of powder intensity data for the $Er_{25}Co_{38}In_{37}$ sample are: a = 4.994(2), b = 4.026(2) and c = 7.054(3) Å.

The compound prolongs the RCo_2In (R = Y, Pr, Nd, Sm, Gd, Tb, Dy, Ho) series. Similar to other RCo_2In, the $ErCo_2In$ structure slightly differs from the $PrCo_2Ga$-type. The Ga(2*f*) and Co(2*e*) sites of $PrCo_2Ga$ occupy Co(2*f*) and In(2*e*) atoms in $ErCo_2In$.

Yu.T and V.B. gratefully acknowledge partial support of this research by the Simons Foundation (Award Number: 1037973).

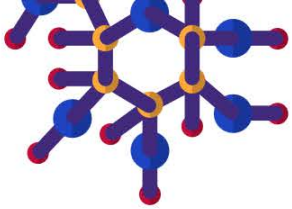

p46

Crystal structure of the new ternary phases in the Nd-Tm-Ge system

Zinoviya Shpyrka, Galyna Didokha, Volodymyr Pavlyuk

Ivan Franko National University of Lviv, Lviv, Ukraine

The ternary compounds $Nd_{0.34}Tm_{0.66}Ge_{1.85}$ and $Nd_{0.2}Tm_{0.8}Ge_{2.013}$ are formed in the Nd–Tm–Ge system at 600°C. The alloys were synthesized by arc melting of pure metals (all with stated purity better than 99.9 wt.%) in an arc furnace under argon atmosphere. The alloys were annealed at 600°C in evacuated quartz ampoules for 720 h, subsequently quenched in ice water, and then examined by powder X-ray diffraction (DRON-4.07 diffractometer, Fe Kα radiation). Single crystal X-ray diffraction (XCalibur Oxford Diffraction diffractometer, Mo Kα-radiation) with a CCD detector was used for the structure studies. The structure was solved by direct methods using SHELXS-86 [1] and refined by SHELXL-97 [2] programs.

The structure of the $Nd_{0.34}Tm_{0.66}Ge_{1.85}$ is orthorhombic, Pearson symbol *oS*24, space group $Cmc2_1$, $DyGe_{1.85}$ structure type, with a = 4.0865(1), b = 29.6897(6), c = 3.9125(1) Å, V = 474.69(2) Å^3. The atomic parameters were refined to R = 0.057 for 356 unique reflections. The structure of the $Nd_{0.2}Tm_{0.8}Ge_{2.013}$ is orthorhombic, Pearson symbol *oS*16, space group *Cmcm*, $ErGe_{2.16}$ structure type, with a = 4.0185(2), b = 15.8379(8), c = 3.8802(2) Å, V = 246.95(2) Å^3. The atomic parameters were refined to R = 0.057 for 163 unique reflections. The neodymium and thulium atoms occupy 4*a* position statistically.

[1] G.M. Sheldrick, SHELXS-86, Program for Crystal Structure Determination, University of Göttingen, Germany, 1986.
[2] G.M. Sheldrick, SHELXL-97, Program for Crystal Structure Refinement, University of Göttingen, Germany, 1997.

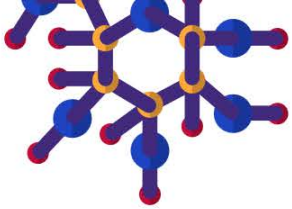

p47

Crystal structure of the $R_{1.33}Ni_3Ga_8$ (R = Tb, Dy, Ho, Er, Tm, Lu) compounds

Nataliya Muts, Yaroslav Tokaychuk, Roman Gladyshevskii

Ivan Franko National University of Lviv, Lviv, Ukraine

The aim of this work was the synthesis and crystal structure determination of new ternary gallides $R_{1.33}Ni_3Ga_8$ (R = rare-earth metal). Samples $R_{10.8}Ni_{24.3}Ga_{64.9}$ (R = Pr, Nd, Sm, Gd, Tb, Ho, Tm, Lu, Yb) were synthesized from bulk metals (R ≥ 99.89 mass%, Ni and Ga ≥ 99.99 mass%) by arc melting under an argon atmosphere and annealed at 600°C under vacuum for 135 days.

The existence of six ternary compounds with $Gd_{1.33}Pt_3Al_8$-type structure (Pearson symbol *hR*51, space group *R*-3*m*) was established by means of X-ray powder diffraction (diffractometer STOE Stadi P) and energy-dispersive X-ray spectroscopy (scanning electron microscope Tescan Vega 3 LMU): $Tb_{1.33}Ni_3Ga_8$ (a = 4.2056(1), c = 37.8913(9) Å), $Dy_{1.33}Ni_3Ga_8$ (a = 4.20103(9), c = 37.8368(9) Å), $Ho_{1.33}Ni_3Ga_8$ (a = 4.19666(9), c = 37.7882(9) Å), $Er_{1.33}Ni_3Ga_8$ (a = 4.19290(8), c = 37.7446(8) Å), $Tm_{1.33}Ni_3Ga_8$ (a = 4.18819(7), c = 37.6980(7) Å), and $Lu_{1.33}Ni_3Ga_8$ (a = 4.1826(1), c = 37.647(1) Å).

The structure type of the ternary $R_{1.33}Ni_3Ga_8$ compounds belongs to the family of linear intergrowth structures with general formula $R_{0.67}T_nM_{2n+m}$ and are composed of six atom layers of the composition $R_{0.67}Ga$ ($R_{0.67}M$) and nine slabs $NiGa_2$ (TM_2). The layers containing the rare-earth metal atoms, which are characterized by disordered distribution of R atoms and Ga-atom triangles, are separated by single and double $NiGa_2$ slabs.

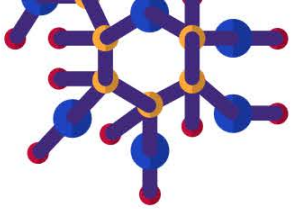

p48

More about the $BaO–Lu_2O_3–CuO$ system

Oksana Zaremba, Mariia-Suzanna Teplinska, Pavlo Demchenko, Vasyl Kordan, Roman Gladyshevskii

Ivan Franko National University of Lviv, Lviv, Ukraine

The present study involved an examination of the interplay among the components of the $BaO–Lu_2O_3–CuO$ system through X-ray diffraction phase and structure analysis (STOE Stadi P, Cu $K\alpha_1$ and DRON 2.0M, Fe $K\alpha$). Polycrystalline samples were synthesized starting from $BaCO_3$, Lu_2O_3, and CuO powders by a two-stage solid-state reaction method at 900°C. Under the conditions of our experiment, the existence of the cuprate $BaLu_2CuO_5$ (structure type BaY_2CuO_5, Pearson symbol *oP*36, space group *Pnma*, a = 12.0286(1), b = 5.5979(1), c = 7.0366(1) Å, R_B = 0.053) was confirmed. This ceramic phase was tested as cathode material of a lithium-ion battery, where commercial metallic lithium was used as anode and a 1M solution of $Li[PF_6]$ salt in a mixture of aprotic solvents (dimethyl carbonate and ethylene carbonate in the ratio 1:1) as electrolyte. Electrochemical lithiation was carried out in the galvanostatic mode (2-electrode prototype Swagelok-cell) at 0.5-1.0 mA/cm^2. The morphology and composition of the sample before and after lithiation were controlled by SEM and EDX (Tescan Vega 3 LMU). As a result of the electrochemical reaction, the $BaLu_2CuO_5$:Li phase was obtained, and its structure remained unchanged (a = 12.0242(2), b = 5.5959(1), c = 7.0341(1) Å, R_B = 0.050). The decrease of the cell volume from 473.81(2) to 473.30(2) Å^3 (–0.11%) indicates that replacement of ions in the original structure takes place during the lithiation. The amount of intercalated Li was 0.22 per f.u.

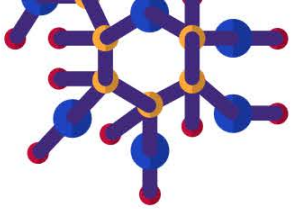

p49

Phase equilibria in the ternary systém Gd–Mn–Zn and electrochemical hydrogenation of the phases

Oksana Zelinska, Nataliya Chorna, Vasyl Kordan, Anatoliy Zelinskiy, Volodymyr Pavlyuk

Ivan Franko National University of Lviv, Lviv, Ukraine

Multicomponent systems containing rare earth and transition metals have essential scientific and practical interest due to various applications, including hydrogen storage devices and metal-hydride batteries. Systematic study of the interaction between the components in such systems allows to determine the relationship between composition, structure, and properties of the phases and search for new materials more purposeful.

The alloys for investigation were synthesized by arc melting of pure components under an argon atmosphere, followed by annealing at 500 °C for two months and quenching in cold water. The phase analysis of the samples was carried out by X-ray powder diffraction, scanning electron microscopy and energy-dispersive X-ray spectroscopy. Electrochemical hydrogenation of the phases was studied in two-electrode «Swagelok»-type cells.

As a result, the interaction of the components in the ternary system Gd–Mn–Zn was studied and the isothermal section of its phase diagram at 500 °C was constructed in a full concentration range. The existence of several Gd–Zn, Gd–Mn and Mn–Zn binary compounds was confirmed. Slight solubility of the third compound was observed in GdZn (4.5 at.% Mn), $GdZn_2$ (4.6 at.% Mn), Gd_3Zn_{11} (3.7 at.% Mn), Gd_2Zn_{17} (3.5 at.% Mn) and $GdMn_2$ (2.5 at.% Zn). No visible solubility was observed in other binary phases. A new ternary compound with the composition $Gd_2Mn_2Zn_{15}$ (Th_2Zn_{17}-type structure, *R*-3*m*, *a* = 9.0076(2) Å, *c* = 13.2629(6) Å) was found in the region of high zinc content, and its crystal structure was refined from single crystal data. The crystal structure of another ternary compound with equiatomic composition GdMnZn ($CaIn_2$-type structure, $P6_3/mmc$, *a* = 4.201 Å, *c* = 7.031 Å) was refined from powder diffraction data.

Electrochemical hydrogenation of the phases confirmed their ability to absorb-desorb hydrogen reversibly from 0.025 H/f.u. for $GdMn_{2-x}Zn_x$ to 1.92 H/f.u. for $Gd_2Zn_{17-x}Mn_x$ and remain stable in the electrolyte (6 M KOH) environment.

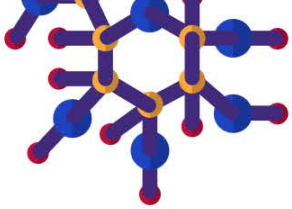

p50

Structural Characterization of Sol-Gel Derived High-Entropy Perovskite $(Y_{0.2}Nd_{0.2}Sm_{0.2}Eu_{0.2}Er_{0.2})AlO_3$

Stanislav Pesternikov, Vitalii Stadnik, Vasyl Hreb, Leonid Vasylechko

Lviv Polytechnic National University, Lviv, Ukraine

Synthesis of high-entropy (HE) aluminate $(Y_{0.2}Nd_{0.2}Sm_{0.2}Eu_{0.2}Er_{0.2})AlO_3$ was achieved through a sol-gel citrate method using $Y(NO_3)_3{\cdot}6H_2O$, Nd_2O_3, Sm_2O_3, Eu_2O_3, Er_2O_3 and $Al(NO_3)_3{\cdot}9H_2O$ as precursors. XRD examination of the product after final heat treatment at 1100 °C for 4 hours revealed formation of single phase material with an orthorhombic perovskite structure. In such a way a fine white powder with the average crystallite size D_{ave} of 127 nm and microstrain values <ε> of 0.1% was obtained. Attempt to synthesis the above material through the sol-gel combustion method was unsuccessful, leading to formation of multiphase material. This study presents a detailed structural characterisation of sol-gel derived high-entropy aluminate $(Y_{0.2}Nd_{0.2}Sm_{0.2}Eu_{0.2}Er_{0.2})AlO_3$ compared against a numerous references $RAlO_3$ compounds and $(R_{1-x}R'_x)AlO_3$ solid solutions with perovskite structure. Full profile Rietveld refinement performed in space group *Pbnm* proves single-phase nature and homogeneity of the HE perovskite synthesized yielded lattice parameters a=5.2514(3) Å, b=5.3011(3) Å, c=7.4428(5) Å, which closely align with those of the isostoichiometric HE aluminate synthesized *via* coprecipitation method [1]. The unit cell dimensions of the HE $(Y_{0.2}Nd_{0.2}Sm_{0.2}Eu_{0.2}Er_{0.2})AlO_3$ perovskite with the average R^{3+} cation radius of 1.110 Å follow well the empirical relations earlier established for $RAlO_3$ rare-earth aluminate series.

[1] Z. Zhao *et al*. *J. Mater. Sci. Technol*. **47** (2020) 45–51.

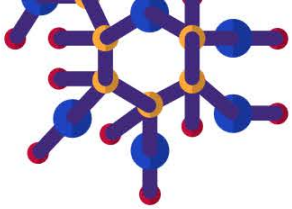

p51

Spark plasma sintering of the $B_{13}C_2$–VB_2 composition

Andriana Ivanushko, Volodymyr Babizhetskyy, Oksana Zaremba, Anatoliy Zelinskiy, Khrystyna Miliyanchuk, Roman Gladyshevskii

Department of Inorganic Chemistry, Ivan Franko National University of Lviv, Lviv, Ukraine

Superhard materials based on $B_{13}C_2$ would find wide application in various industries. These materials, characterized by their exceptional hardness and durability, are in demand due to their suitability in the production of cutting tools, protective coatings, and other industrial applications where high mechanical resistance is required.

Ceramic materials were synthesized from high-purity $B_{13}C_2$ and VB_2 powders by spark plasma sintering at a maximum temperature of 1900°C and a pressure of 70 MPa under argon atmosphere. The initial content of VB_2 in the powder mixtures $B_{13}C_2$+VB_2 was 47 wt.%.

X-ray powder diffraction patterns collected from the surface of the synthesized pellet, showed two phases: $B_{13}C_2$ and VB_2. $B_{13}C_2$ adopts its own rhombohedral structure type, whereas the crystal structure of VB_2 belongs to the structure type AlB_2. Results of the structure analysis of the $B_{13}C_2$–VB_2: $B_{13}C_{1.80(6)}$, *R*-3*m*, *a* = 5.6109(7) Å, *c* = 12.102(3) Å, *V* = 329.95(9) Å^3, B_{ov} = 1.7(4) Å^2, B1 18*h* 0.4413(12) 0.5587(12) 0.0463(15), B2 18*h* 0.5069(15) 0.4931(15) 0.192(2), (0.10(3)B+0.90(3)C) 6*c* 0 0 0.120(3), B3 3*a* 0 0 0 occ. = 0.80(6); VB_2, *P*6/*mmm*, *a* = 3.0033(2) Å, *c* = 3.06437(19) Å, *V* = 23.936(3) Å^3, B_{ov} = 1.04(15) Å^2,V 1*a* 0 0 0, B 2*d* $^1/_3$, $^2/_3$, $^1/_2$.

Optimized synthesis conditions made it possible to achieve a relative density of 96.8 %. The hardness measured by the Vickers method for the $B_{13}C_2$–VB_2 ceramic material was 24.1 GPa.

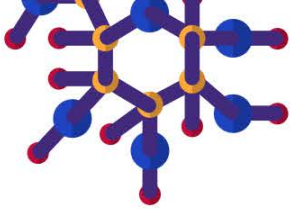

p52

Synthesis method for single crystals of the compound Ti_3SiC_2

Anastasiia Broda[1], Nastasiya Klymentiy[1], Svitlana Pukas[1], Raul Cardoso-Gil[2], Yuri Grin[2], Roman Gladyshevskii[1]

[1]Ivan Franko National University of Lviv, Lviv, Ukraine. [2]Max-Planck-Institute for Chemical Physics of Solids, Dresden, Germany

The compound Ti_3SiC_2 belongs to the family of MAX phases. The most widely utilized method for synthesizing MAX phases is a liquid/solid-state reaction (SSR), which relies on high-temperature reactions between elemental starting powders [1].

The compound Ti_3SiC_2 was obtained by sintering mixed powders of Ti, Si and C in an induction furnace under an argon atmosphere at 1100°C for about 30 min. After that, the sample was placed in a high-temperature furnace for annealing. The annealing was carried out in an argon atmosphere for 108 h at 1475°C. The XRD analysis identified Ti_3SiC_2 as the main phase (85 mass%) with TiC (15 mass%). The crystal structure of Ti_3SiC_2 was investigated using single crystal XRD analysis.

The compound Ti_3SiC_2 is a representative of its own structure type: Pearson symbol *hP*12, space group $P6_3/mmc$, a = 3.0683(1), c = 17.6704(5) Å. The Ti atoms occupy two Wyckoff positions: 2*a* (0, 0, 0; $U_{iso/eq}$ = 0.0064(2) Å^2) and 4*f* (⅓, ⅔, 0.13530(3); 0.0069(1) Å^2). The C atoms occupy a position 4*f* (⅓, ⅔, 0.57243(17); 0.0070(4) Å^2), and the Si atoms a position 2*b* (0, 0, ¼; 0.0116(3) Å^2). The structure is characterized by layers of edge-sharing $\underline{C}Ti_6$-octahedra that alternate with layers of Si atoms, which are located at the centers of trigonal prisms [2].

[1] J. Gonzalez-Julian, *J. Am. Ceram. Soc.* **104** (2021) 659-690.
[2] W. Jeitschko, H. Nowotny, *Monatsh. Chem.* **98** (1967) 329-337.

This work was carried out under the EIRENE Grants of the Max-Planck-Institute for Chemical Physics of Solids (Dresden, Germany).

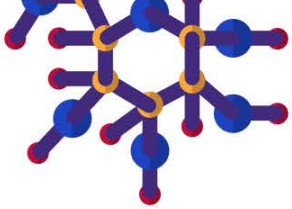

p53

Exploring high magnetocrystalline anisotropy in $Ni_{50}Mn_{25}Ga_{20}Fe_5$ single crystals

Taras Kovaliuk[1], Milan Klicpera[1], Denys Musiienko[2], Ross Harvey Colman[1]

[1]Charles University, Prague, Czech Republic. [2]Czech Academy of Sciences, Prague, Czech Republic

The magnetic shape memory effect is a near-unique multiferroic property of the Ni_2MnGa Heusler alloy family (and it's off-stoichiometry or substituted derivatives). The effect relies on the synergistic combination of high magneto-crystalline anisotropy, high magnetic moment, and low energy required to move twin domain boundaries, known as the twinning stress [1]. Despite extensive searching, no alternatives to the Ni-Mn-Ga alloys have been found to have the required combination of these properties at room temperature. Instead much research has been focused on the incremental improvement of the current capabilities of Ni-Mn-Ga alloys through either substitutional doping [2], or defect reduction in the crystal manufacturing process [3,4].

Recently, we have investigated the effects of Fe substitution [2,5,6]. Substitution of Fe for Ga, with the general formula $Ni_{50}Mn_{25}Ga_{25-x}Fe_x$ is a solid solution for $x < 10$, and results in the rapid increase of the martensitic transformation temperature, from ~200 K at $x = 0$, to ~310 K at $x = 5$. At 5% Fe substitution cooling results in a cascade of transformations between martensite variants, including the pseudo-tetragonal 10M structure (with lowest twinning stress), the 14M modulated phase, and the orthorhombic non-modulated structure. The preparation of single crystals has allowed the detailed investigation of anisotropic magnetic, elastic and transport properties. This contribution will highlight our results of these investigations.

[1] O. Heczko, *Mater. Sci. Technol.* **30**, (2014) 1559.
[2] V. Kopecký, M. Rameš, P. Veřtát, R.H. Colman, and O. Heczko, *Metals (Basel)*. **11**, (2021) 850.
[3] P. Cejpek, L. Straka, M. Veis, R. Colman, M. Dopita, V. Holý, and O. Heczko, *J. Alloys Compd*. **775**, (2019) 533.
[4] D. Musiienko, F. Nilsén, A. Armstrong, M. Rameš, P. Veřtát, R.H. Colman, J. Čapek, P. Müllner, O. Heczko, and L. Straka, *J. Mater. Res. Technol.* **14**, (2021) 1934.
[5] A. Armstrong, F. Nilsén, M. Rameš, R.H. Colman, P. Veřtát, T. Kmječ, L. Straka, P. Müllner, and O. Heczko, *Shape Mem. Superelasticity* **6**, (2020) 97.
[6] M. Klicpera, T. Kovaliuk, K. Drastichová, P. Cejpek, K. Uhlířová, M. Kratochvílová, B. Vondráčková, J. Valenta, and R.H. Colman, *J. Alloys Compd.* **908**, (2022) 164543.

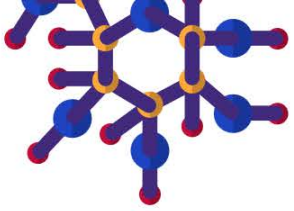

List of Authors

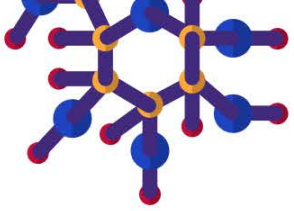

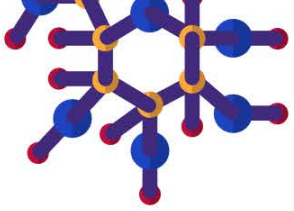

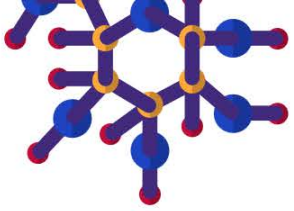

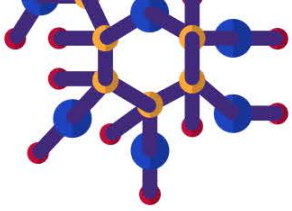

Laser diode floating zone furnace

Pinpoint laser heating system with energy saving

Beam profile

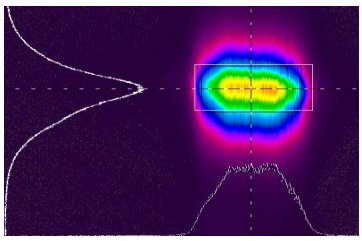

Ruby

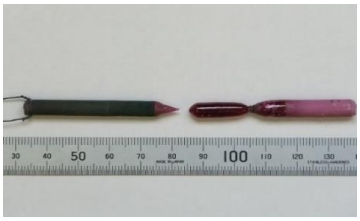

Ni_3Ta

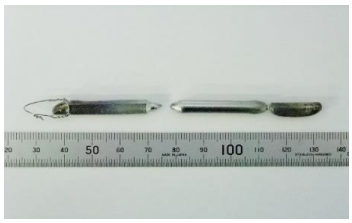

LDFZ furnace

(Model :FZ-LD-5-200W-II-VPO-PC)

≪SPEC≫

* 5 laser diode units
* Max temperature : 2,800℃
* Total power : 1,000W
* Seal : O-ring
* Wavelength : 976 nm
* Cooling system : Chiller
* Pressure : 0.95MPa
* Vacuum : 6.7×10^{-3}Pa
* Control : PC and manual with remote control

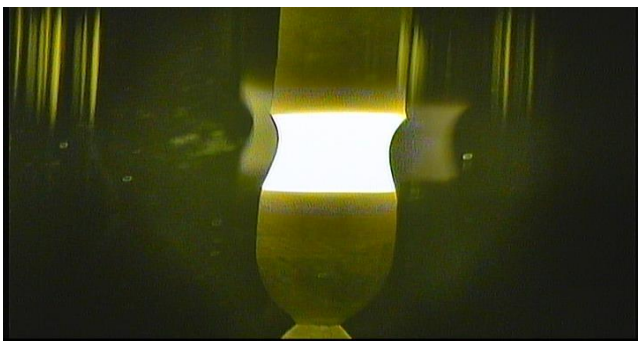

Crystal Systems Corporation

Four mirror floating zone furnace

Uniform temperature profile on the circumference of sample rod during crystal growth

Xenon lamp furnace

(Model :FZ-T-12000-X series)

≪SPEC≫

* Four mirrors
* Xenon lamp
* Max. temperature : 3,000℃
* Total power : 12,000W
* Seal : O-ring or Magnetic liquid
* Pressure : 0.95MPa
* Vacuum : 6.7×10^{-3}Pa
* Control : PC and manual with remote control

Halogen lamp furnace

(Model: FZ-T-10000/4000/2000-Hseries)

≪SPEC≫

* Four mirrors
* Halogen lamp
* Max. temperature : 2,200℃
* Total power : 600 - 6,000W
* Seal : O-ring or Magnetic liquid
* Pressure : 0.95MPa
* Vacuum : 6.7×10^{-3}Pa
* Control : PC and manual with remote control

Crystal Systems Corporation